Characterisation of the Gene Regulatory Network for Posterior Segmentation in *Parasteatoda tepidariorum*

Anna Schönauer

Degree awarded by
Oxford Brookes University

The thesis is submitted in partial fulfillment of the requirements of the award of Doctor of Philosophy

July 2016

Acknowledgments

First of all, I would like to thank Alistair for inspiring me with his enthusiasm for evo-devo and spiders, because it certainly wasn't the weather that convinced me to come to the UK. I really appreciate that no matter how busy you were, you were always available and supportive. Thank you for providing many opportunities throughout the PhD. Alongside an exciting research project, you connected me with the scientific community through various conferences and summer schools. You also encouraged me to take part in organising the seminar series, various outreach activities and spurred me on to give as many public talks as possible (you were right, it is the best training).

A substantial contribution to my PhD experience was made by the people I worked with over the last 3 and a bit years: thank you Maarten for teaching me the first steps into spider research; Evelyn thank you for showing me all your in situ tricks; Isabel and Kentaro for helping me out with all sorts of random things in the lab. Thank you to all the current lab members: Daniel, Chris, Dani, Pedro, Sebastian, Jo, Alex, Georgie, Chrissy, Claudia and Michaela – you are a lovely bunch to work with, but also to have a good chat over a pint or two! I also want to thank the other PhD students in Brookes for being such a good group for sharing complaints but also relishing in the excitement when experiments actually worked!

Obviously, a very big thank you to Harri, who went through all the ups and the downs with me, and there were a lot. Whenever I was struggling he was

always there to convince me that I could do it and that there wasn’t anything else I would rather do.

I am forever grateful to my family, who have always supported me in every way they could, even without really knowing what I was up to and offering me a wonderful home during my write-up exile time.
Danke Mama, Papa, Judith und Baby Nora für eure Unterstützung in jeglicher Form, Zuspruch und die schöne Zeit zuhause im Schreib-Exil!

Abstract

My PhD project focused on the identification of components and the architecture of the gene regulatory network that controls the formation of the segment addition zone (SAZ) and posterior segments in the spider *Parasteatoda tepidariorum*. Analysis of the formation and function of the SAZ among arthropods suggests that Wnt and Delta-Notch signaling regulated this process ancestrally in an analogous mechanism to that regulating somitogenesis in vertebrates. However, it remained unknown how the two major signaling pathways interact during the formation of the SAZ and regulate other putatively downstream segmentation genes, such as *even-skipped (Pt-eve)* and *runt* (*Pt-run-1*). Therefore, I studied the interactions between *Delta* (*Pt-Dl*) and its receptor *Notch* (*Pt-N*) and the Wnt ligand gene *Wnt8* (*Pt-Wnt8*). I showed that *Pt-Dl* initially activates *Pt-Wnt8* in the posterior SAZ, but conversely inhibits *Pt-Wnt8* expression in the anterior SAZ. Furthermore, I observed the dynamic expression of *Pt-eve* and *Pt-run-1* in the SAZ and the forming segments, suggesting an important role in posterior development. Moreover my results show that the expression of *Pt-eve* and *Pt-run-1* is regulated by the read out of Delta-Notch and Wnt signaling via *caudal (Pt-cad)*, which might be a mechanism ancestral to all arthropods.

To investigate the function of Wnt signaling in more detail in spiders, I also studied the evolution and expression of Frizzled receptors (Fz) during spider embryogenesis. Four Fz genes (*Pt-fz1, Pt-fz2, Pt-fz4a, Pt-fz4b*) have been identified in *Parasteatoda* and analysis of the expression of the frizzled receptor genes throughout embryonic development suggests an involvement in neuroectoderm development, segmentation and development of anterior

structures. Moreover, the early ubiquitous and later segmental expression of *Pt-fz1* shows that this gene is a good candidate receptor for Wnt8 in *Parasteatoda*.

Table of contents

Table of Figures

List of tables

Abbreviations

aa	amino acid
bp	base pairs
°C	degrees Celsius
Cas9	caspase 9 endonuclease
C-terminal	carboxy-terminal
cDNA	copy DNA
Ch	cheliceres
CRISPR	clustered regularly interspaced palindromic repeats
d	dorsal area
DAPI	4-6-diamidino-2-phenylindol
ddH_2O	double-distilled water
DIG	Digoxigenin
DNA	deoxyribonucleic acid
dsRNA	double stranded deoxyribonucleic acid
eRNAi	embryonic RNAi
h	hour
HR	homologous recombination
INT/BCIP	2-[4-iodophenyl]-3-[4-nitrophenyl]-5-phenyltetrazolium chloride)/ 5-bromo-4-chloro-3-indolyl-phosphate
L	walking leg
Lb	labrum
ml	millilitre
NBT/BCIP	nitro blue tetrazolium/5-bromo-4-chloro-3-indolyl-phosphate
NHEJ	non-homologous end joining
nt	nucleotide
N-terminal	amino-terminal
O	opisthosomal
PcL	precheliceral lobe
PCR	polymerase chain reaction
Pp	pedipalp
pRNAi	parental RNAi

RNA	ribonucleic acid
RNAi	RNA interference
RhodB	Rhodamine B isothiocyanate–Dextran
rpm	rotations per minute
RT	reverse transcription
µg	microgram
µl	microliter
SAZ	segment addition zone
sgRNA	short guide RNA
st	stage of development
Sto	stomodaeum
wt	wild-type

1. Introduction

1.1. Evolution & Development

The development of a single-celled zygote into a multicellular organism requires complex molecular mechanisms and tightly regulated developmental programs. Evolutionary developmental biology seeks to compare the genetic regulation of developmental processes in a phylogenetic framework to uncover ancestral and derived features of development and the underlying molecular mechanisms (Carroll, 2008; Gilbert et al., 1996; Hall, 2003). One question that has been of great interest to evolutionary developmental biologists since the emergence of this field is the origin and evolution of segmentation among animals (Davis and Patel, 1999; Davis and Patel, 2002; De Robertis, 2008; McGregor et al., 2009; Tautz, 2004).

1.2. Segments

Various groups of animals exhibit some kind of reiterated body structures (Couso, 2009): echinoderms, hemichordates and molluscs are composed of an array of coelomic cavities of mesodermal origin, separated by epithelia, which has been described as primary segmentation (Tautz, 2004). The formation of segments from undifferentiated posterior tissue, as found in arthropods, annelids and chordates, has been specified as secondary segmentation (Tautz, 2004) (see fig. 1).

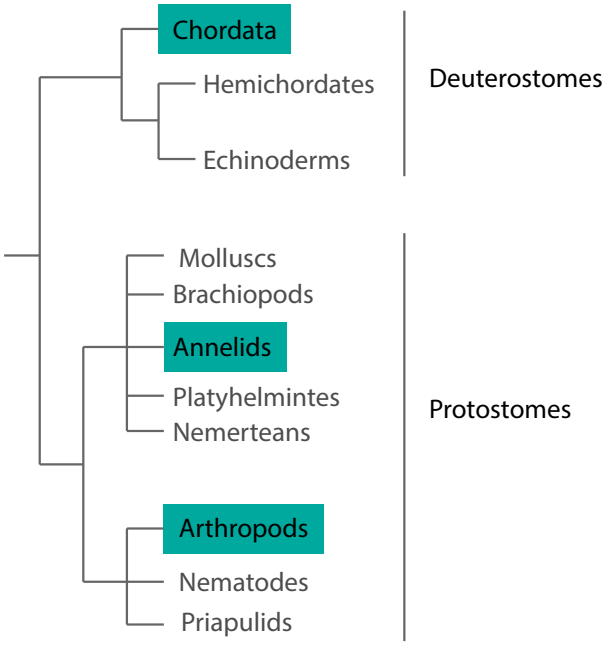

Figure 1 | Segmented body plans among bilateria. Phylogenetic tree depicting the relationships of bilateria with segmented groups highlighted in green. Figure adapted from Prud'homme et al., 2003 .

Although, these three extant bilaterian phyla are segmented along their antero-posterior axis, it is highly disputed if this characteristic derived from a common segmented ancestor or if the process of segment formation has evolved multiple times independently in the different lineages (Aulehla and Herrmann, 2004; Balavoine and Adoutte, 2003; Chipman, 2010; Couso, 2009; Damen, 2007; Davis and Patel, 1999; Erwin and Davidson, 2002; Graham et al., 2014; Patel, 2003; Peel, 2008; Peel et al., 2005; Pourquie, 2003; Scholtz, 2002; Tautz, 2004). Indeed, vertebrates, arthropods and annelids with segmented bodies are more closely related to unsegmented groups in their phyla than they are to each other (Aguinaldo et al., 1997; de Rosa et al., 1999) (see fig. 1).

1.3. Evolutionary scenarios of segmentation

There are three possible explanations for the evolution of segmentation (Davis and Patel, 1999) (see fig. 2). Firstly, it has been suggested that the common bilaterian ancestor was unsegmented and segmentation has evolved independently in all three bilaterian phyla. In support of this, it has been argued that only minor similarities in the mechanisms for segment formation can be detected, due to the independent evolution of segments (see fig. 2 A) (Davis and Patel, 1999). And furthermore that similarities in regulation have evolved through the parallel recruitment of pre-existing gene-regulatory modules (Chipman, 2010).

The second theory is that the common ancestor of bilateria, the urbilateria, exhibited a segmented body and therefore segmentation is homologous among bilaterian animals. This theory suggests that the whole genetic toolkit for segment formation was present in the common segmented ancestor and this explains similarities in the regulation of segmentation in extant phyla (Davis and Patel, 1999; De Robertis and Sasai, 1996; Kimmel, 1996; Patel, 2003) (see fig. 2 B).

A third hypothesis, is that segmentation evolved independently after the protostome/deuterostome split and therefore segmentation is homologous among arthropods and annelids, but evolved independently in vertebrate chordates (see fig. 2 C). This assumes that the annelid/arthropod clade share a segmented ancestor and hence exhibits a significantly high degree of similarities and major differences compared to vertebrates (Scholtz, 2002). Furthermore, this theory comprises the loss of segmentation in the

unsegmented phyla of Ecdysozoa and Lophotrochozoa (Davis and Patel, 1999).

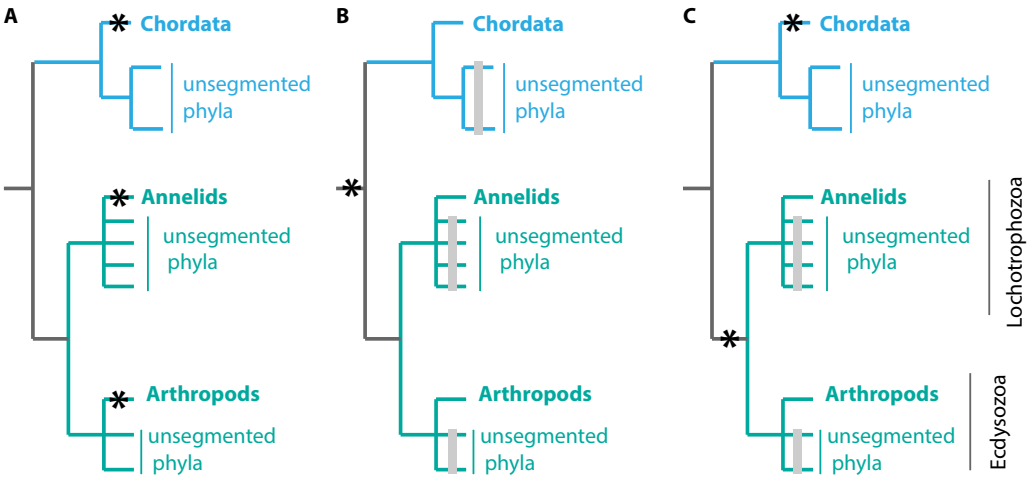

Figure 2 | Evolutionary scenarios of segmentation. (A) Segmentation arose independently in all three phyla. **(B)** A common segmented ancestor for all three groups with loss of segmentation among the unsegmented phyla. **(C)** Homology of segments among annelids and arthropods and independent segmentation in chordates. Deuterostomia in blue; Protostomia in green. Asterisks indicated the acquisition of segmentation; solid grey blocks indicate the loss of segmentation (modified after Davis and Patel 1999).

The “segmented common ancestor theory” (see fig. 2 A) was countered with the argument of parsimony: it appears easier to evolve segmentation 3 times independently, than to achieve the loss in numerous unsegmented phyla (Chipman, 2010). In addition it seems unlikely that a complex and highly advantageous trait like segmentation would have been lost (Chipman et al., 2004). Furthermore is has been claimed, that the existence of a segmented bilaterian ancestor is unlikely simply due to a lack of fossil evidence (Erwin and Davidson, 2002). Nevertheless, it has been argued that the losses of segmentation are not impossible to achieve, because the unsegmented groups are clustered and segmentation could have been lost early in the evolutionary history of extant unsegmented phyla (Davis and Patel, 1999).

Indeed the involvement of Delta/Notch signaling in arthropod segmentation, as shown in *Periplaneta* and the spiders *Cupiennius* and *Parasteatoda* as well as in vertebrates has also been interpreted as further evidence for the possibility of a common segmented ancestor (De Robertis, 2008; Oda et al., 2007; Peel and Akam, 2003; Pueyo et al., 2008; Stollewerk et al., 2003). Further support for a common segmented ancestor from analysis of regulatory mechanisms underlying segmentation includes the dynamic expression of *her1*, the vertebrate ortholog of the arthropod pair-rule gene *hairy*, commencing very early on in vertebrate development (Kimmel, 1996). Moreover, it appears that *hedgehog* (*hh*) is necessary for the maintenance of segmental borders in arthropods and annelids implying a segmented common ancestor of these phyla (Dray et al., 2010; Farzana and Brown, 2008; Ingham and McMahon, 2001). It has also been suggested that a gradient emerging from the anterior, like the *Drosophila* bicoid gradient, would not be able to pattern the posterior in short germ arthropods as it cannot reach the posterior, hence a posterior signaling centre must have regulated segmentation ancestrally. Hence, the homeodomain transcription factor *caudal* (*cad*), which is involved in patterning the posterior of *Drosophila* embryos, as well as in other arthropods like its Cdx orthologs in vertebrates, again evidences similarities in posterior development between distantly related segmented phyla (Lall and Patel, 2001).

On the contrary, other authors have claimed that some parts of the genetic toolkit, like signaling pathways and their individual components, like transcription factors are employed in many different aspects of development

and hence, to derive homology and a common origin from such genetic modules appears incorrect (Erwin and Davidson, 2002).

Another explanation for the observation of common mechanisms, with a varying composition of factors involved and changes in their regulation, is the generation of the GRN of segmentation by convergent evolution. In this process, an already established network, acquires new components after an evolutionary event, like a whole genome duplication, through co-option of the duplicated factors (Minelli, 2015). It has been suggested that for example the generation of repeated structures by the Delta-Notch and the Wnt signaling pathways displays a co-opted function of their ancient role in axis elongation (Chipman, 2010).

1.4. Mechanisms of Segmentation

1.4.1. Segmentation in Vertebrates

Three different developmental events, the formation of somites, the subdivision of the hindbrain into rhombomeres and the formation of the pharyngeal arches are regarded as segmentation processes in vertebrates (Graham et al., 2014). However, only the sequential formation of the somites from the pool of undifferentiated presomitic mesoderm (PMS) cells, displays an analogous mechanism to the segmentation process in arthropods (Graham et al., 2014). It is important to emphasise, that vertebrate somites arise from the mesoderm, in contrast to ectodermal arthropod segments. However, the mode of segment or somite formation, respectively from a posterior pool of

undifferentiated cells, regulated by dynamic gene expression is at least an analogous mechanism.

Somite formation in vertebrates is regulated by opposing gradients of gene expression, which sequentially subdivide the PMS into smaller subunits (Kageyama et al., 2012; Pourquie, 2001) (Fig. 3). In the 'clock and wavefront' model for somite formation first proposed by Cooke and Zeeman, 1976 the periodic production of somites in the PSM is regulated through the cyclical expression of members of the *hairy/enhancer of split* (*Hes*)-gene family (Takke and Campos-Ortega, 1999) (see fig. 3). In the mouse, *Hes7* forms an auto-regulatory feedback loop, in which the unstable *Hes7* protein represses its own transcription resulting in oscillating *Hes7* expression in the PSM (Nomura-Kitabayashi et al., 2002). However, the synchronicity of expression in the PSM is only achieved through cell-to-cell signaling via Delta/Notch, where *Delta* activates *Notch* in a neighboring cell to initiate *Hes7* expression (Cooke, 1998; Jiang et al., 2000). The interface between the site of somite differentiation and the posterior oscillatory gene expression has been described as the wave front (Kageyama et al., 2012). The wave front is generated by a rostral to caudal FGF gradient (Dubrulle et al., 2001) (see fig. 3). The low levels of FGF and high levels of Notch in the anterior finally trigger the expression of a regulator of somite formation, *Mesp2* (Kageyama et al., 2012; Saga, 2007) (see fig. 3). Additionally, a gradient of *Wnt3a* helps to set the boundary for somite formation and maintains oscillations (Aulehla and Herrmann, 2004). Low levels of *Wnt3a*, inhibit the oscillation and allow differentiation to occur (Aulehla and Herrmann, 2004) (see fig. 3)

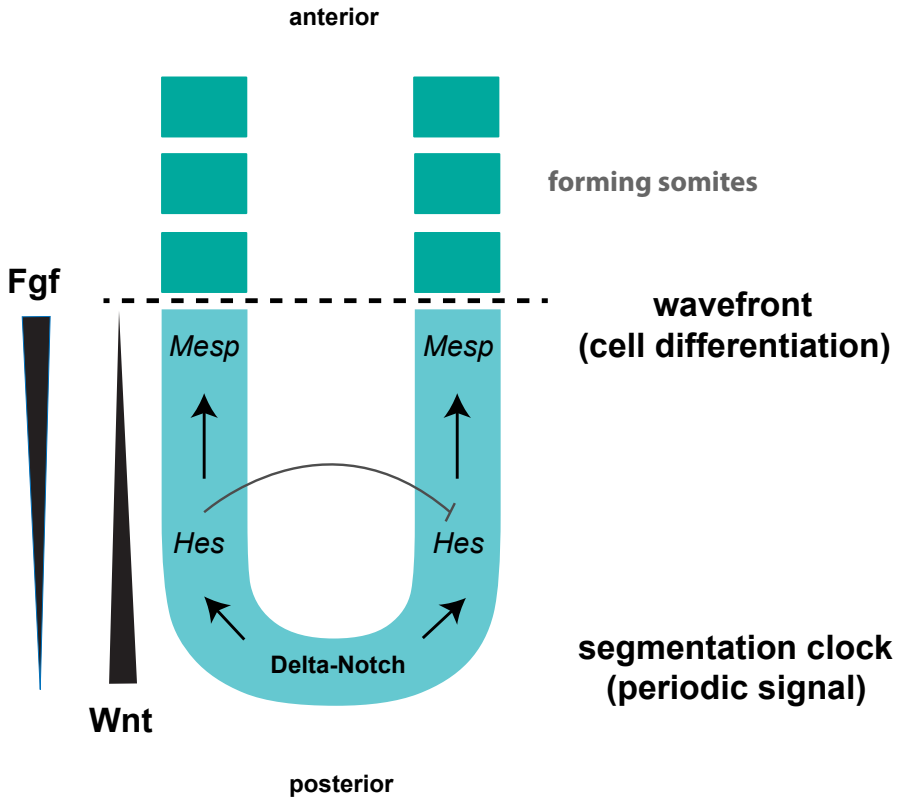

Figure 3 | Vertebrate somitogenesis. Delta-Notch signaling at the posterior conveys the periodic signal in the presomitic mesoderm (PSM; light blue), where it activates *Hes*-gene expression. *Hes*-genes form an auto-regulatory feedback loop, which leads to oscillatory expression. Wnt and FGF signaling establish opposing gradients in the PSM. *Mesp* expression at the wavefront is activated and allows cell differentiation and hence somite formation in periodic intervals.

1.4.2. Segmentation in Annelids

Segment addition in annelids occurs at larval and juvenile stages. In the marine annelid, *Platynereis dumerilii (Pdu),* the first signs of morphological segmentation become apparent at the swimming larval stage (Fischer et al., 2010). After an elongation phase, where the larva develops into a worm with three distinct segments, the larva settles and continues to form segments sequentially from the segment addition zone (SAZ) (de Rosa et al., 2005; Fischer et al., 2010).

The relative expression domains of the segment polarity gene orthologs *hedgehog* (*Pdu-hh*), *engrailed* (*Pdu-en*) and the Wnt ligand *Pdu-Wnt1/wg* (Dray et al., 2010; Prud'homme et al., 2003) are reminiscent of the parasegmental boundary described in *Drosophila,* where *wg* is expressed anterior of *en* overlapping with *hh* expression (Martinez-Arias and Lawrence, 1985) (see also section 1.3.3.1. “The *Drosophila* paradigm”).

Furthermore, inhibition of Hedgehog (Hh) signaling in *Platynereis* leads to the loss of the segmental groove, the segments acquire an ovoid shape and germ band elongation is disrupted (Dray et al., 2010). Hence, Hh signaling is critical for boundary maintenance in nascent segments prior to morphological segmentation in this annelid (Dray et al., 2010), as has been found in arthropods (Farzana and Brown, 2008).

Furthermore, expression data of the *Platynereis* homologues of the two segmentation genes *caudal* (*Pdu-cad)* and *even-skipped* (*Pdu-eve*) in the SAZ and in forming segments of *Platynereis*, suggest that they have a function in segmentation because they are expressed in domains and at developmental time points comparable to what has been observed in arthropods (de Rosa et al., 2005). Phylogenetic analysis identified 13 *Hes*/*Hey*-related genes in *Platynereis* (Gazave et al., 2014), which are known to be part of the oscillatory gene expression and downstream targets of Delta/Notch signaling in vertebrate somitogenesis (Kageyama et al., 2012). However, there is no functional data available for the *Hes/Hey*-related genes in *Platynereis.*

Leeches undergo direct embryonic development and form segments sequentially from teloblast cells, embryonic stem cells, which in turn form

columns of segmental founder cells (Weisblat et al., 1984). Morphologically, the first signs of segmentation become obvious after the fusion of the two bilateral germ bands, when the germ band divides from anterior to posterior into repeated units (Bissen and Weisblat, 1989; Zackson, 1982). However, expression data of the *even-skipped* homologs in the leeches *Helobdella robusta* (*Hro*) and *Theromyzon trizonare* (*Ttr*) do not support a role for these genes in segmentation (Song et al., 2002), unlike in *Platynereis* (de Rosa et al., 2005). Indeed knockdown of *Hro-eve* suggests a role in cell proliferation and neurogenesis, rather than segmentation in this leech (Song et al., 2002). Furthermore, analysis of *hes*-genes in the two leeches (*Hro-hes*, *Ttr-hes*) does not support a function in segmentation, again in contrast to *Platynereis* (Song et al., 2004).

Whilst the molecular organization of segment boundaries in *Platynereis* displays similarities with the *Drosophila* parasegmental boundaries and the expression of the segmentation genes *caudal* and *even-skipped* suggest a role in segmentation, studies in the two leeches could not confirm an involvement of *even-skipped* in segmentation (de Rosa et al., 2005; Dray et al., 2010; Martinez-Arias and Lawrence, 1985; Song et al., 2002).

Although the analysis of the relative expression patterns of segmentation gene orthologs show analogy with vertebrates and arthropods (Dray et al., 2010; Prud'homme et al., 2003), the diverse developmental processes and the limitations of functional tools in annelids make the study of segmentation and also the comparison with other segmented phyla challenging (Balavoine, 2014).

1.4.3. Segmentation in Arthropods

The phylum name Arthropoda is derived from the Greek words for “jointed” (arthros) and “feet” (podes), as all arthropods exhibit jointed appendages. All arthropods also display a sclerotized cuticle, the exoskeleton, which encloses the whole body and is shed during growth. Furthermore, the arthropod body is composed of segments along the antero-posterior axis and their nervous system is located ventrally (Anderson, 1973; Scholtz, 1998). It has been hypothesised that the modular body plan of arthropods has facilitated flexibility for adaption to the requirements of the diverse habitats and so has majorly contributed to the success of these animals (Stansbury and Moczek, 2013).

The Drosophila paradigm

Segmentation in arthropods has been most intensely studied in *Drosophila*, which employs a derived mode of segment formation among arthropods where the specification of the cephalic, thoracic and abdominal segments occurs almost simultaneously along the anterior-posterior axis (Davis and Patel, 2002; Ingham, 1988; Lawrence, 1992; Nusslein-Volhard and Wieschaus, 1980; Pankratz and Jäckle, 1993; Peel et al., 2005). This specification of segments in the fruit fly is regulated by a well characterised segmentation cascade (Scott and Carroll, 1987) (see fig. 4).

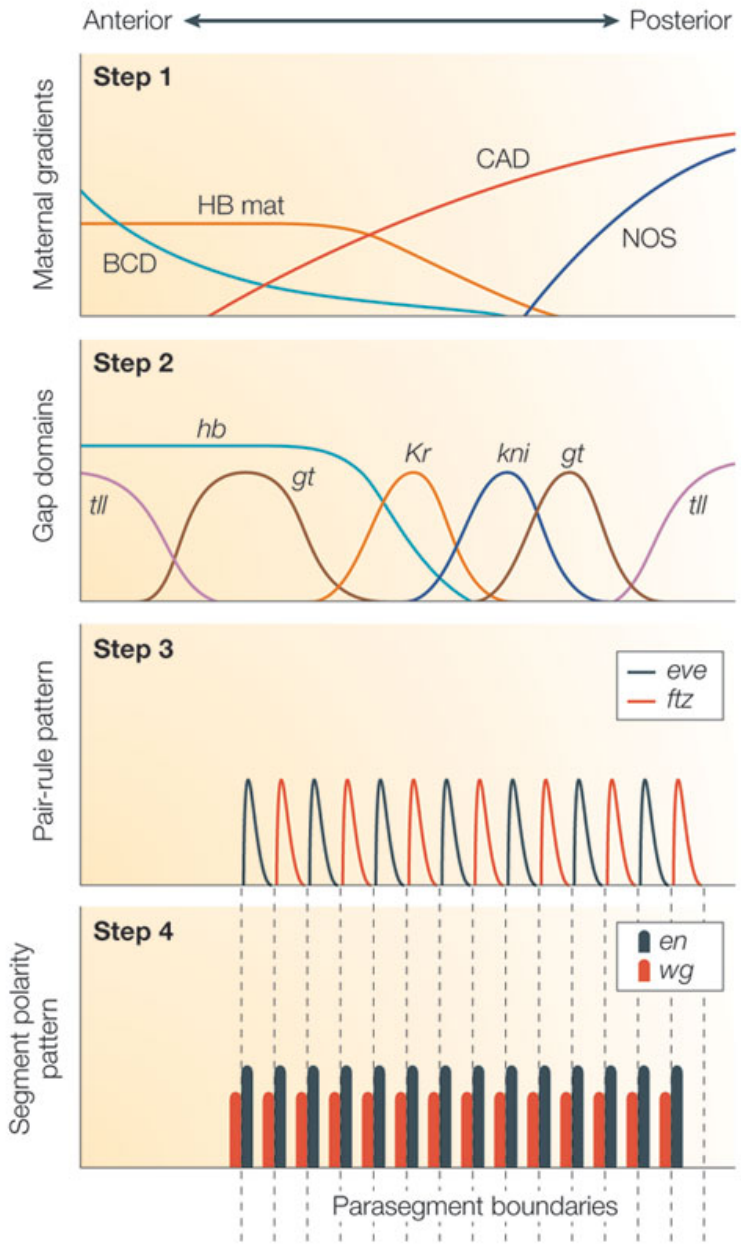

Figure 4 | The *Drosophila* segmentation gene cascade. Maternal transcripts bicoid (BCD) and nanos (NOS) are localized to the anterior and posterior pole, respectively; hunchback (HB) and caudal (CAD) are expressed ubiquitously (**Step 1**). The output of the maternal effect genes activates zygotically expressed gap genes (tailless, tll; gt, giant; Kr, Krüppel; kni, knirps) at specific positions along the A-P axis (**Step 2**). The primary (*hairy, even-skipped, runt*) and secondary (*fushi tarazu, paired*) pair-rule genes interpret the aperiodic expression of the maternal effector and gap genes, to generate a periodic stripe pattern, predicting the parasegmental boundaries (**Step 3**). Odd- and even-numbered segments express different combinations of pair-rule genes. The parasegmental boundary is established between the *engrailed* domain anteriorly and the *wingless* domain posteriorly (**Step 4**). Picture is taken from (Peel et al., 2005).

Initially, localized maternal transcripts are translated and establish long-range transcription factor gradients in the syncytial blastoderm, which in turn regulate zygotic downstream factors (Rivera-Pomar et al., 1995; St Johnston and Nusslein-Volhard, 1992). Unique to higher diptera, including *Drosophila*, is the maternally deposited factor *bicoid,* which is translated upon fertilisation to form an anterior to posterior gradient that activates gap genes in a concentration dependent manner (Berleth et al., 1988; Driever and Nusslein-Volhard, 1988b; Lehmann and Nusslein-Volhard, 1991; St Johnston and Nusslein-Volhard, 1992; Stauber et al., 1999) (see fig 4, step1). Bicoid has also been shown to directly repress the translation of the initially uniformly distributed maternal factor *caudal* (*cad*) in the anterior (Macdonald and Struhl, 1986).

Subsequently, maternal coordinate genes trigger the asymmetric expression of gap genes within the blastoderm (see fig. 4, step 2). Gap genes in turn activate pair-rule gene expression and spatially regulate and refine their alternating expression together with maternal inputs and auto-regulatory feedback of pair-rule genes themselves (Carroll, 1990; Frasch and Levine, 1987; Gaul and Jackle, 1990). The double-segmental pair-rule pattern further activates the single-segmental expression of segment polarity genes, delineating the borders of the parasegments and compartments of the future segments (Rivera-Pomar and Jackle, 1996) as the parasegments, are out of phase with the true segmental boundaries (Martinez-Arias and Lawrence, 1985) (see fig. 4, step 4). Typically, *engrailed (en)* is expressed in the anterior portion of the parasegment, which corresponds to the posterior of the future segment and *wingless (wg)* specifies the posterior of the parasegment

(Kornberg et al., 1985; Martinez-Arias and Lawrence, 1985) (see fig. 4, step 3 and 4 and fig. 5). *En* activates the expression of *hedgehog* (*hh*), which binds the *patched* (*ptch*) receptor on *wg* expressing cells. This in turn activates *wg*, maintaining its expression and thereby defining the parasegmental borders (Heemskerk et al., 1991; Ingham et al., 1991; Mohler and Vani, 1992) (see fig. 5). *en* and *wg* do not only delineate the parasegments in *Drosophila*, but have been shown to exhibit conserved relative expression in other arthropods (Damen, 2007; Patel et al., 1989b).

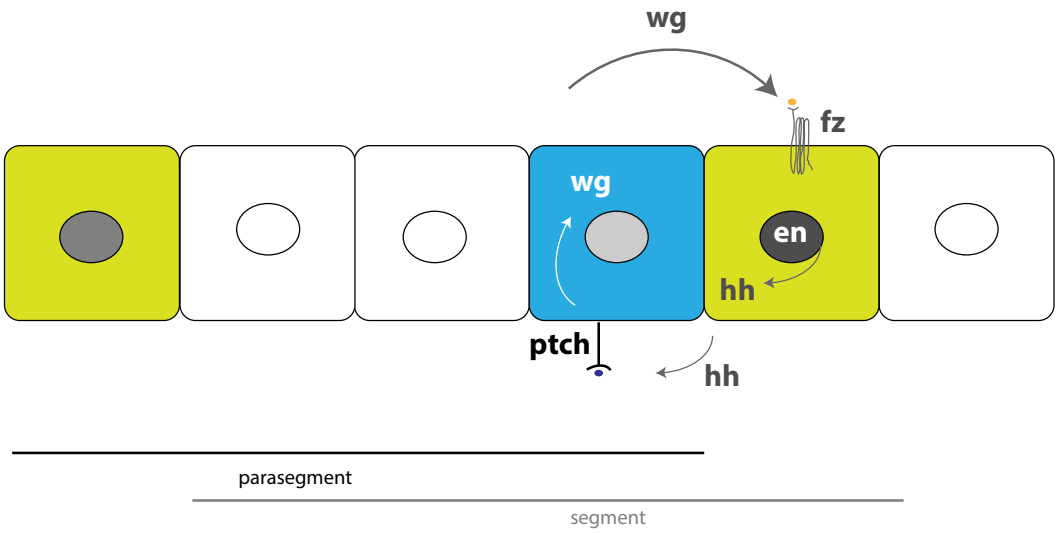

Figure 5 | Maintenance of the parasegmental boundary in *Drosophila*. After the establishment of the parasegmental boundaries through the pair-rule genes, *wg* protein diffuses to the neighbouring cells, binds to the frizzled (*fz*) receptor on *en* expressing cells (Bhanot et al., 1996). Subsequently *en* activates *hh* expression, which in turn binds the *patched* (*ptch*) receptor in *wg* expressing cells, leading to an activation of wg expression (Ingham et al., 1991; Mohler and Vani, 1992).

Finally, the combinatorial expression of gap, pair-rule and segment polarity genes regulate the Hox genes, which determine the segment identity (Affolter et al., 1990; Akam, 1987; Harding et al., 1985; Irish et al., 1989; Lewis, 1978; Pearson et al., 2005).

In contrast to *Drosophila*, most other arthropods are short or intermediate germ arthropods, which specify a species-specific number of anterior segments at the blastoderm stage and form posterior segments consecutively from the SAZ, and in some cases add segments also during post embryonic stages (Davis and Patel, 2002) (see fig. 6).

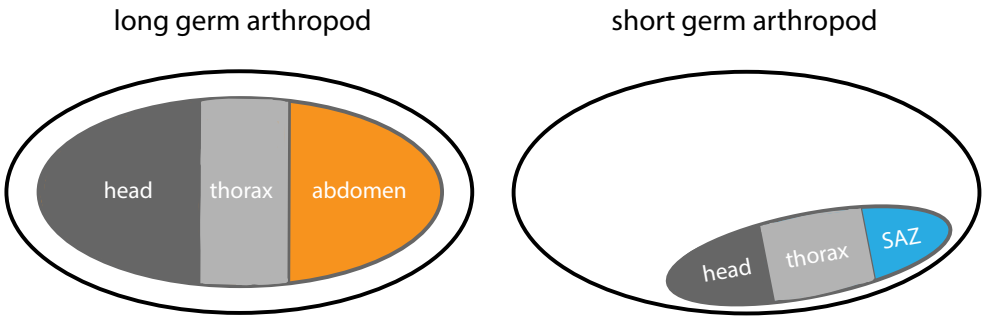

Figure 6 | Long and short germ arthropod segmentation. In long germ arthropods, the head (dark grey), the thorax (light grey) and the abdomen (orange) are specified almost simultaneously. In contrast, short germ arthropods pattern their head (dark grey) and thorax (light grey) early in embryonic development and form posterior segments from the segment addition zone (SAZ; blue).

This sequential addition of segments also occurs in a cellularised environment, suggesting that different molecular mechanisms may regulate segment formation in long germ arthropods compared to short germ arthropods (Peel et al., 2005). For example in *Drosophila* the patterning of the future segments occurs through long-range transcription factor gradients, which is not possible in a cellular environment (Davis and Patel, 2002; Pankratz and Jäckle, 1993). However, despite the common conception that all future segments of *Drosophila* are specified simultaneously, a succession in the appearance of pair-rule and segment polarity stripes can be observed, with anterior stripes

showing up first (Bothma et al., 2014; Janssens et al., 2014; Pankratz et al., 1990). These observations led to the suggestion that the successive segmentation gene expression appearance is a remnant of secondary growth and the ancestral cell-cell based mode of segmentation was not entirely replaced by a morphogen gradient driven process in *Drosophila* (Tautz, 2004). Despite the in depth knowledge about segmentation in the long germ insect *Drosophila*, the gene regulatory network (GRN) responsible for the set up of the SAZ and the sequential segment formation from this tissue in short germ arthropods remains poorly understood.

Segmentation in short germ arthropods

Orthologs of maternal factors

In *Drosophila*, Bicoid is an important maternal factor, however it represents a derived characteristic, not found outside of Diptera (Driever and Nusslein-Volhard, 1988a; McGregor, 2005; Stauber et al., 1999). Cad is also important during Drosophila embryogenesis and is distributed in a reciprocal gradient to Bcd along the anterior-posterior axis with the maximum at the posterior (Mlodzik and Gehring, 1987).

Moreover, *cad* is expressed in the embryonic posterior of many arthropods and *cad* RNAi knockdown experiments cause posterior defects (Copf et al., 2004; Dearden and Akam, 2001; Olesnicky et al., 2006; Shinmyo et al., 2005). Furthermore, *cad* regulates the expression of anterior gap genes in *Tribolium* and *Gryllus,* which suggests a role at the top of the segmentation gene cascade (Copf et al., 2004; Shinmyo et al., 2005).

The most recent studies in *Tribolium* revealed that the graded expression of *caudal* (*Tc-cad*) also modulates the frequency of *even-skipped (Tc-eve),* resulting in oscillating waves of *Tc-eve* expression (Copf et al., 2004; El-Sherif et al., 2014). Hence, it has been suggested that *Tc-cad* acts a morphogen, which regulates the rate of pair-rule gene expression in *Tribolium* (El-Sherif et al., 2014). These findings are in great contrast to the static *even-skipped* expression, regulated by the combinatorial action of gap genes in *Drosophila* (Frasch and Levine, 1987).

Gap gene orthologs

In most short germ arthropods, gap gene expression commences early in the germ rudiment in broad domains overlapping several future segments, however the relative expression is not conserved (Bucher and Klingler, 2004; Liu and Kaufman, 2004a; Liu and Kaufman, 2004b; Liu and Patel, 2010). Furthermore, the functional analysis of gap genes in e.g. *Tribolium*, *Oncopeltus* and *Gryllus* shows a more complex picture than in *Drosophila* and in some cases the knockdown causes malformation rather than a lack of several adjacent segments (Bucher and Klingler, 2004; Liu and Kaufman, 2004a; Liu and Kaufman, 2004b; Mito et al., 2005; Schroder, 2003).

In *Parasteatoda*, the development of the prosoma requires *hunchback (hb)* and *distal-less (Dll)* expression and there is evidence that these genes perform gap gene-like functions in this spider (Pechmann et al., 2009; Schwager et al., 2009). *Dll* is expressed in a broad domain in the presumptive L1 segment at early stages, whereas the homologous mandibular segment in

insects lacks *Dll* and is expressed in the homologous segment only at low levels in other mandibulate arthropods (Pechmann et al., 2011).

In insects, *hb* mainly regulates pair-rule and HOX gene expression and causes homeotic transformations in knockdown experiments (Liu and Kaufman, 2004a; Marques-Souza et al., 2008; Mito et al., 2005). In *Parasteatoda hb* is expressed before morphological segmentation and causes a loss of adjacent segments in RNAi experiments (Schwager et al., 2009). Therefore, it has been proposed that *hb* acts like a gap gene in the spider and is responsible for the correct expression of target genes, rather than HOX gene regulation (Schwager et al., 2009).

Pair-rule gene orthologs

In the short germ insect *Tribolium* pair-rule genes are expressed with double-segmental periodicity like in *Drosophila*, which resolves into single-segmental expression through splitting of those primary stripes or intercalation of secondary stripes (Brown et al., 1997; Goto et al., 1989; Maderspacher et al., 1998; Patel et al., 1994). However, the knockdown of *Tc-eve*, *Tc-run* and *Tc-odd* does not result in the classic pair-rule phenotypes exhibiting the loss of alternating segments, but causes severe truncations in all three cases (Choe et al., 2006). On the other hand, *Tc-slp* and *Tc-prd*, were shown to occur in double segmental periodicity and produce pair-rule gene phenotypes with the loss of alternating segments in RNAi experiments (Choe and Brown, 2007). These observations led to the conclusion, that pair-rule genes act on two different functional levels and the hierarchy as described in *Drosophila,* is maintained in *Tribolium* (Choe et al., 2006).

Whilst primary pair-rule genes are regulated by maternal factors and gap genes in *Drosophila,* a different mechanism of pair-rule regulation has been proposed in *Tribolium* (Choe et al., 2006; Frasch and Levine, 1987): *Tc-eve* has been shown to activate *Tc-run* expression, which in turn activates *T-odd* expression (Choe et al., 2006). The subsequent repression of *Tc-eve* by *Tc-odd* finally closes a pair-rule gene circuit in *Tribolium* (Choe et al., 2006). Hence, it can be concluded that certain aspects of the derived *Drosophila* segmentation still represent ancestral aspects of insect segmentation, but there is also variation in the precise regulation and roles of pair-rule genes (Choe and Brown, 2007; Patel et al., 1994).

In contrast to the double segmental periodicity of pair-rule genes in some insects, the orthologues of these genes exhibit single segment periodicity in short germ arthropods like spiders and during the addition of the final few segments in the centipede *Strigamia* (Brena and Akam, 2013; Leite and McGregor, 2016; Schoppmeier and Damen, 2005a).

For example, in the spider *Cupiennius salei*, the primary pair-rule gene orthologues *hairy* (*Cs-h*), *even-skipped* (*Cs-eve*) and *runt* (*Cs-run*) are expressed dynamically in the SAZ and with single-segmental periodicity in nascent segments (Damen et al., 2000). Furthermore, the secondary pair-rule gene orthologs *paired* (*Cs-opa)*, *Cs-odd related 1* (*Cs-odd-r1*) and *sloppy-paired (Cs-slp)* are likely to be involved in segmentation, due to their expression in the anterior SAZ and nascent segments (Damen et al., 2005).

The *Strigamia* pair-rule gene ortholog expression of *Sm-eve*, *Sm-run*, *Sm-odd, Sm-h* precede morphological segmentation and establish a double-segmental pattern in the peri-proctodeal area, and were therefore suggested to perform a

homologous function to primary pair-rule genes in *Drosophila* (Chipman and Akam, 2008; Chipman et al., 2004). Initially, *Sm-eve1* is expressed in a double-segmental pattern, out of phase with the double-segmental *Sm-Dl* expression (Brena and Akam, 2013). Subsequently, *Sm-eve1* and *Sm-Dl* were observed to resolve into single segmental stripes through splitting or intercalations (Brena and Akam, 2013). However, a detailed analysis of the expression of *Sm-Dl* and *Sm-eve1* revealed a striking change in pair-rule periodicity in the centipede, towards the end of the segmentation process (Brena and Akam, 2013). Interestingly, for the formation of the approximately 10 last trunk segments the initially dynamic expression slows down and *Sm-eve* is expressed uniformly in the peri-proctodeal area, which resolves into single-segmental stripes, co-expressed with *Sm-Dl* (Brena and Akam, 2013).
The dynamic expression in the posterior of the centipede, with the switch from double to single-segmental periodicity, has lead to the conclusion that oscillatory gene expression with single-segmental pair-rule gene expression represents the ancestral mechanism for the generation of segments. Furthermore, it has been suggested that the double-segmental patterning of the majority of trunk segments may be an adaption to the rapid development of centipedes (Brena and Akam, 2013; Damen, 2004; Leite and McGregor, 2016).

Segment polarity gene orthologs

Analysis of the segment polarity orthologs in the *Cupiennius* implies that the functional organisation of parasegmental boundaries is an ancestral feature of arthropods (Damen, 2002). In the spider, two copies of *engrailed* have been

identified (*Cs-en1, Cs-en2*) and *wingless* (*Cs-wg*) together with a Wnt ligand (*Cs-Wnt5-1*) have been proposed to define the parasegmental boundary. The combined expression of *Cs-en1* and *Cs-en2* cover the posterior of the functional unit, where *Cs-wg* and *Cs-Wnt5-1* in conjunction specify the domain just anterior to that. Indeed, the relative expression of *wg* and *en* expression at the segmental borders appears to be conserved across all arthropods (Jaynes and Fujioka, 2004; Marie and Bacon, 2000; Patel et al., 1989a; Patel et al., 1989b).

Wnt and Delta-Notch signaling in arthropod segmentation

While Delta-Notch signaling is not involved in regulating *Drosophila* segmentation (Peel et al., 2005), it has been found that this pathway is crucial for segment formation in several short germ arthropods.

In the cockroach *Periplaneta*, it has been demonstrated that components of the Delta-Notch pathway are expressed in dynamic stripes in the SAZ and the nascent segments emerging from the posterior (Pueyo et al., 2008). Furthermore, *Pa-N* is crucial for SAZ establishment and maintenance, segment formation and expression of the downstream factors *Pa-h* and *Pa-en* (Pueyo et al., 2008). Note also that *Pa-h* exhibits single segmental periodicity, unlike in *Drosophila* (Pueyo et al., 2008). Further analysis of the molecular mechanism of segment addition in *Periplaneta,* revealed that the sequential formation of segments is regulated by oscillating levels of gene expression, which originate from the SAZ (Chesebro et al., 2012) (see fig. 7). More specifically, *Pa-Wnt1* initially activates *Pa-cad* in the posterior, forming a signaling centre responsible for the set up and maintenance of the SAZ (see

fig. 7). *Pa-cad* is expressed in a broad domain, maintaining SAZ cells in an undifferentiated state (see fig. 7). Subsequently, *Pa-Wnt1* expression activates *Pa-Delta* in the posterior and establishes a positive feedback loop, which regulates cyclic expression of *Pa-Dl* (see fig. 7). It is thought that if *Pa-Delta* expression reaches a certain threshold it can pass through the *Pa-cad* domain and trigger segmentation gene expression like *Pa-en* anteriorly (Chesebro et al., 2012) (see fig. 7).

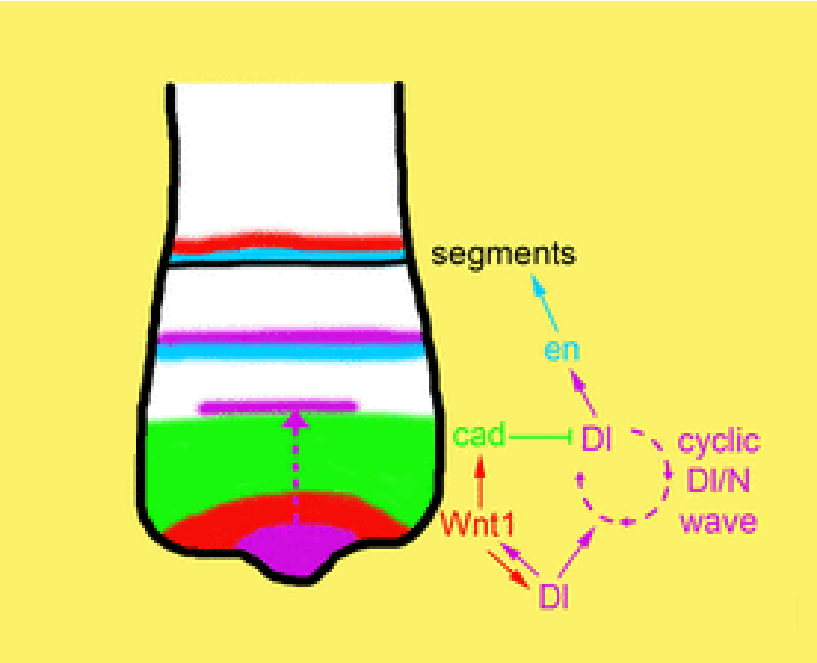

Figure 7 | The *Periplaneta* posterior organiser. In the cockroach, Delta expression (violet) emanating from the posterior and Wnt1 (red) form a positive feedback loop, activating each others expression. Wnt1 also activates cad expression (green) in a broad domain in the anterior GZ, both required to establish the growth zone (GZ) maintain the cells in an undifferentiated state. Cad on the other hand represses Dl expression in the anterior GZ and thereby inhibits segment formation. Cycling Dl expression passes through the cad domain and enables segment formation in the cad negative area. Subsequently the segment polarity network is activated, with en (blue) and Wnt1 delineating the segmental borders. Picture modified from (Chesebro et al., 2013).

The involvement of Delta/Notch signaling during segmentation in a chelicerate was first shown in *Cupiennius*, where *Delta-1*, *Cs-Delta-2* and *Notch* (*Cs-N*)

are expressed in the SAZ and resolve into stripes in nascent segments later, prior to morphological segmentation (Stollewerk et al., 2003). Functional analysis of all three genes using RNAi knockdown resulted in malformation of the segments with indistinct borders, irregular shapes and an enlarged SAZ. Moreover, the expression pattern of *Cs-h* was perturbed in the SAZ and the forming segments in these RNAi embryos (Stollewerk et al., 2003). Therefore the authors concluded that Notch-signaling is necessary for segment patterning and the establishment of sharp segmental borders in *Cupiennius* (Stollewerk et al., 2003).

It was also shown that Delta/Notch signaling in spider segmentation acts via the down stream targets *Suppressor of hairless* and *Presenillin* (Damen, 2002; Stollewerk et al., 2003). The two copies of *Suppressor of hairless* (*Cs-Su(H)-1*, *Cs-Su(H)-2*) and *Presenillin* (*Cs-Psn*) are expressed ubiquitously at early stages and specific *Cs-Su(H)-2* segmental expression comes on at later stages. RNAi knockdown of *Cs-Su(H)-1* and *Cs-Su(H)-2* caused identical phenotypes, where segmentation is blocked after the formation of three irregular-shaped opisthosomal segments and an enlarged SAZ. Moreover, the expression of both *Cs-en* and *Cs-h* is lost in the *Cs-Su(H)-1* and *Cs-Su(H)-2* knockdown embryos (Damen, 2002; Schoppmeier and Damen, 2005b; Stollewerk et al., 2003). The effect of *Cs-Psn* knockdown is similar to what has been observed for *Cs-Su(H)-1* and *-2*, however, five segments are formed before posterior development stops. Also, segment shape and size are affected, but in contrast to *Cs-Su(H)-1* phenotypes, the head lobes do not develop properly and appendages in the prosoma are shortened or missing, but the SAZ is unaffected. Expression of *Cs-h* and *Cs-Delta-1* is abolished in

the posterior of the *Cs-Psn* RNAi embryos (Schoppmeier and Damen, 2005b). These results show that Delta-Notch signaling in spiders activates the same downstream cascade as in vertebrate somitogenesis and that Notch signaling in spiders is responsible for SAZ and segment border formation analogous to it's function in vertebrates (Ferjentsik et al., 2009).

In *Parasteatoda*, the ligand *Delta* (*Pt-Dl*) and the receptor *Notch* (*Pt-N*) exhibit expression in the SAZ and stripes in opisthosomal segments (Oda et al., 2007). Functional analysis of these genes also shows that both are required for the development of the SAZ and subsequent generation of segments. Knockdown of *Pt-Dl* or *Pt-N* cause an abnormal thickening of the tissue at the developing posterior of the germ disc. These early phenotypes develop into different posterior phenotypes ranging from embryos with reduced opisthosomal tissue, with a normal prosoma, to a complete loss of the opisthosoma and disorganised anterior regions of these germ bands. Cells in the aggregated caudal region of *Pt-Dl* or *Pt-N* RNAi embryos strongly express the mesodermal marker *twist* (*Pt-twi*) (Yamazaki et al., 2005) and lack expression of the posterior determinant gene *caudal* (*Pt-cad*) (see fig. 8). This indicates that the specification of caudal ectoderm fails in *Pt-Dl* RNAi embryos due to the insufficient downstream activation of *Pt-cad* and the over expression of *Pt-twi* (Oda et al., 2007).

The Wnt-signaling pathway is also crucial for posterior spider segments. In *Parasteatoda,* knockdown of the ligand *Wnt8* (*Pt-Wnt8*) results in malformation and truncation of the opisthosoma. Moreover, it was shown that the lack of *Pt-Wnt8* leads to a misregulation of *Pt-Dl* and the Delta-Notch

downstream factor *hairy* (*Pt-h*) in the SAZ (McGregor et al., 2008b). Like in vertebrates, these results suggest that Wnt signaling is involved in the regulation of Delta/Notch signaling in spiders. It has been speculated that *Pt-Wnt8* might be responsible for establishing and maintaining the pool of posterior, undifferentiated SAZ cells and the specification of caudal ectoderm through repression of *Pt-twi* and activation of *Pt-cad* (McGregor et al., 2009). Summarising the results in *Parasteatoda*, the loss of *Pt-Delta* or *Pt-Wnt8* causes opisthosomal truncations in the most severe cases (McGregor et al., 2008b; Oda et al., 2007). Furthermore, it has been shown that both signaling pathways regulate the posterior determinant gene *Pt-cad* (McGregor et al., 2008b; Oda et al., 2007) (see fig. 8).

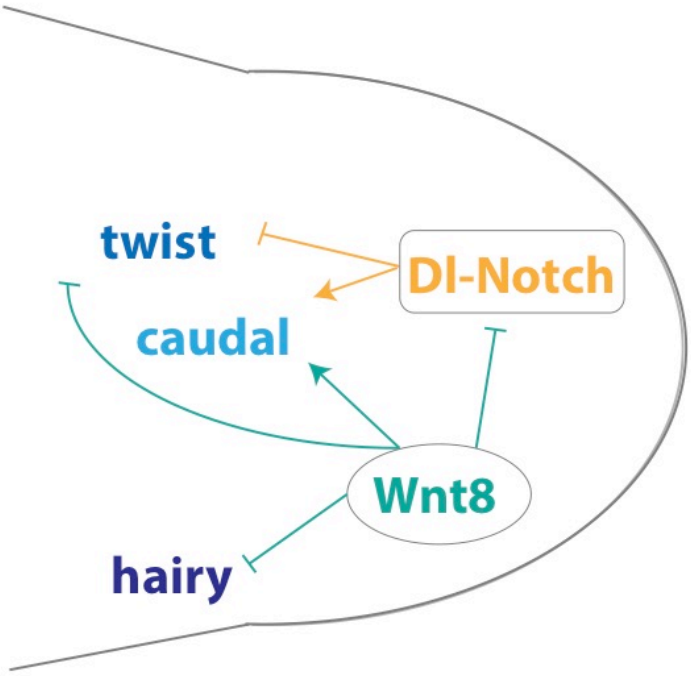

Figure 8 | Summary of the GRN of posterior segmentation in *Parasteatoda*. It has been shown in RNAi knockdown experiments that Delta and Notch activate (orange arrow) caudal and repress twist expression in the posterior of the SAZ (Oda et al., 2007). Further it could be shown that Wnt8 represses twist and hairy, but activates caudal (green arrow) expression in the spider (McGregor et al., 2008b).

Components of the Delta-Notch pathway have also been suggested to be involved in segmentation of the centipede *Strigamia maritima (Brena and Akam, 2013)*. Dynamic levels of gene expression have been described in the peri-proctodeal area, which resolve into stripes in the developing trunk segments for *Sm-eve2* and *Sm-Delta*. At the blastoderm stage oscillatory expression of those two genes arises from around the blastopore and later from two lateral patches at the forming proctodeum, suggesting that those structures embody the posterior signaling centre. A change in expression of those genes from oscillatory double segmental to static single segmental expression occurs in order to pattern the last trunk segments (Brena and Akam, 2013). In another study, *Sm-Delta* and *Sm-Notch* expression were observed over the course of segmentation in correlation with expression of the pair-rule gene homologues *Sm-eve* and *Sm-hairy*. It could be shown that the dynamic expression patterns for all genes investigated, correlated in terms of periodicity in the posterior. It was hence suggested, that the pair-rule genes examined, are regulated by Delta/Notch signaling during *Strigamia* segmentation, as it has been described in other arthropods (Chipman and Akam, 2008).

Taken together, the analysis of the regulation of the formation and function of the SAZ among several arthropods suggest that Wnt and Delta-Notch signaling regulated this process ancestrally, in a mechanism similar to the regulation of somitogenesis in vertebrates (Bolognesi et al., 2008; Chesebro et al., 2012; McGregor et al., 2008b; Oda et al., 2007; Stollewerk et al., 2003).

1.5. *Parasteatoda tepidariorum* as a model to study arthropod segmentation

1.5.1. Chelicerates

Chelicerates branch at the base of arthropods and therefore are the sister group to myriapods, crustaceans and hexapods (Giribet and Edgecombe, 2012; Giribet, 2005; Regier et al., 2010) (see fig. 9). The origin of chelicerates has been dated back to the Cambrian, over 500 million years ago using the fossil records and molecular data (Dunlop, 2010; Rota-Stabelli et al., 2013). The chelicerates can be divided into the euchelicerates and the pygnogonid sea spiders with both exhibiting a pair of chelicere and chelifore appendages, respectively (Dunlop and Arango, 2005; Weygoldt and Paulus, 1979) (see fig. 9).

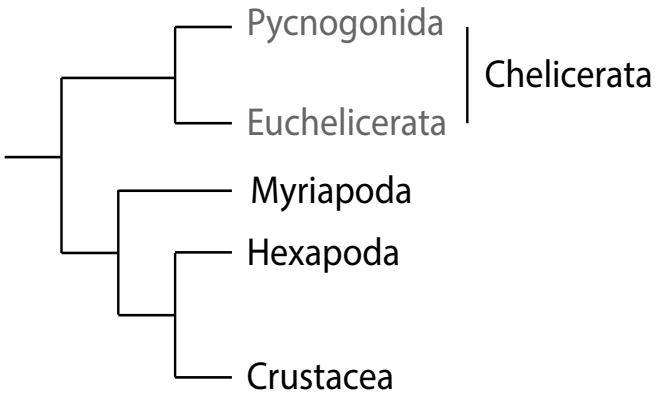

Figure 9 | Arthropod phylogeny. Within the arthropod phylogeny, chelicerates (pycnogonida and euchelicerata) branch at the base. Crustaceans and hexapods are the most derived groups and therefore at the top of the tree. The myriapods form a sister group to the insect/crustaceans clade. (Regier et al., 2010; Rota-Stabelli et al., 2011; Weygoldt and Paulus, 1979)

Owing to their phylogenetic position, chelicerates can contribute greatly to our understanding of ancestral arthropod features and providing a good reference

point for hypotheses about the molecular mechanisms of development and the body plan of the last common ancestor of bilateria (Schwager et al., 2015). The genomes of the two-spotted spider mite (*Tetranychus urticae*), a scorpion (*Mesobuthus martensii*), three spiders (*Stegodyphus mimosarum, Acanthoscurria geniculate, Parasteatoda tepidariorum*) and a horseshoe crab species (*Limulus polyphemus*) have been sequenced and analysed (Cao et al., 2013; Grbic et al., 2011; Nossa et al., 2014; Sanggaard et al., 2014 ; Schwager et al., 2016, in prep.). Interestingly, large variation in the genome sizes, as well as differences in the predicted gene content have been observed among chelicerate genomes. It has been suggested that events like whole genome duplications, for example in *Limulus* (Nossa et al., 2014), or extensive gene loss, as found in *Tetranychus* (Grbic et al., 2011), are responsible for this variation among chelicerate genomes.

1.5.2. *Parasteatoda* the model organism

The basal phylogenetic position of chelicerates among arthropods (Regier et al., 2010; Rota-Stabelli et al., 2011), as well as the well described embryonic development (Anderson, 1973; Kanayama et al., 2010; Mittmann and Wolff, 2012), and the availability of molecular tools, have made the common house spider *Parasteatoda tepidariorum* a powerful model organism in the field of evolutionary developmental biology (Hilbrant et al., 2012; McGregor et al., 2008a).

Parasteatoda is a cobweb making spider native to the neotropics, but is now a ubiquitous species. Females make cocoons containing up to 400 embryos

about every 5 days, all year around under laboratory conditions. Due to the short fertilization process, which takes about three minutes, embryos develop synchronously within one cocoon, which is particularly advantageous for developmental studies. Embryos of all embryonic stages can be fixed and used for in situ hybridisation and antibody staining to study mRNA and protein expression, respectively (Prpic et al., 2008a; Prpic et al., 2008c). Furthermore, gene function can be studied in *Parasteatoda* with RNA interference. Double-stranded RNA (dsRNA) injected into adult females results in the embryos in several cocoons exhibiting a knockdown effect (Prpic et al., 2008b). While injecting a single cell of an embryo at 16- and 32-cell stages with dsRNA generates clones of cells lacking gene function (Kanayama et al., 2010). Moreover the *Parasteatoda* genome has been sequenced in addition to transcriptomic resources (Posnien et al., 2014 , Schwager et al., in prep) and microRNA expression data (Leite et al., 2016).

1.5.3. *Parasteatoda* development

Upon fertilization, the first synchronized nuclear divisions take place in the center of the spherical egg. The energids start to migrate towards the periphery after about five divisions and cellularise at around the 16-cell stage (see fig. 10 A). Cells divide further and aggregate at one hemisphere to form the blastoderm (see fig. 10 A). The blastopore forms in the center of the germ disc upon gastrulation and invagination processes occur. After blastopore closure, the cumulus, a cluster of mesenchymal cells in the center of the germ disc, migrate underneath the ectodermal cell layer towards the rim of the germ

disc (see fig. 10). This process specifies the DV axis and initiates the transformation from a germ disc to a germ band (see fig. 10). The embryo then acquires a fan-like shape, whereby the caudal lobe forms from the central region of the previous germ disc. The sequential addition of opisthosomal segments from the posterior SAZ follows, and the nervous system and appendages begin to form along the AP axis (see fig. 10 A). At late stages of embryonic development, inversion occurs during which the embryo encloses the yolk and internal organs like the heart, digestive tract, and brain develop (see fig. 10 A). Embryonic development until hatching takes about 8 days and then it takes another 12 weeks for the spiderlings to develop to adulthood at 25 °C (Anderson, 1973; Kanayama et al., 2010; Mittmann and Wolff, 2012; Schwager et al., 2015) (see fig. 10 A, B).

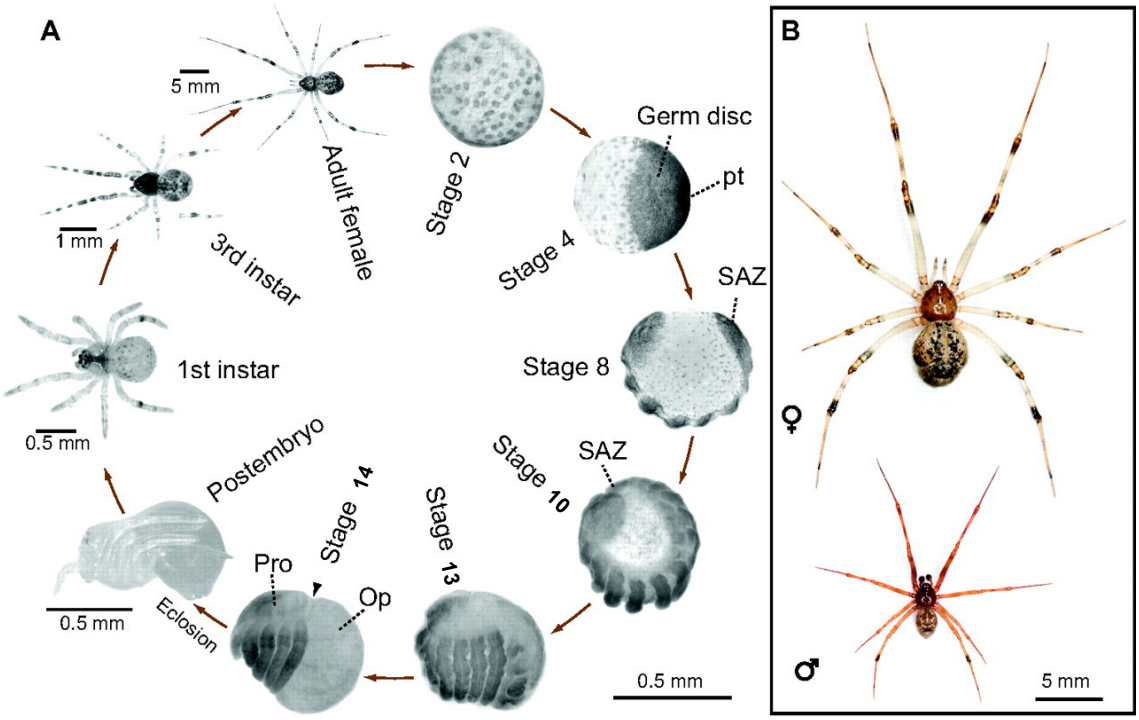

Figure 10 | *Parasteatoda* embryonic development. (A) At stage 2 cellularisation is complete and the germ disc including the primary thickening (pt) in the center forms at stage 4. At stage 8, the germ band with the segment addition zone (SAZ) has developed. At stage 10 the germ band has elongated and the limbs are becoming morphologically visible. Inversion occurs between stage 10 – 13, marked by the internalisation of yolk. At stage 14 the embryo is fully developed with a clear constriction (arrowhead) between prosoma (Pro) and opisthosoma (Op). After hatching the postembryo develops into the 1st instar, which exits the cocoon. The 3rd instar represents a free-foraging instar stage. **(B)** Adult female (♀) spider at the top, male (♂) adult spider at the bottom**.** Picture taken from (Hilbrant et al., 2012; Rota-Stabelli et al., 2011). Staging was carried out after (Mittmann and Wolff, 2012; Regier et al., 2010) and the picture was modified from (Hilbrant et al., 2012).

1.6. Aims of the thesis

Further investigating the GRN of posterior development in the basally branching arthropod *Parasteatoda tepidariorum* will not only help elucidate the mechanisms involved in regulating short germ segmentation in arthropods and the evolution of these processes in arthropods and other metazoans.

Therefore, I set out to address the following questions in my PhD thesis:

1. **Investigating the dynamic interactions of Delta-Notch and Wnt signaling in Parasteatoda**
    - Characterising the expression and role of the receptor *Pt-Notch*
    - Investigating the interactions between Delta/Notch and Wnt signaling
    - Investigating the *Pt*-Delta protein localisation using CRISPR

2. **Characterisation of downstream targets of Wnt and Delta-Notch signaling**

- Characterising the expression and role of *Pt-caudal*
- Analysing expression patterns of pair-rule orthologs

3. **Characterisation of the GRN underlying posterior segmentation**
    - Examining the effect of Delta-Notch and Wnt signaling on the downstream factors *Pt-eve and Pt-run-1*
    - Understanding the regulatory impact of *Pt-cad* on the pair-rule genes orthologue *Pt-eve and Pt-run-1*

- Investigating interactions between pair-rule gene orthologues in *Parasteatoda*

4. Analysis of Frizzled receptors in *Parasteatoda*

- Identification of Frizzled receptor genes
- Characterisation of the expression of Frizzled receptor genes during embryonic development

2. Materials & Methods

2.1. Spider culture, Embryo collection, fixation and staging

The spider culture at Oxford Brookes was initially founded with spiders from Göttingen (Germany). Adult spiders were kept separately in *Drosophila* vials (175 mm multipurpose container, Greiner) with coconut husk (generic from pet shop) and fed with banded crickets (size 2, Livefoods direct) twice a week. Mated females produce a cocoon every 3-5 days, whereby only up to 5 consecutive cocoons were taken from one female to ensure good quality of the embryos. The cocoons were collected daily and kept separately from the mother in petri dishes, with a piece of Whatman paper dampened with tap water to keep the spiderlings in a humid environment. Starting from a few days after hatching, the spiderlings were fed with vestigial flies twice a week. When the juvenile spiders reached the body size of about 5 mm, they were transferred to separate vials. The spider culture was kept at 25°C and embryos were fixed as described in Akiyama-Oda and Oda (2003). Embryos were staged according to Mittmann and Wolff (2012).

2.2. General molecular biology

2.2.1. RNA extraction and cDNA synthesis

Embryos of the stages 5 to 9 (see fig. 10) were collected and stored at -80°C. From a mix of those stages total RNA was extracted using the RNeasy Lipid Tissue Mini Kit (Qiagen). cDNA was synthesised from total RNA with the QuantiTect Reverse Transcription Kit (Qiagen).

2.2.2. PCR

Gene-specific cDNA fragments for in situ probe generation of dsRNA preparation were amplified with primers designed with Primer3 (http://primer3.ut.ee) using the One*Taq* 2x Master Mix (New England Biolab, NEB). The primers were only designed to cover a sequence of the coding region of the genes examined.

25 µl reaction mix	
forward primer (10 mM)	0.5 µl
reverse primer (10 mM)	0.5 µl
template DNA	variable
One*Taq* 2x MasterMix	12.5 µl
ddH_2O	to 25 µl

PCR program		
initial denaturation	94°C 30 s	
denaturation	94°C 30 s	x 35 cycles
annealing	45-68°C 30 s	
extension	68°C 1min/kb	
final extension	68°C 5 min	
final hold	10°C	

Parasteatoda Frizzled sequences are available from the Assembled Searchable Giant Arthropod Read Database ASGARD: *Pt-fz1* (Locus 7239), *Pt-fz2* (Locus 1), *Pt-fz 4-1* (Locus 7239) and *Pt-fz 4-2* (Locus 2608) (Zeng and Extavour, 2012). *Pt-Sfrp*, *Pt-cad*, *Pt-eve*, *Pt-Dl*, *Pt-run-1, Pt-odd, Pt-slp* and *Pt-opa* sequences were obtained from the *Parasteatoda* transcriptome (Posnien et al., 2014).

gene name	product size	forward primer	reverse primer	method
Pt-fz1	980 bp	CCCGAACATGGATTGGTGTG	CCTTCGGCACAATCCCAAAT	ISH
Pt-fz2	589 bp	TTCATCAGTTTTGGCCAT	ACCTTTGCTTCCTTCTGGATTGG	ISH
Pt-fz4-1	569 bp	GCTCCGTATGGACTGGCATCT	TTTCCTTTGCAGTTTCGGCTATT	ISH
Pt-fz4-2	721 bp	ATATTCTGAAGCCTCCGAGAGAA	TTCGGATCAGTACTATTACATTA	ISH
Pt-Sfrp	754 bp	GGTAGGAAAACTGTCGATCTGTG	TTGGCTTGAACAGATATGCACAT	ISH
Pt-eve	731 bp	GCAGGGTCTTCGAACTTCAG	GTTGGAAGAGTTGCGTCGTT	ISH, RNAi
Pt-cad	1005 bp	TGTTGATGGGAGATGGTTCC	AAAGCCCCTTTCGAAGATGT	ISH
Pt-cad F1	456 bp	ATGTATTCCCCTACAGCTAGAC	ATCGCTGGAAACTGCAACAATAG	RNAi
Pt-cad F2	429 bp	GGTATGAGTGGTACTGAATCACC	TCAGTAGATACTAATATTTGCTATATT TAGAG	RNAi
Pt-Wnt8	see (McGregor et al., 2008b)			ISH, RNAi
Pt-Dl	967 bp	ACAAACCACACGGCTTTTTC	GCTTGGTCAAGCAGTCATCA	ISH, RNAi
Pt-N F1	701 bp	TGCAGCACATTCGAGACATG	CCGAGCCATTGTCTTCATCG	ISH, RNAi
Pt-N F2	675 bp	GTTCTCCTGGGCTAATGGGT	TCTTCTGGTGATGAGCTGCA	RNAi
Pt-run-1	amplified with universal primers from a plasmid obtained from Wim Damen, University of Jena (Germany)			ISH
Pt-run-1 F1	741 bp	ATGCATTTACCAGCAGATTCAGTGA G	AACAGCGAGAGTGACATCCAAATTATA	RNAi
Pt-run-1 F2	792 bp	TCTCCAACATCTCAAGATTCATGTT C	TCAGTATGGCCTCCATAGACCT	RNAi
Pt-odd	912 bp	AGCTCCTCCAGTGATGTCGT	TTGTGGCAAATGTCACAGGT	ISH
Pt-opa	771 bp	CCACGTAAAGCATGCAACAA	TCGCTCTTTAAAGCACATATTCAC	ISH
Pt-twi	amplified with universal primers from a plasmid obtained from Wim Damen, University of Jena (Germany)			ISH
Pt-slp	901 bp	ATCCGCCAAAGTCCAGAAA	TCAATCCTTGGAAGTCCATCA	ISH

Table 1| Primer sequences for all gene used in in situ and dsRNA experiments. Gene name; size of the product generated with the respective primer pair; sequence of the forward and reverse primer in 5'-3' orientation; method (ISH, in situ hybridisation; RNAi, RNA interference) the fragment was used for. All primers were designed to cover a fragment of the coding region of the respective gene.

The PCR product was loaded on a 1% agarose gel and the specific band was purified from the gel using the NucleoSpin Gel and PCR Clean-up kit (Machery-Nagel).

2.2.3. Cloning

Subsequently, the PCR product was ligated into the TOPO PCR4 vector using the TOPO TA kit (cloning of *Taq*-polymerase amplified PCR products, Invitrogen), according to the manufacturers guidelines:

The ligation was transformed into OneShot TOP10 chemically competent cells (Invitrogen) according to the standard heat shock transformation protocol:

- TOP10 cells are thawed on ice
- 2 µl of the TOPO cloning reaction is added to the cells, mixed gently and incubated on ice for up to 30 min
- TOP10 cells are heat-shocked in a water bath at 42°C for 30 sec and immediately transferred to ice
- 250 µl S.O.C. medium (Invitrogen) is added and incubated in a shaking incubator at 200 rpm, at 37 °C for 1 hour
- 50 µl of the transformed cells were plated on Lennox Broth (LB) plates with ampicillin (100 µg/ml) and incubated at 37 ° C over night

2.2.4. Colony PCR and overnight cultures

Colonies were then picked for PCR using the One*Taq* 2x Master Mix (NEB) and plated and numbered on a Lennox Broth (LB) plates with ampicillin (100 µg/ml), to track the colonies. The PCR product was loaded on a 1% agarose gel and checked for the correct product size. Colonies with the correct insert size were grown in 5 ml liquid LB cultures with ampicillin (100 µg/ml) at 37 °C in a shaking incubator over night.

Plasmid mini preparations were made from the liquid cultures using the EZNA Plasmid Mini Kit I (VWR) according to the manufacturers guidelines and verified with Sanger sequencing (Eurofins).

reaction mix		
PCR product	0.5 – 4 µl	mix the reaction gently and incubate at room temperature for 5 minutes
salt solution	1 µl	
water	up to 5 µl	
TOPO vector	1 µl	

2.2.5. Sequencing

Plasmids and PCR products were sequenced with the value-read service of Eurofins Genomics (Germany). Alignments of sequences and *in silico* design of constructs were done in SnapGene Version 2.8.

2.2.6. In situ probe synthesis

RNA probes were labelled with Digoxigenin (DIG; Roche) and detected with an alkaline phosphatase conjugated anti-DIG antibody (Fab fragments, Roche) using the substrate nitro blue tetrazolium/5-bromo-4-chloro-3-indolyl-phosphate (NBT/BCIP) (Roche), resulting in purple/blue staining.

For double in situ hybridisation, the second probe was labelled with fluorescein (Roche) and detected with an alkaline phosphatase conjugated anti-fluorescein antibody (Fab fragments, Roche) and INT (2-[4-iodophenyl]-3-[4-nitrophenyl]-5-phenyltetrazolium chloride)/BCIP (Roche), resulting in orange staining.

2.3. In situ hybridisation protocol

In situ hybridisations were carried out according to the whole-mount protocol for spiders (Prpic et al., 2008d) with minor modifications. In order to decrease the background in the staining reaction, the anti-DIG and anti-fluorescein antibodies were pre-absorbed over night at 4°C with stage 6 to 8.2 embryos. Note that in situ hybridisation staining reactions on control and experimental (RNAi) embryos were carried out for the same time. For double in situ

hybridisations, the first staining reaction was stopped by incubating the samples for 15 minutes at 65°C with inactivation buffer (50 ml hybridisation buffer B, 0.1 ml 10% Tween-20, 1.5 ml 10% SDS). The embryos were then washed twice with PBS-T for 15 minutes and twice for 20 minutes. Subsequently, the embryos were incubated in blocking solution for 30 minutes and then with the anti-Fluorescein antibody at a dilution of 1:2000 in blocking solution (Roche) for 3 hours. Nuclear staining was performed by incubation of embryos in 1 µg/ml 4-6-diamidino-2-phenylindol (DAPI) in PBS with 0.1% Tween-20 for 30 minutes and subsequently washed with PBS-T with 0.1% Tween-20 twice for 5 minutes.

2.4. RNAi interference

2.4.1. Double stranded RNA preparation

To generate double stranded RNA (dsRNA), PCR fragments (for primer sequences and fragment sizes see table 1) of the coding regions were amplified from plasmids using universal primers, which both contain a 5' T7 promoter binding site (Fwd T7 5'-TAA TAC GAC TCA CTA TAG GG-3',
Rev T7/T3 5'-TAA TAC GAC TCA CTA TAG GGA ATT AAC CCT CAC TAA AGG GA-3'). The introduction of the T7 promoter sequence on the antisense strand, using the Rev T7/T3 primer, allows the *in vitro* transcription of both strands in one reaction.

The PCR was carried out as described in chapter 2.2.2. and the PCR product was purified from a 1% agarose gel using the NucleoSpin Gel and PCR Clean-up kit (Machery-Nagel).

PCR products were used as templates for *in vitro* reverse transcription of both strands with the MegaScript T7 transcription kit (Invitrogen) according to the manufacturers guidelines. dsRNA was then generated by annealing the transcripts in a water bath starting at 95°C, and then slowly cooled down to room temperature. The dsRNA was then adjusted to a concentration of 1.5 to 2.0 µg/µl for injections.

2.4.2. Parental RNAi (pRNAi)

For each gene, at least three adult female spiders were injected according to the protocol by Akiyama-Oda and Oda (2006). 2 µl dsRNA was injected into the opisthosoma of spiders at concentrations of 1.5-2.0 µg/µl every two to three days up to a total of five injections. The injected spiders were mated after the second injection. Embryos from injected spiders were fixed for gene expression and phenotypic analyses two and four days after egg laying approximating to stages 6 to 9.2. Embryos from GFP injected control females were generated and treated as described above.

2.4.3. Embryonic RNAi (eRNAi)

Embryonic injections were carried out as described in Kanayama et al. (2010) with minor changes (GC100F-10 capillaries, Harvard Apparatus; needle puller PC-10, Narishige or Femtotip II sterile injection capillary 0.5 µm, Eppendorf). Embryos were injected at the 8 or 16 cell stage with an injection mix composed of 10 µl Fluorescein isothiocyanate (FITC)-dextran (2 µg/µl, MW 10 000, Sigma), 10ul Biotin-dextran (2 µg/µl, MW 10 000, Sigma) and 5 µl

dsRNA (1.5 to 2.0 µg/µl) and fixed when they reached developmental stages 6 or 7. In order to visualise the clones of eRNAi cells, the co-injected Biotin-dextran was detected with the Vectastain ABC-AP kit, which was carried out according to the manufacturers protocol (Vector Laboratories) following the *in situ* hybridisation. At least 200 embryos were injected for each gene of interest to ensure that multiple independent clones were generated in the SAZ.

2.5. Synthesis and overexpression of capped mRNA

The pSP64-*cad*-eGFP-PolyA plasmid was generated by Christian Bonatto Paese. In order to synthesise capped mRNA, the pSP64-*cad*-eGFP-PolyA plasmid was linearized with *Nhe*I (Promega) according to the manufacturers protocol, the respective band cut from a 1% agarose gel and purified using the NucleoSpin Gel and PCR Clean-up kit (Machery-Nagel). The linearized plasmid was used as a template for the SP6 transcription reaction with mMESSAGE mMACHINE® SP6 Transcription Kit (Ambion™) following the manufacturer's instructions. Capped mRNAs was injected as described by Kanayama et al., 2010 .

2.6. CRISPR construct generation for the C-terminal tagging of *Pt-Dl*

The CRISPR/Cas9 system can be used to either introduce mutations through error-prone non-homologous end joining (NHEJ) or to insert a sequence of interest at a specific locus through homologous recombination (HR) (Baena-

Lopez et al., 2013; Bassett et al., 2013; Gratz et al., 2014). In order to introduce double strand breaks (DSB) at a given locus in the genome, a synthetic guide RNA (sgRNA) binds the Cas9 endonuclease and directs the complex to the target sequence through complementary base pairing. The sgRNA contains the complementary target sequence of about 20 nucleotides at the 5' end, followed by a protospacer adjacent motiv (PAM), which is necessary for the Cas9 endonuclease activity and a loop structure at the 3' end for the recognition by the Cas9 (see fig. 11).

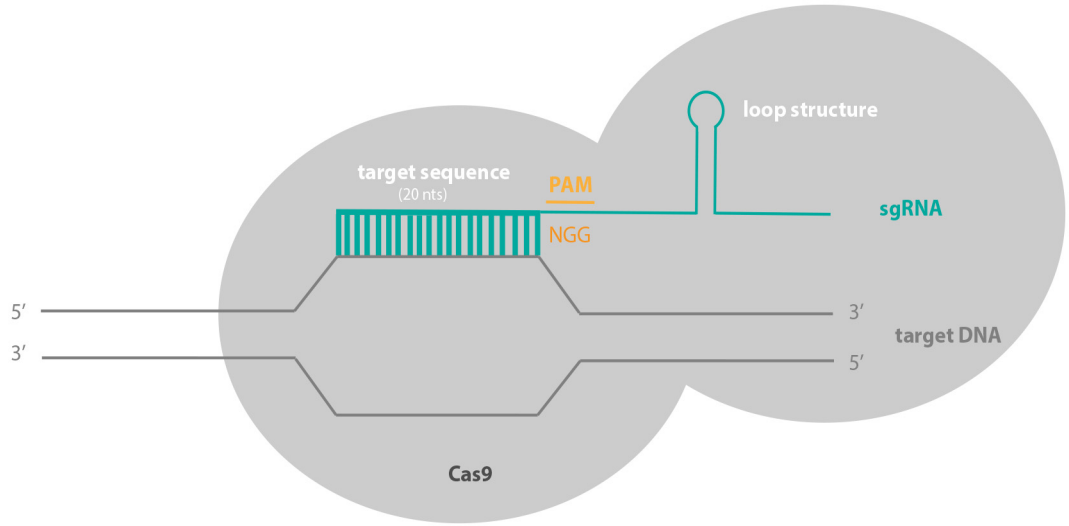

Figure 11 | The Cas9 complex. The sgRNA contains the 20 nucleotide long target sequence, followed by the PAM sequence (NGG). The loop structure at the 3' end of the sgRNA is responsible for the incorporation into the Cas9 complex.

For the C-terminal tagging of *Pt*-Delta, the 3' and 5' homology arm (3'HA, 5'HA) were cloned into the multiple cloning sites (MCS) of the pHD-dsRed plasmid, which contains the fluorescent marker cassette dsRed (*Discosoma sp.* red fluorescent protein) and the translation termination signal SV40 (simian vacuolating virus 40) (see fig. 12). The pHD-dsRed plasmid was gifted to Pedro Gaspar.

The 5' homology arm (HA) contains 1 kb upstream of the *Pt-Dl* stop codon (*Pt-Dl* coding sequence, excluding the stop codon TAA) and the 3'HA contains 1 kb of the intergenic region (no Augustus gene prediction) upstream of the *Pt-Dl* coding region (see fig. 12).

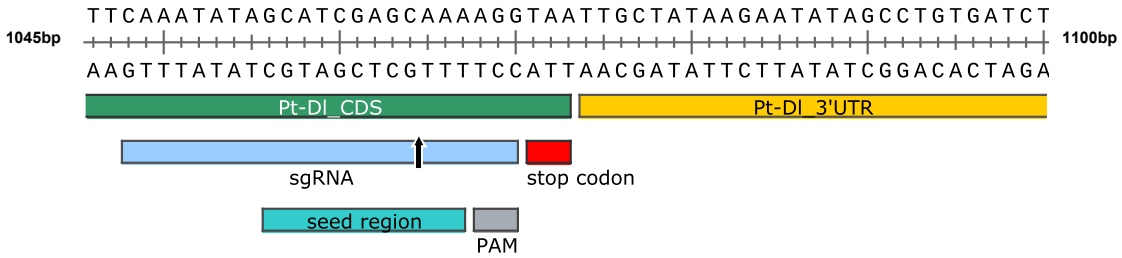

Figure 12 | sgRNA priming site. 55bp region of the 5'homology arm region (Pt-Dl CDS, Pt-Dl 3'UTR containing the sgRNA priming site (sgRNA, blue bar). The Cas9 cut site is located 3 bases upstream of the PAM sequence (grey bat), indicated by a black arrow. The endogenous Pt-Dl stop codon (TAA) is marked with a red bar. The seed region (turquoise bar) is crucial for the recognition by the sgRNA and must not contain PCR amplification errors.

To generate the C-terminal fusion of *Pt-Dl* with the dsRed cassette, a 314 bp region between the MCS for the 5'HA and the dsRed cassette had to be excised from the original plasmid and an AarI recognition site was inserted 5' of the dsRed cassette. Primers were designed to amplify the vector backbone from the 3' end of the MCS of the 5'HA (pHD_dsRed_3'HA_AarI_fwd: CACGCACCTGCAATTGCCGCGATGGCCTCCTCCGAGGACGTCA, pHD_dsRed_3'HA_AarI_rev: TGCATATGTCCGCGGCCGCTAG) up to the start of the dsRed cassette, including the AarI recognition sequence. Two non-polar amino acids (Alanin, GCC/GCG) were added between the AarI site and the dsRed start codon, to maintain the reading frame.

The vector backbone was amplified from the original plasmid using the Q5 High Fidelity DNA Polymerase, according to the protocol (NEB).

25 µl reaction mix	
5X Q5 Reaction Buffer	5 µl
10 µM dNTPs	0.5 µl
forward primer (10 µM)	1.25 µl
reverse primer (10 µM)	1.25 µl
template DNA	variable
Q5 High-Fidelity DNA Polymerase	0.5 µl
ddH_2O	to 25 µl

PCR program		
initial denaturation	98°C 30 s	
denaturation	98°C 30 s	x 35 cycles
annealing	50-72°C 30 s	
extension	72°C 20-30 sec/kb	
final extension	72°C 2 min	
final hold	10°C	

The PCR product was loaded on a 1% agarose gel and the specific band was purified from the gel using the NucleoSpin Gel and PCR Clean-up kit (Machery-Nagel).

2.6.1. Q5 Site-directed mutagenesis

The purified PCR product was treated with the Kinase-Ligase-DpnI enzyme mix according to the manufacturers protocol (Q5 Site-directed Mutagenesis Kit, NEB), to eliminate possible contamination with the template plasmid and circularisation of the PCR product at room temperature. Subsequently, the circularized product was transformed into chemically competent TOP10 cells (Invitrogen) according to the standard heat shock transformation protocol

(also see chapter 2.2.3), plated on LB plates with ampicillin (100 µg/ml) and incubated at 37 °C over night.

Following, colony PCR was carried out and liquid cultures of positive clones were generated (see chapter 2.2.4). Plasmid preparations were performed and sent for Sanger sequencing (see chapter 2.2.5).

To enable the insertion of the 3' and 5'HA, primers were designed containing the specific and the restriction enzyme recognition sequence:

3'HA_SapI_fwd: CACGGCTCTTCCTATttgctataagaatatagcctgtgatctag,

3'HA_SapI_rev: CACGGCTCTTCGGACtacggtgatttttggatttaaaatcaagg,

5'HA_AarI_fwd: CACGCACCTGCCACATCGCcaatccctgccttaatgg,

5'HA_AarI_rev: CACGCACCTGCGTGTCGGCccttttgctcgatgctatatttga

The 3' and 5'HA regions were amplified from genomic DNA (obtained from Daniel Leite) with the Q5 High Fidelity DNA polymerase (NEB) and purified using the NucleoSpin Gel and PCR Clean-up kit (Machery-Nagel). Subsequently, the mutagenized pHD-dsRed plasmid (introduced AarI sites) and the 5' HA fragment were digested with AarI (ThermoFisher) according to the manufacturers protocol at 37 °C for 4 hours. The 5' HA fragment was purified with the NucleoSpin Gel and PCR Clean-up kit (Machery-Nagel). Afterwards, the 5' HA fragment was ligated into the digested pHD-dsRed plasmid with the T4 DNA Ligase system (Promega) according to the manufacturers protocol at 15°C over night (see fig. 13). The ligated product was transformed into chemically competent TOP10 cells (Invitrogen) according to the standard heat shock transformation protocol, plated on

Lennox Broth (LB) plates with ampicillin (100 µg/ml) and incubated at 37 °C over night.

Afterwards colony PCR was performed and positive colonies cultured in 5ml liquid LB cultures with ampicillin (100 µg/ml) at 37 °C in a shaking incubator over night. Plasmid mine preparations were made from the liquid cultures using the EZNA Plasmid Mini Kit I (VWR) and verified with Sanger sequencing. The protocol for restriction and ligation was repeated for the 3'HA (see fig. 13). The final plasmid was verified with Sanger Sequencing and the LB cultures were used to prepare a glycerol stock for long-term storage at -80°C.

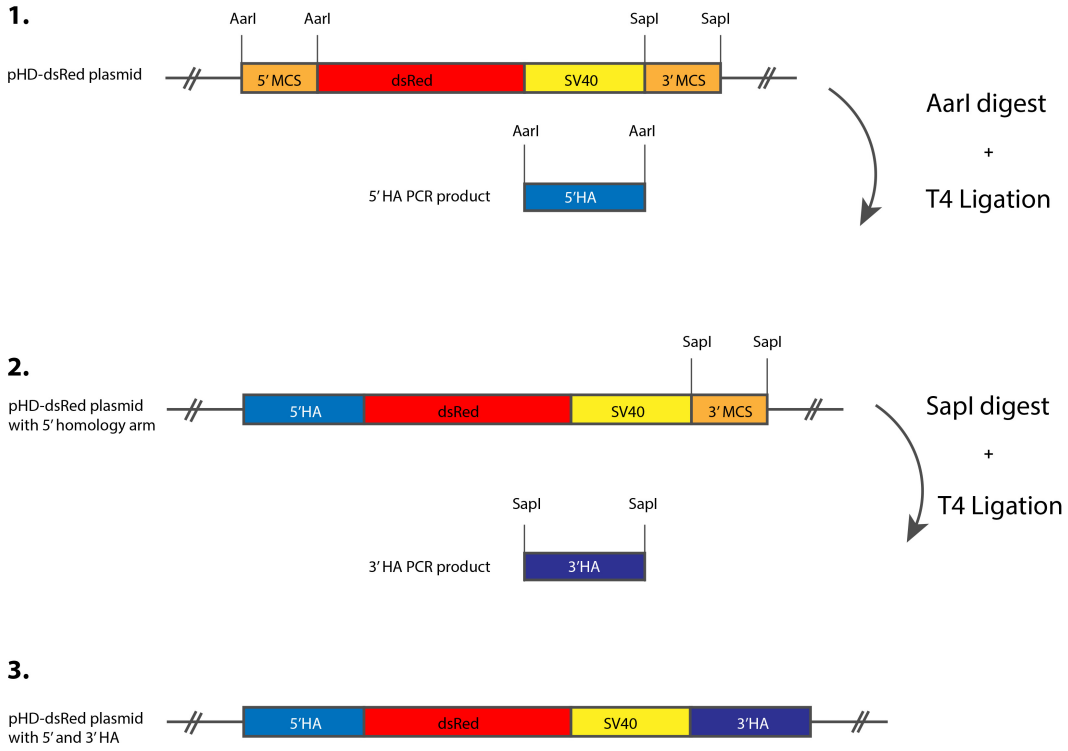

Figure 13 | Cloning of the 5' and 3' homology arms (5'/3'HA). The pHD-dsRed plasmid contains a 5' multiple cloning site (MCS) flanked by AarI restriction sites (light blue), followed by the dsRed (red) and SV40 (yellow) cassette, adjacent to a 3' MCS flanked with SapI sites (orange). The 5'HA PCR product (light blue) contains AarI restriction cut sites at the 5' and 3' end. First, the plasmid and the 5'HA PCR product were digested with AarI, respectively and then ligated with the T4 ligase (1). In the second step, the newly generated plasmid and the 3'HA PCR product (light blue) were digested with SapI and further ligated with the T4 ligase (2). The obtained plasmid comprises the 5'HA, in frame with dsRed and SV40 and the 3'HA (3).

2.6.2. Short guide RNA (sgRNA) design and synthesis

The sgRNA guides the Cas9 endonuclease to the region of interest and the precise cut site is determined by the PAM sequence (NGG). The forward primer, containing the cut site close to the stop codon and the PAM sequence, for the amplification of the *Pt-Dl*-sgRNA, were predicted using the online tool http://crispr.mit.edu. In order to synthesise the sgRNA with a T7 polymerase *in vitro* transcription reaction, a T7 promoter sequence was added 5' of the gene specific sequence. 3' of the gene specific sequence, an overlap with the sgRNA reverse primer was added (5' GAAATTAATACGACTCACTATAGGN$_{18\text{-}20nt\ gene\ specific\ sequence}$**GTTTTAGAGCTAGAAATAGC 3';** the font indicates the overlapping region with the sgRNA reverse primer). The sgRNA reverse primer (sgRNA_rev AAAAGCACCGACTCGGTGCCACTTTTTCAAGTTGATAACGG ACTAGCCTTATTTTAACTT**GCTATTTCTAGCTCTAAAAC**; the bold part of the sequence indicates the overlapping region with the sgRNA forward primer) is a universal primer, containing the stem loop structure for the incorporation of the sgRNA into the Cas9 complex.

The *Pt-Dl*-sgRNA template was amplified using the Phusion polymerase (NEB) as follows:

reaction mix

ddH_2O	67 µl
5x HF buffer	20 µl
10 µM dNTPs	2 µl
Phusion DNA polymerase	1 µl
sgRNA_fwd primer (10 µM)	5 µl
sgRNA_rev primer (10 µM)	5 µl
	100 µl

PCR program

98°C 30 s
98°C 10 s
60°C 30 s } x 35 cycles
72°C 15 s
72°C 10 min
4°C hold

The PCR product was purified with the NucleoSpin Gel and PCR Clean-up kit (Machery-Nagel) purification kit and eluted in 30ml elution buffer. The PCR product was used as a template for *in vitro* transcription with the T7 MegaScript kit (Invitrogen, Life Technologies), according to the manufacturers protocol.

reaction mix

6 µl nuclease free water	incubate at 37°C for 4h
2 µl ATP (75 mM)	
2 µl CTP (75 mM)	
2 µl GTP (75 mM)	
2 µl UTP (75 mM)	
2 µl 10x reaction buffer	
2 µl PCR product (150 ng/ml)	
2 µl l enzyme mix (T7)	
20 µl	

The reaction was incubated with 1µl TurboDNAse (included in the kit) at 37°C for 15 minutes. To stop the reaction 115µl nuclease free water and 15µl ammonium acetate stop solution were added.

The sgRNA was precipitated by adding 150µl phenol:chloroform:isoamyl alcohol (24:24:1), pH 7 and vortexing thoroughly for 30 seconds. After a spin cycle of 10000 g for 3 minutes at room temperature, the upper layer was transferred into a fresh tube and precipitated with 150µl isopropanol at -20°C for at least 15 minutes. After another spin cycle at 17000 g for at least 15 minutes at 4°C, the supernatant was discarded and the RNA pellet was washed with 500µl ethanol. The ethanol wash was repeated, the pellet dried briefly and resuspended in 30µl ddH_2O. The sgRNA was run on a gel and the concentration measured on a NanoVue spectrophotometer (GE lifesciences).

2.6.3. CRISPR injection protocol

The guidelines for the preparation of the CRISPR injection mix were obtained from Andrew Bassett (University of Oxford). The sgRNA, the Cas9 protein (also gifted from Andrew Bassett) and the donor plasmid were assembled as follows:

	volume	final concentration
water	15 ul	
10x buffer	2 ul	1x
~1 ug/ul Cas9	1 ul	50 ng/ul
0.5 ug/ul sgRNA	1 ul	25 ng/ul

10x buffer

200 mM	HEPES pH 7.5	200 ul (1 M)
1000 mM	KCl	500 ul (2 M)
25 mM	MgCl2	12.5 ul (2 M)
5%	glycerol	100 ul (50%)
1 mM	EDTA	2 ul (0.5 M)
5 mM	DTT	50 ul (0.1 M)
	Water	135.5 ul
		1 ml

The injection mix was pre-incubate at 37°C for 10 min. Afterwards the donor plasmid was added at a concentration of 500 ng/ul DNA.

2.7. Data documentation

Embryos were imaged using a Leica fluorescence stereomicroscope equipped with a Jenoptik ProgRes C3 digital camera. Brightfield and UV channel images were merged using Adobe Photoshop CS6, which was also used for linear corrections of brightness, contrast, and colour values. Images for the *Pt-cad* overexpression experiment were taken with a Zeiss Axio Zoom V16 stereomicroscope, equipped with an Axiocam 506 monoand a colour digital camera.

2.8. Protein sequence alignments

Blastp (www.blast.ncbi.nlm.nih.gov) was used to identify sequence conservation with the Pt-Eve homeodomain and Pt-Sfrp frizzled-like CRD domain. Species with the highest conservation were aligned manually.

2.9. Phylogenetic analysis

The nucleotide sequences of all species included were obtained from NCBI (http://www.ncbi.nlm.nih.gov). The phylogentic analysis was carried out using the "one click" method of the online tool "*Phylogeny.fr: robust phylogenetic analysis for the non-specialist" (Dereeper et al., 2008).* The program uses MUSCLE for the sequence alignment (Edgar, 2004), GBlocks for sequence curation (Castresana, 2000), PhylML for the maximum-likelihood phylogeny analysis (Guindon et al., 2010) and the TreeDyn software for the graphical output (Chevenet et al., 2006).

3 Results Chapter 1: Dynamic interactions between *Pt-Dl, Pt-N* and *Pt-Wnt8* regulate posterior segmentation in *Parasteatoda*

It has been shown previously that both Wnt and Delta-Notch signaling are crucial for the formation of the SAZ and the sequential formation of segments from this tissue in *Parasteatoda* (McGregor et al., 2008b; Oda et al., 2007). Indeed, it is likely that this involves interplay between these two pathways, because it was shown that in *Pt-Wnt8* RNAi knockdown embryos *Pt-Dl* expression is established normally, but subsequently fails to clear and persists in the posterior (McGregor et al., 2008b). This suggests that *Pt-Wnt8* is necessary for dynamic *Pt-Dl* expression. However, it is unclear if *Pt-Dl* also regulates *Pt-Wnt8*. Therefore I investigated the expression, roles and interactions between Delta-Notch and *Wnt8* signaling during posterior development in *Parasteatoda* in more detail.

3.1 The role of *Pt-Dl* in posterior development in *Parasteatoda*

As previously reported, *Pt-Dl* expression commences early in embryonic development at mid stage 4 in a few ectoderm cells around the rim of the germ disc and then in future mesodermal cells in the centre of the germ disc at a slightly later stage (Oda et al., 2007). During stage 6, after *Pt-Dl* expression has cleared from posterior SAZ cells, this gene is expressed in a salt and pepper pattern adjacent to a more diffuse posterior domain in anterior SAZ cells (Oda

et al., 2007) (see fig. 14 A). In contrast, *Pt-Wnt8* expression is weaker in anterior SAZ cells, where it overlaps with *Pt-Dl* expression, compared to the stronger expression of *Pt-Wnt8* detected in posterior SAZ cells (see fig. 14 B). Although this aspect of *Pt-Wnt8* expression was noticed previously, it was suggested it might be a gradient in expression rather than a domain of where *Pt-Wnt8* expression is specifically down regulated (McGregor et al., 2008b).

To investigate the role of *Pt-Dl* further, I knocked down the expression of this gene using pRNAi. This treatment resulted in the loss of *Pt-Wnt8* expression in the posterior of the SAZ, but conversely gave rise to stronger *Pt-Wnt8* expression in anterior SAZ cells (see fig. 14 C). This suggests that *Pt-Dl* is required to activate *Pt-Wnt8* expression in posterior SAZ cells but then when *Pt-Dl* expression reaches the anterior SAZ cells it is involved in down-regulating *Pt-Wnt8* possibly to facilitate the formation of segments from this tissue.

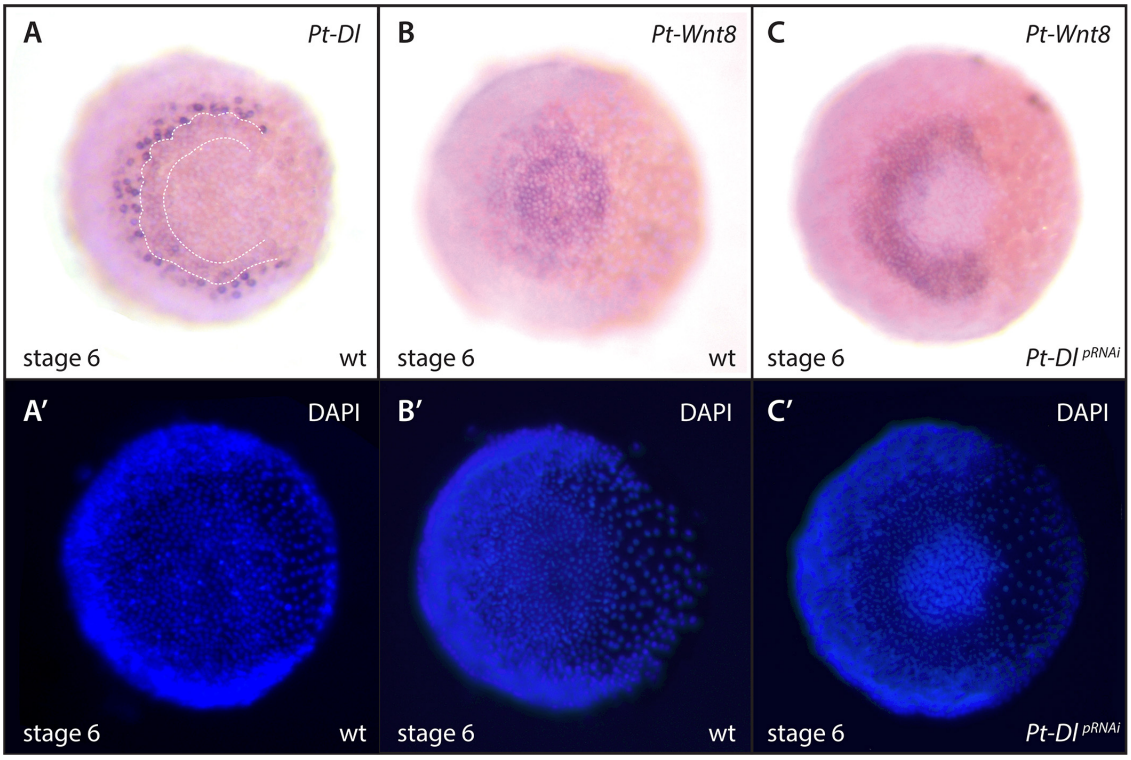

Fig.14 | The effect of *Pt-Dl* on *Pt-Wnt8*. Whole mount stage 6 embryos, ventral view **(A-C)**. Panels **A-C** show bright field images and **A'-C'** show fluorescent images with the nuclear staining DAPI of the same embryo, respectively. In wild-type embryos at stage 6, *Pt-Dl* is expressed as a salt and pepper pattern next to a more diffuse domain (indicated by dashed lines) in anterior SAZ cells (**A**). At stage 6, *Pt-Wnt8* is strongly expressed in posterior SAZ cells (**B**). Expression of this gene is comparatively weaker in anterior SAZ cells where *Pt-Dl* is expressed at this stage. *Pt-Wnt8* is also expressed in a cell row at the anterior of the germ band. (**B**). In *Pt-Dl* pRNAi embryos at stage 6, *Pt-Wnt8* expression is lost in posterior SAZ cells but this gene is conversely expressed more strongly in anterior SAZ cells compared to wild-type (**C**).

3.2 The role of *Pt-N* in posterior development in *Parasteatoda*

To study Delta-Notch signaling in posterior development in *Parasteatoda* further, I then characterised the expression of *Pt-N* in the embryos of this spider. The expression of *Pt-N* commences at stage 5 in a two to three cell wide band around the germ disc (see fig. 15 A). Slightly later, a second ring of *Pt-N* expression appears more centrally (data not shown). After the dorsal opening and the formation of the germ band at stage 6, diffuse expression appears in

the posterior SAZ (see fig. 15 B). The posterior SAZ expression then becomes stronger and the anterior domain forms a broad band at stage 7 (see fig. 15 C). *Pt-Delta,* as well as *Pt-Notch* expression commence at the rim of the germ disc at a similar stage (around stage 5) (see fig. 15 A, Oda et al., 2007). *Pt-Delta* initially clears from the posterior at stage 6, however, *Pt-N* is expressed diffusely in the whole SAZ area at stage 6 and 7 (see fig. 15 B, C). Furthermore, *Pt-Delta* and *Pt-N* expression resolve into anterior stripes, although the *Pt-N* stripe appears uniform, whereas *Pt-Delta* expression displays a diffuse stripe adjacent to a more anterior stripe that has a salt and pepper pattern (see fig. 14 A, fig 15 B, C).

It has been reported previously that pRNAi against *Pt-N* has a similar effect to the knockdown of *Pt-Dl* in early *Parasteatoda* embryos and that the expression of *Pt-Dl* is disrupted in *Pt-N* RNAi embryos (Oda et al., 2007). Therefore, I next tested if *Pt-N* expression was reciprocally regulated by *Pt-Dl*. pRNAi against *Pt-Dl* leads to the loss of *Pt-N* expression in the anterior but stronger *Pt-N* expression in the posterior SAZ (see fig. 15 D). Thus the RNAi results suggest that *Pt-N* might inhibit *Pt-Delta* in posterior cells and activate its expression in the anterior of the SAZ, reminiscent of the effect of *Pt-Dl* on *Pt-Wnt8* (see fig. 14).

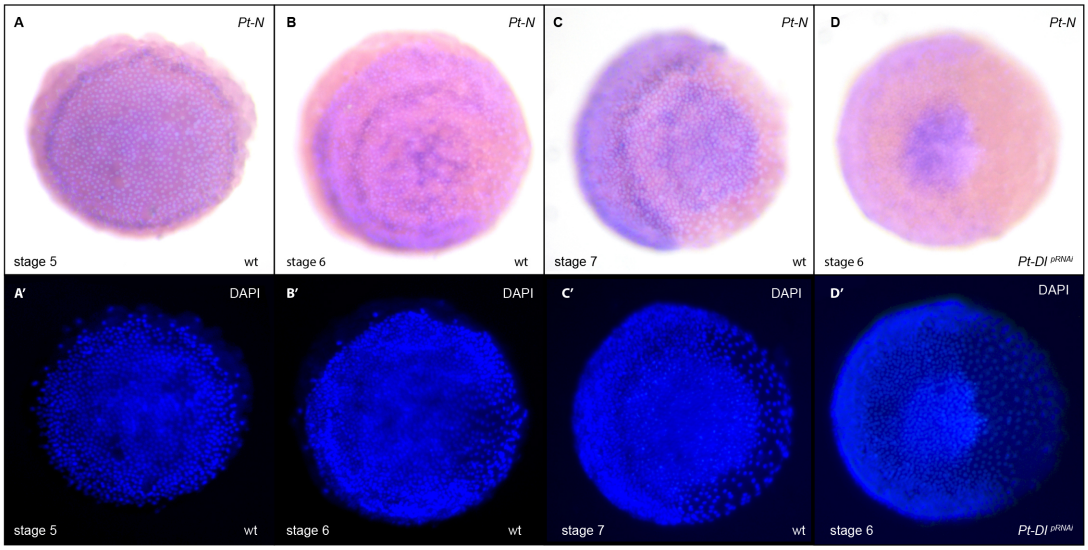

Figure 15 | *Pt-N* expression and the effect of *Pt-Dl* on *Pt-N*. In wild-type embryos *Pt-N* is expressed in a 2-3 cells wide band around the rim of the germ disc at stage 5 (**A**). At stage 6, *Pt-N* is expressed in a salt and pepper pattern in the posterior and in a stripe domain in the anterior SAZ (**B**). Later at stage 7, *Pt-N* is expressed in the posterior SAZ and in a broad domain in the anterior portion of the germ band (**C**). Expression of *Pt-N* is lost in the anterior and is strongly expressed in the posterior SAZ in *Pt-Dl* parental RNAi embryos at that stage (**D**). Images **A'-D'**; show fluorescent staining with the nuclear marker DAPI of the respective bright field images **A-D**. **A** shows a germ disc stage embryo, panels B-D show posterior views of whole mount embryo with ventral oriented to the left.

To determine if *Pt-Wnt8* is also regulated by *Pt-N*, I next examined *Pt-Wnt8* expression in *Pt-N* pRNAi embryos. I found that *Pt-Wnt8* also requires *Pt-N* (see fig. 14 B), reminiscent of the effect of *Pt-Dl* on *Pt-Wnt8* expression (see fig. 16 C). More precisely, *Pt-Wnt8* expression is restricted to an area in the posterior where the cell number is increased as a consequence of the *Pt-N* knockdown (Oda et al., 2007). These findings confirm that Delta-Notch signaling is necessary to first activate *Pt-Wnt8* expression in posterior SAZ cells during stage 5, but subsequently down-regulates *Pt-Wnt8* in anterior SAZ cells, possibly to facilitate the formation of segments from this tissue (see fig 15 and fig. 16).

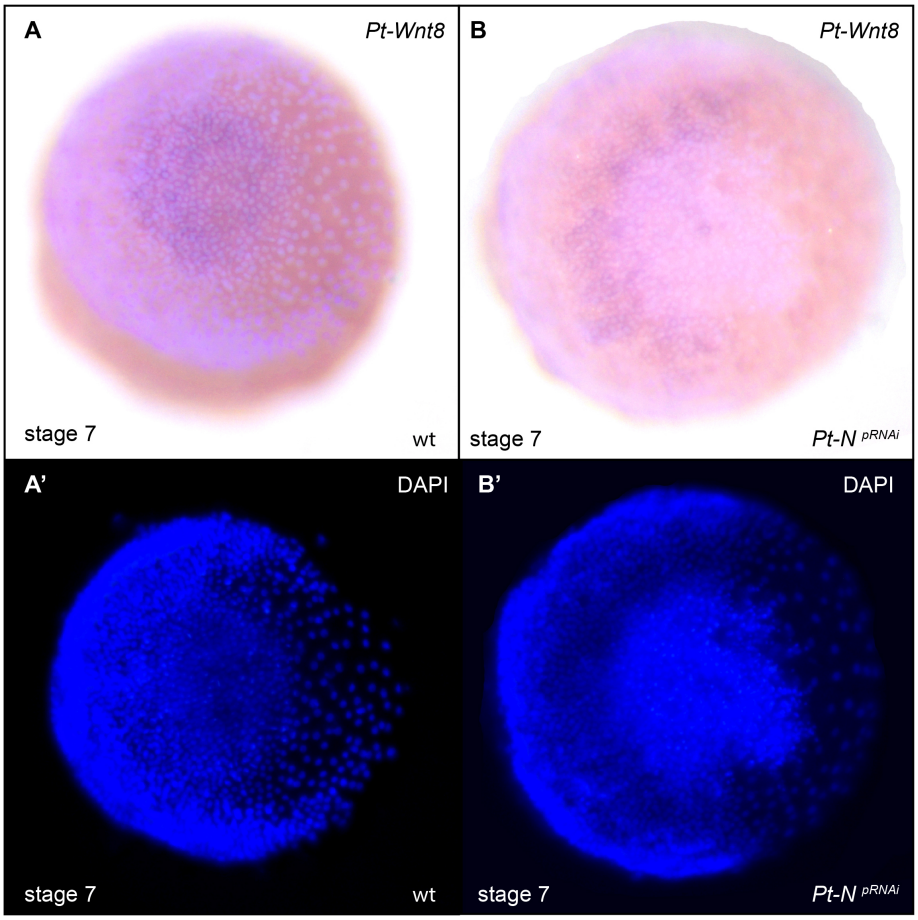

Fig.16 | *Pt-N* regulates *Pt-Wnt8* expression. In wild-type embryos at stage 7, *Pt-Wnt8* is expressed in the posterior SAZ cells and more weakly in the anterior SAZ cells (**A**). Expression of *Pt-Wnt8* is lost in the posterior, but is expressed more highly in the anterior SAZ in *Pt-N* parental RNAi embryos at that stage (**B**). Images **A'-B**; show the fluorescent staining with the nuclear marker DAPI of the respective bright field images **A, B**. All panels show posterior views of whole mount embryos with ventral oriented to the left.

3.3 Investigating *Pt-Dl* protein localisation *in vivo* using CRISPR

Many previous studies examined the function and interactions of components regulating segmentation in arthropods only at the mRNA level (Chesebro et al., 2012; Chipman and Akam, 2008; Choe et al., 2006; McGregor et al., 2008b; Pueyo et al., 2008; Sarrazin et al., 2012; Stollewerk et al., 2003). However, expression pattern analysis and RNAi knockdown entail the caveat that they

might not convey a complete picture, because the expression levels and the location of the protein is likely to make a significant contribution to our understanding of gene function and the underlying molecular mechanisms (Gilles and Averof, 2014). Thus, it was an objective of this thesis to try to establish a different experimental approach to investigate the localization of GRN proteins that appear to exhibit dynamic expression throughout posterior development in *Parasteatoda*. In particular, *Pt*-Dl represents an interesting candidate for this study because its expression changes in association with the formation of posterior segments in the spider (Oda et al., 2007).

The Clustered Regular Interspersed Repeats / Caspase9 (CRISPR/Cas9) - genome editing method utilises modified components of a bacterial defence mechanism to introduce nucleotide specific double strand breaks (Bassett and Liu, 2014; Bhaya et al., 2011; Sander and Joung, 2014). CRISPR/Cas9 induced mutagenesis has already been successfully used for genome editing in various model organisms, including several arthropods (Auer et al., 2014; Bassett et al., 2013; Friedland et al., 2013; Gilles et al., 2015; Kistler et al., 2015; Nakanishi et al., 2014; Nakayama et al., 2013; Wei et al., 2014). In *Parasteatoda,* the knock-in of a fluorescent reporter via CRISPR/Cas9 at the *Pt*-Delta locus would enable the tracking of *Pt*-Delta protein at any stage of development in live embryos. Thereby, dynamic protein expression in the SAZ and the forming segments could be visualized throughout segmentation to further investigate the activity of a putative molecular clock regulating segmentation in *Parasteatoda*. In order to visualize *Pt-Delta* protein expression *in vivo,* a plasmid for the fusion of the fluorescent marker red fluorescent protein (dsRed) in frame with the *Pt-Delta*

coding region was generated. As the C-terminal tagging of the Delta protein with a fluorescent marker has been shown to be functional in *Drosophila* (Hagedorn et al., 2006), the sgRNA was designed against 20 nucleotides upstream of the *Pt-Delta* stop codon. This design ensures the seamless transcriptional transition of the *Pt-Delta* transcript to dsRed and thereby generates the C-terminal tagging of the *Pt*-Delta protein. The constructs also comprises the SV40 polyadenylation signal to ensure transcriptional termination (Wu and Alwine, 2004) (see fig 12).

I then injected 670 embryos with the *Pt-Dl*-CRISPR construct together with the fluorescent marker FITC, to track the clones *in vivo* (see chapter 2.6.3) and checked for a fluorescent signal every 24 hours for up to 4 consecutive days. The embryos displayed a very high survival rate of over 90% and I could detect the fluorescent dye FITC in somatic clones (see fig. 17), however, no dsRed signal could be detected at any of the time points observed.

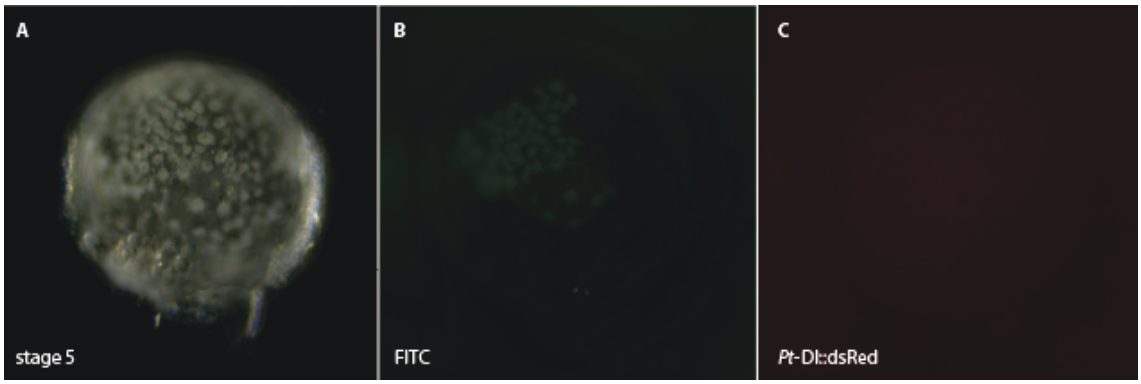

Fig.17 | *Pt*-Dl::dsRed knock-in using CRISPR. Panels **A-C** show the same embryo at stage 5. Panel **A** shows a bright field image of the injected embryo. The FITC signal in panel **B** visualizes the clone of cells comprising the injection mix. Panel **C** shows that no dsRed signal could be detected in the respective clone area.

This suggests that the integration of the *Pt-Dl*-CRISPR construct was not successful for various methodological reasons, which will be discussed in the following. Furthermore the integration of the *Pt-Dl*-CRISPR construct requires HR, which has been shown to be less efficient than NHEJ (Cong et al., 2013; Platt et al., 2014; Wang et al., 2013), hence an increase in the number of injected embryos, might enhance the probability of a positive result.

3.4 Discussion

3.4.1 The role of *Pt-N* and *Pt-Dl* in the posterior of *Parasteatoda*

In this work I showed that *Pt-Dl* is required for the activation of *Pt-Wnt8* in the posterior, but represses its expression in the anterior SAZ (Schonauer et al., 2016). This suggests that *Pt-Dl* facilitates the expression of *Pt-Wnt8* and that Delta-Notch signaling has a dual effect on *Pt-Wnt8* expression in the SAZ (Schonauer et al., 2016). Moreover, it was previously shown that that *Pt-Wnt8* is required to maintain a pool of cells in the posterior SAZ of *Parasteatoda* and regulate cyclical expression of *Pt-Dl* (McGregor et al., 2008b). Therefore, these complex regulatory interactions of Delta-Notch and *Pt-Wnt8* in the posterior of *Parasteatoda* embryos suggests that the formation and maintenance of the SAZ and the subsequent formation of segments from this tissue requires a functional compartmentalisation of the SAZ. This is consistent with findings in other arthropods (Brena and Akam, 2013; Chesebro et al., 2013).

In the centipede *Strigamia*, expression analysis showed that *Sm-Dl* and *Sm-cad* are expressed out of phase with each other: the initial double segmental pattern in the posterior disc, a population of undifferentiated cells from which the

segments form, as well as the segmental expression in the forming trunk segments do not overlap between those two genes (Brena and Akam, 2013; Chipman et al., 2004).

Furthermore, study of the cockroach has shown that a positive feedback loop of *Pa-Wnt1* and *Pa-Dl* in the posterior in conjunction with *Pa-cad* repressing *Pa-Dl* in the more anterior region of the growth zone (GZ), are responsible for oscillating gene expression passing through the GZ (Chesebro et al., 2013). This functional subdivision of the *Periplaneta* GZ maintains the GZ cells in an undifferentiated state and ensures stimuli of differentiation at regular intervals at the anterior (Chesebro et al., 2013).

Therefore studies of *Parasteatoda* and other arthropods suggest that the SAZ can be subdivided into a posterior region that maintains a pool of undifferentiated cells and an anterior region, where the cells differentiate and nascent segments are forming. However, further work on spiders and other arthropods is needed to determine how these regions are specified and regulated and if common mechanisms are used across arthropods.

In *Parasteatoda Pt-Dl* and *Pt-N* expression are both activated at a similar stage, in potentially overlapping domains at the rim of the germ disc and in the SAZ (see fig.15 A, Oda et al., 2007). However while *Pt-Dl* clears from the posterior, *Pt-N* expression remains diffusely in the whole SAZ area at the same stage (see fig. 14 A and fig. 15 B). Due to those differences in expression dynamics between *Pt-Dl* and *Pt-N*, it has been suggested that *Pt-N* might be responsible for the maintenance of *Pt-Wnt8* in the posterior and *Pt-Dl* required for *Pt-Wnt8*

repression in the anterior SAZ, whilst the overall effect on *Pt-Wnt8* in both the *Pt-Dl* and the *Pt-N* knockdown experiments appears similar (Schonauer et al., 2016).

Pt-Dl and *Pt-N*, expression at least in the SAZ appears to overlap, however, *Pt-N* appears to be expressed more diffusely compared to the distinct *Pt-Dl* expression (see fig.14 A and fig. 15 B). Together with the effect of *Pt-Dl* and *Pt-N* expression and vice versa in reciprocal RNAi knockdown experiments, might be indicative of a regulatory feedback interaction in the Delta-Notch pathway (Oda et al., 2007; Schonauer et al., 2016).

Interestingly, it has been shown in *Drosophila* and in vertebrates that Delta and Notch undergo complex regulatory interactions, whereby Delta *trans*-activates Notch by binding to the receptor and reciprocally *cis*-inhibits *Notch* activity in the same cell (de Celis and Bray, 1997; del Alamo et al., 2011; Micchelli et al., 1997). This *cis*-inhibition mechanism increases the specificity of the signaling interaction, as the cell becomes unresponsive for signals from other cells, facilitating the generation of distinct cell fates in a pool of previously uniform neighbouring cells (del Alamo et al., 2011; Sprinzak et al., 2010). Furthermore it could be shown that *fringe* modulates ubiquitously expressed *Notch* in certain developmental compartments, like the dorsal of the *Drosophila* wing (Irvine, 1999; Takeuchi and Haltiwanger, 2010). This increases the affinity for *Delta* over the second ligand *Serrate,* contributing to border formation in developmental processes, like the dorsal and ventral compartment of the fly wing (Irvine, 1999; Takeuchi and Haltiwanger, 2010).

3.4.2 Investigation Pt-Dl protein localisation using CRISPR

To better decipher if these or similar interactions between Dl and N are involved in segment addition in spiders it is necessary to study their protein localization. Hence, I set out to label Pt-Dl protein with the fluorescent marker dsRed using the genome editing method CRISPR. However, in the few attempts I undertook, I could not detect a fluorescent signal in the injected embryos. Nevertheless, the negative results for the CRISPR injections rely on a small number of injected embryos and only one concentration of sgRNA, Cas9 protein and donor plasmid has been tested. For the injection mix, I used the recommended concentrations for *Drosophila*. Given more time for these experiments I would inject different concentrations of sgRNA, because it has been shown to have a great influence on the targeting efficiency in *Drosophila* (Ren et al., 2014). Furthermore, I would co-inject multiple sgRNAs targeting the same locus (there are several sgRNA options available in the online prediction), as this has proven to increase the cutting efficiency of the Cas9 endonuclease in *Drosophila* (Ran et al., 2013) with the caveat that this could result in off target effects. While the basic requirements, like microinjection, are already available in *Parasteatoda*, it is now a matter of testing and optimizing various parameters in order to establish CRISPR successfully in the spider.

4 Results Chapter 2: Downstream targets of Wnt and Delta/Notch signaling

In previous studies of *Parasteatoda* posterior segmentation, it has been shown that *Pt-cad* and the mesodermal specification gene *twist* (*Pt-twi*) are expressed in the SAZ and the developing opisthosomal segments (Oda et al., 2007; Yamazaki et al., 2005). Furthermore, it could be shown that *Pt-cad* and *Pt-twi* are responsible for the correct formation of mesoderm and caudal ectoderm in the posterior of the developing embryo and that both factors are downstream targets of Wnt and Delta/Notch signaling in the spider (McGregor et al., 2008b; Oda et al., 2007; Yamazaki et al., 2005).

It has been concluded from *Pt-Dl* knockdown experiments, where *Pt-cad* expression is lost and caudal ectoderm is not able to form, that *Pt-cad* is downstream of Delta/Notch signaling. However, it has been suggested that *Pt-cad* cannot be directly activated by *Pt-Dl*, as a significant time difference of more than 10 hours between the onset *Pt-Dl* transcription at late stage 4 and initiation of *Pt-cad* transcription at mid stage 6 has been observed (Oda et al., 2007). To better understand the regulation and role of *Pt-cad* therefore, I first aimed to characterise the expression of *Pt-cad* in greater detail throughout the stages of posterior segment formation.

4.1 Expression of the *caudal* ortholog in *Parasteatoda*

From mid stage 6 on *Pt-cad* is expressed in a circular domain in the SAZ (see fig. 18 A), from which it then clears centrally (see fig. 18 B). Subsequently, *Pt-cad* is expressed in a broad anterior crescent shaped domain and a posterior circular domain (see fig. 18 C). At late stage 7, *Pt-cad* expression appears in the mesoderm of the prosoma in a 1 cell wide stripe and is also strongly expressed in the anterior portion of the O1 segment and throughout the SAZ (see fig. 18 D). The stripe of expression in the prosoma broadens in width to up to 3 cells, whereas expression in the forming O1 segment fades (see fig. 18 E). At this stage, *Pt-cad* is expressed throughout the entire SAZ with stronger expression at the anterior and in a posterior domain (see fig. 18 E). At stage 8.2, *Pt-cad* is expressed strongly in the SAZ and shows faint expression in O2 and strong expression in a 4-5 cells wide stripe in the presumptive L4 segment (see fig. 18 F).

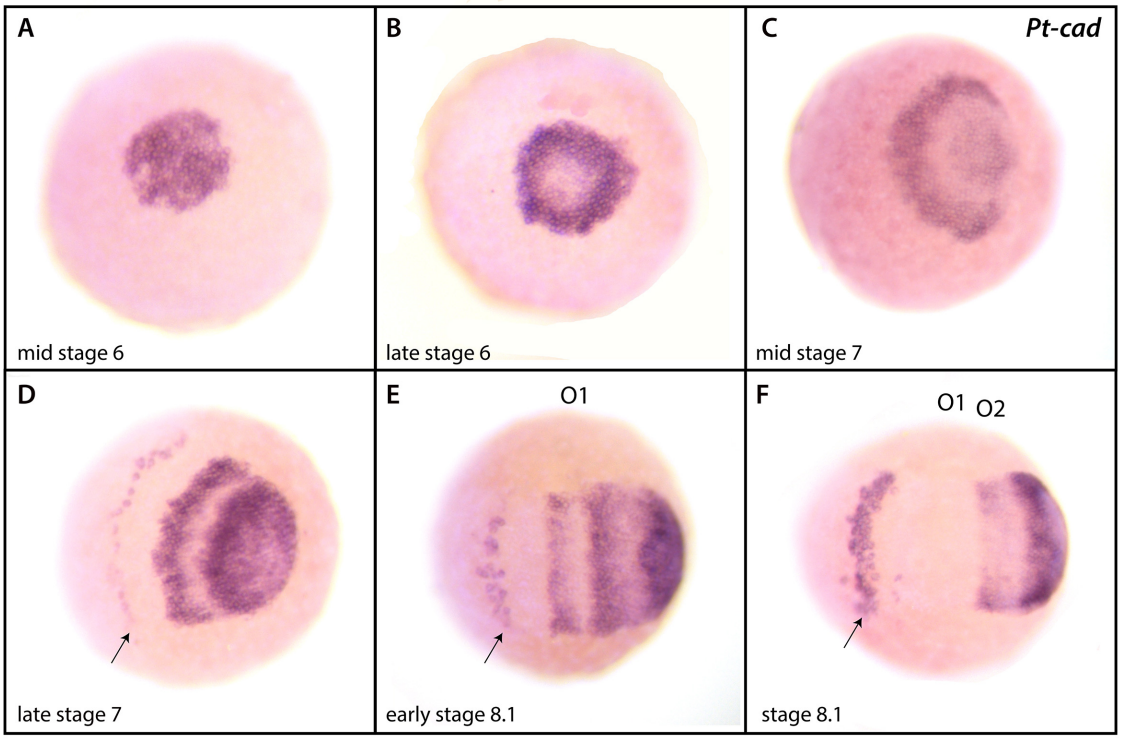

Fig.18 | *Pt-cad* wildtype expression during stages 6-8.1. Whole mount embryos in a ventral view of stage 6 embryos **(A, B)** and opisthosomal germ band **(C-F)**, respectively. In all panels anterior is to the left and embryos are counterstained with DAPI. *Pt-cad* expression starts in a circular domain in the centre of the germ disc at stage 6 **(A)** and subsequently clears from the centre slightly later **(B)**. At mid stage 7, two distinct expression domains within the SAZ can be found; a circular one in at the posterior and a crescent shaped domain at the anterior portion of the SAZ **(C)**. Further, at late stage 7, *Pt-cad* is expressed strongly in the SAZ, the anterior portion of the O1 and in a stripe (black arrow) in the mesoderm of the prosoma **(D)**. *Pt-cad* is strongly expressed in the posterior and a stripe in the anterior portion the SAZ, the anterior portion of O1 and the stripe in the prosoma increases in width to up to 3 cells (black arrow) **(E)**. The prosomal domain becomes broader with up to 5 cells in width (black arrow), the expression in O1 has disappeared, strong expression has developed in the newly formed O2 segment and *Pt-cad* is still expressed in the SAZ **(F)**.

4.2 *Pt-cad* is not required for dynamic *Pt-Dl* expression in the posterior

Previous studies have investigated *Pt-Delta* and *Pt-cad* expression in relation to each other and also studied the effect of *Pt-Delta* on *Pt-cad* in the posterior (Oda et al., 2007). Based on its dynamic expression throughout posterior development, *Pt-cad* represents a potential candidate gene to feed back to Delta-Notch signaling pathway (Oda et al., 2007) to generate repetitive gene expression associated with the formation of each new segment.

Therefore the effect of *Pt-cad* embryonic RNAi knockdown on *Pt-Delta* expression was analyzed at stage 7, when *Pt-Dl* and *Pt-cad* are expressed in distinct domains but do exhibit overlap in the SAZ (chevrons, fig. 19 A).

In the embryonic RNAi experiment, no effect on the expression level of *Pt-Dl* could be observed in *Pt-cad* knockdown clones in

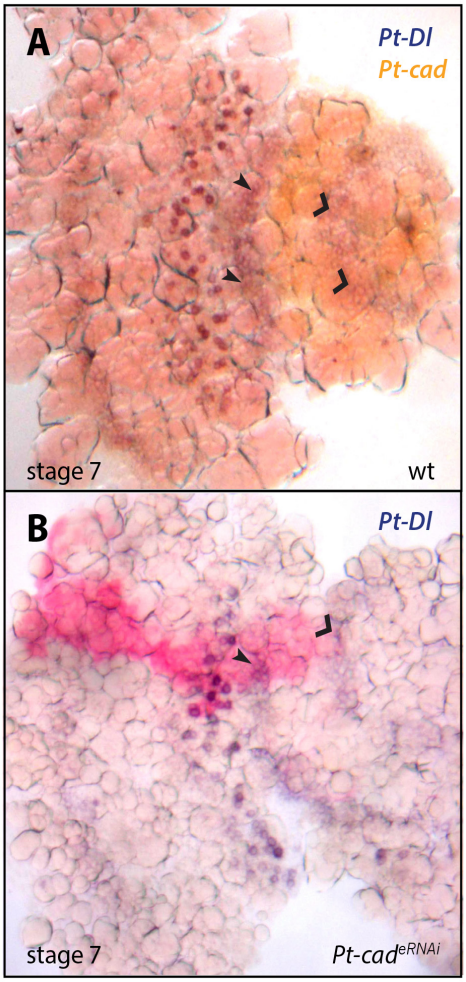

Fig.19 | The effect of *Pt-cad* on *Pt-Dl* Whole mount embryos in a ventral view of stage 6 embryos **(A-B)**. Flat mount embryos with the anterior to the left and the posterior to the right. In wild-type embryos at stage 7 *Pt-Dl* (blue) and *Pt-cad* (orange) are expressed in distinct but also overlapping domains (indicated by chevrons and arrowheads) in the SAZ (**A**). In *Pt-cad* eRNAi knockdown cell clones (red), *Pt-Dl* expression (blue) appears unaffected.

the SAZ that overlapped with cells that express both *Pt-Dl* and *Pt-cad* in wild-type embryos (see fig. 19 B). This suggests that *Pt-cad* is not involved in the regulation of *Pt-Dl* during posterior development in *Parasteatoda*.

4.3 Characterizing the expression of pair-rule orthologs throughout segmentation in *Parasteatoda*

Comparative studies have shown that components of the *Drosophila* segmentation cascade are involved in segmentation in both long and short germ arthropods (Choe et al., 2006; Copf et al., 2004; Damen et al., 2000; Dearden et al., 2002; Liu and Kaufman, 2005; Mito et al., 2005; Shinmyo et al., 2005). For example, the pair-rule orthologs in the spider *Cupiennius* have dynamic expression in the SAZ and are subsequently expressed in posterior segments (Damen et al., 2005).

In order to identify potential downstream targets of Delta-Notch and Wnt signaling during *Parasteatoda* segmentation, expression of the pair-rule gene orthologs *even-skipped* (*Pt-eve), runt (Pt-run-1), odd-skipped (Pt-odd-1), odd-paired (Pt-opa) and sloppy-paired (Pt-slp)* were characterized throughout posterior development.

4.3.1 *S*tructure and expression of the *Parasteatoda even-skipped* ortholog

A single *even-skipped* ortholog (*Pt-eve*>aug3.g17585.t1, Scaffold2587:24766..40760, +strand) was identified in the *Parasteatoda*

genome (Schwager et al., in prep) (see fig. 20). One *Pt-eve* transcript is transcribed from the + strand and the coding region is 884 bp.

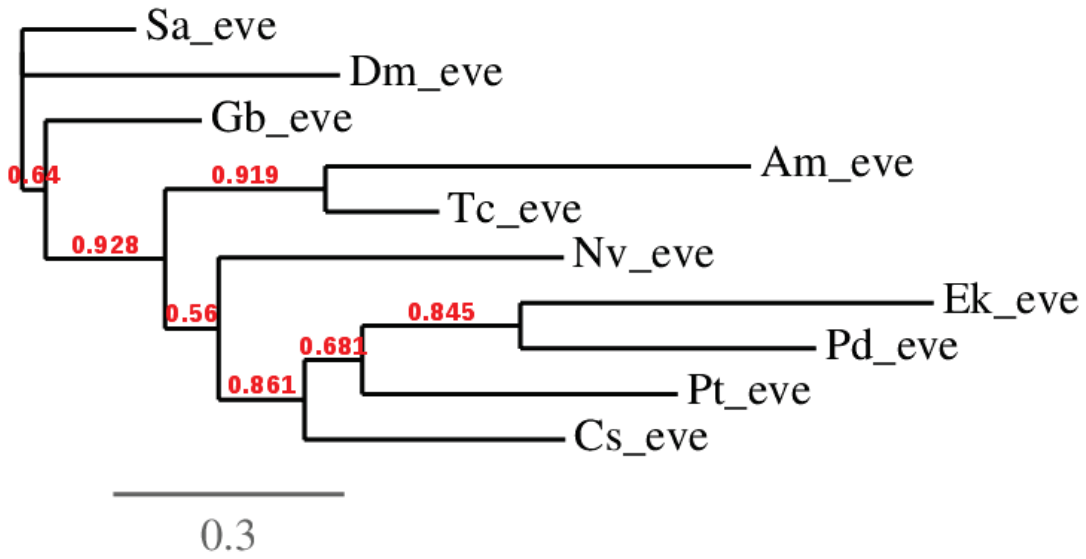

Figure 20| Phylogenetic analysis of the *Drosophila even-skipped* orthologs. The gene trees were built by maximum likelihood analysis in PhyML (Guindon and Gascuel, 2003); branch support values (approximate Likelihood-Ratio Test) are indicated in red. The scale bar at the bottom left indicates the branch length, which is proportional to the number of substitutions per site. *Schistocerca americana* (*Sa*), *Drosophila melanogaster (Dm), Gryllus bimaculatus (Gb), Tribolium castanaeum (Tc), Apis mellifera (Am), Nasonia vitripennis (Nv), Euperipatoides kanangrensis (Ek), Parasteatoda tepidariorum (Pt), Cupiennius salei (Cs), Platynereis dumerilii (Pd).*

The Augustus annotation for the *Parasteatoda even-skipped* ortholog predicts 3 exons with sizes of 178 bp (exon1), 182 bp (exon2) and 438 bp (exon3). Furthermore, the 2 annotated introns exhibit a large difference in size (intron1 = 12210 bp, intron2 = 2908 bp). Analysis of the predicted Pt-Eve protein (255 aa) identified a DNA-binding homeodomain (51 aa), spanning exons 2 and 3 (see fig. 21 A). The homeodomain alignment using BLASTp revealed high conservation in comparison with other arthropods (see fig. 21 B).

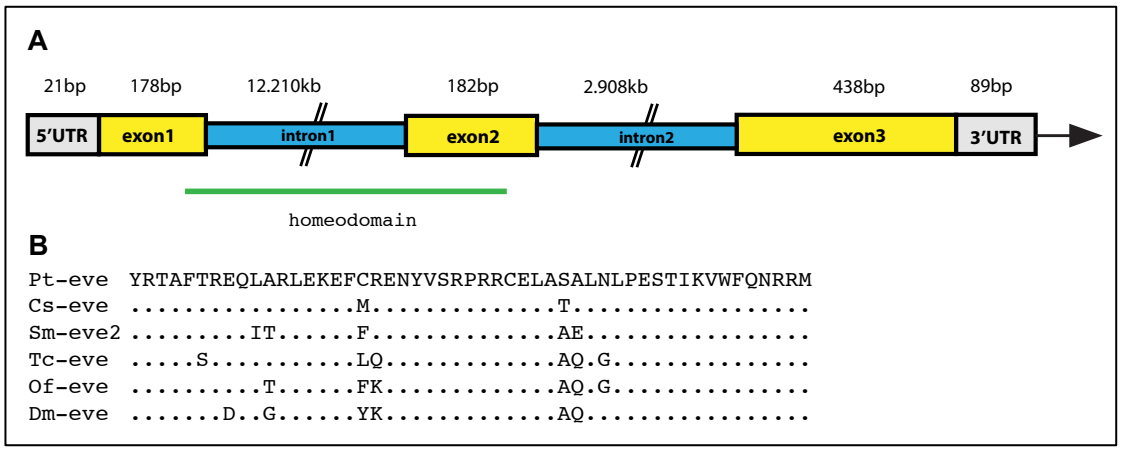

Figure 21 | *Pt-eve* structure and homeodomain sequence analysis. *Pt-eve* comprises 3 exons (exon1 178bp, exon2 182 bp, exon3 438bp). Alignment of *even-skipped* homeodomains **(B)** Identical aa are represented with dots and sequences are in order of similarity identified in protein BLAST. *Cupiennius salei* (*Cs*), *Strigamia maritima* (*Sm*), *Tribolium castaneum* (*Tc*), *Oncopeltus fasciatus* (*Of*), *Drosophila melanogaster* (*Dm*).

In situ hybridisation showed that *Pt-eve* exhibits dynamic expression in the SAZ that resolves into stripes of expression in nascent segments over the course of posterior development (see fig 22 A-H). *Pt-eve* is first expressed in a small circular expression domain of approximately 15 cells in the SAZ at stage 6, during the transition from the germ discs to the germ band stage (data not shown). This expression domain then increases in diameter (fig. 22 A), but concomitantly the centre clears (fig. 22 B) to form a transient ring of expression (fig. 22 C). This ring shaped expression domain is broken by the loss of *Pt-eve* expression in the most posterior cells to form a stripe of expression of approximately 3 cells in width in the nascent O1 segment during stage 7 (fig. 22 D). At this stage, expression of *Pt-eve* is again observed in a circular domain in the most posterior cells of the SAZ (fig. 22 D), which again clears centrally (fig. 22 E) and then breaks to form a second stripe in the presumptive O2 segment, as expression begins to narrow and fade in the older O1 stripe of expression (fig. 22 F). Subsequently, *Pt-eve* expression undergoes similar dynamic cycles

of strong expression in the SAZ followed by clearance of expression from this region and expression in the forming segments. As *Pt-eve* stripes form in nascent segments, the expression in the older, more anterior, segments fades. Therefore, during formation of O3 (fig. 22 G) and the remaining posterior segments, *Pt-eve* expression is only observed in the two or rarely the three most posterior (and thus youngest) segments as well as dynamically in the SAZ. Expression is also seen in the developing nervous system in older prosomal and opisthosomal segments (fig. 22 H).

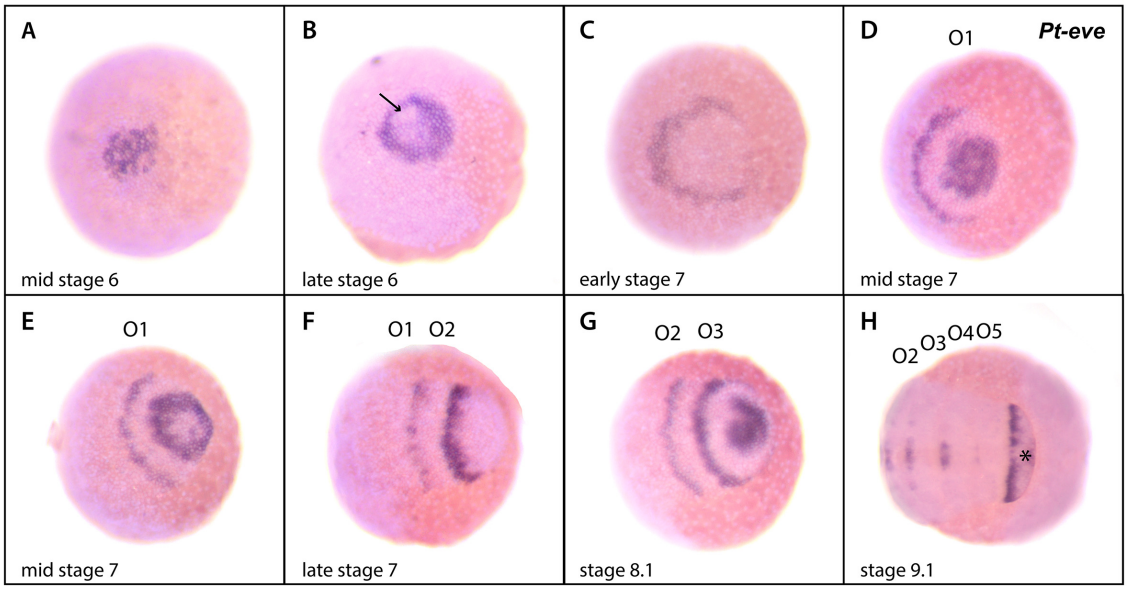

Figure 22 | *Pt-eve* exhibits dynamic expression in the SAZ and in nascent segments. Whole mount embryos in a ventral view of stage 6 embryos **(A-C)** and opisthosomal germ band **(D-H)**, respectively. In all panels anterior is to the left and embryos are counterstained with DAPI. **(A)** *Pt-eve* is expressed in a circular domain in the SAZ at mid stage 6 and clears centrally (black arrow) at late stage 6 **(B)**. The expression in the posterior portion of the SAZ clears entirely and *Pt-eve* is expressed in a crescent shaped domain at the anterior of the SAZ **(C)**. During mid stage 7 *Pt-eve* expression returns strongly in the SAZ and continues to be expressed in the forming O1 segment **(D)**. Another cycle of clearance from the SAZ can be observed during mid stage 7 **(E)**, followed by emerging strong expression in the nascent O2, whereby expression in the posterior portion of O1 narrows **(F)**. At stage 8.1 strong expression in the SAZ and the newly formed O3 and O2 segment can be observed **(G)**. Later, Pt-eve expression can be found in the developing nervous system and mostly the anterior portion of the SAZ (H).

4.3.2 Expression of the *Parasteatoda runt-1* ortholog

In the *Parasteatoda* genome 2 runt paralogs (*Pt-run-1*>aug3.g2762.t1, Scaffold 413:813549..851485; *Pt-run-2*> aug3.g6543.t1, Scaffold 772:494170..494699) were identified, however only one paralog exhibits segmental expression (Evelyn Schwager, personal communication), which suggests an involvement in posterior development and will be referred to as *Pt-run-1* (see fig. 23).

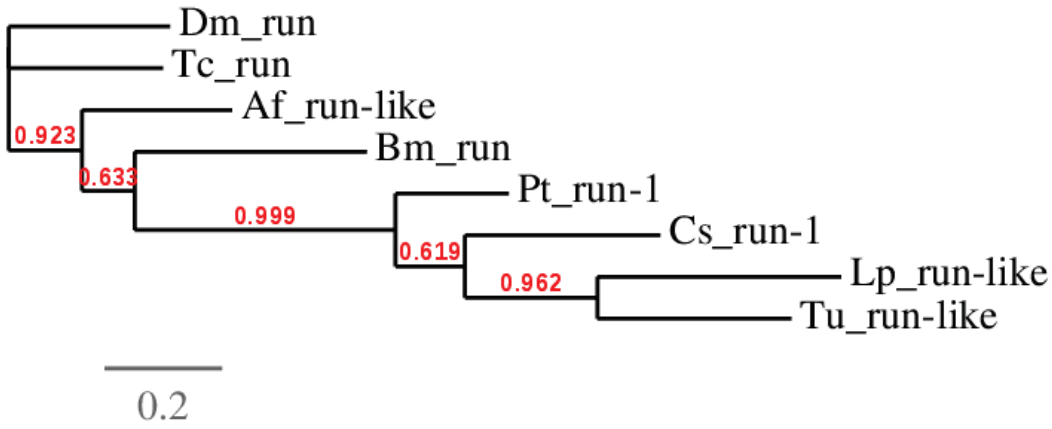

Figure 23 | Phylogenetic analysis of the *Drosophila runt* orthologs. The gene trees were built by maximum likelihood analysis in PhyML (Guindon and Gascuel, 2003); branch support values (approximate Likelihood-Ratio Test) are indicated in red. The scale bar at the bottom left indicates the branch length, which is proportional to the number of substitutions per site. *Drosophila melanogaster (Dm), Tribolium castanaeum (Tc), Apis florea (Af), Bombyx mori (Bm), Parasteatoda tepidariorum (Pt), Cupiennius salei (Cs), Limulus polyphemus (Lp), Tetranychus urticae (Tu).*

The *Pt-run-1* transcript is transcribed from the + strand and the coding region is 1.5 kb in length. The Augustus annotation for the *Parasteatoda run-1* ortholog predicts 5 exons and 4 introns, which exhibit a significant difference in size (intron1= 10140 bp, intron2 = 22390 bp, intron3 = 2739 bp, intron4 = 104 bp).

Pt-run expression commences in a circular domain in the forming SAZ (Fig. 24 A). This expression domain clears from the centre and forms a ring shaped expression domain at the anterior of the SAZ (see fig. 24 B). *Pt-run* expression then resolves into a stripe in the future O1 segment, while a new cycle of

expression is observed in the posterior of the SAZ (see fig. 24 C). Low levels of *Pt-run-1* expression at the anterior of O1 and a strong stripe expression domain at the anterior of the SAZ can be found at stage 8.1 (see fig. 24). A stripe in the nascent O2 segment forms and expression again clears from the SAZ (see fig. 24 E). While segments are added from the posterior, *Pt-run* expression fades from the O1 segment, but is still expressed in O2 and appears again as a circular domain in the SAZ area (see fig. 24 F).

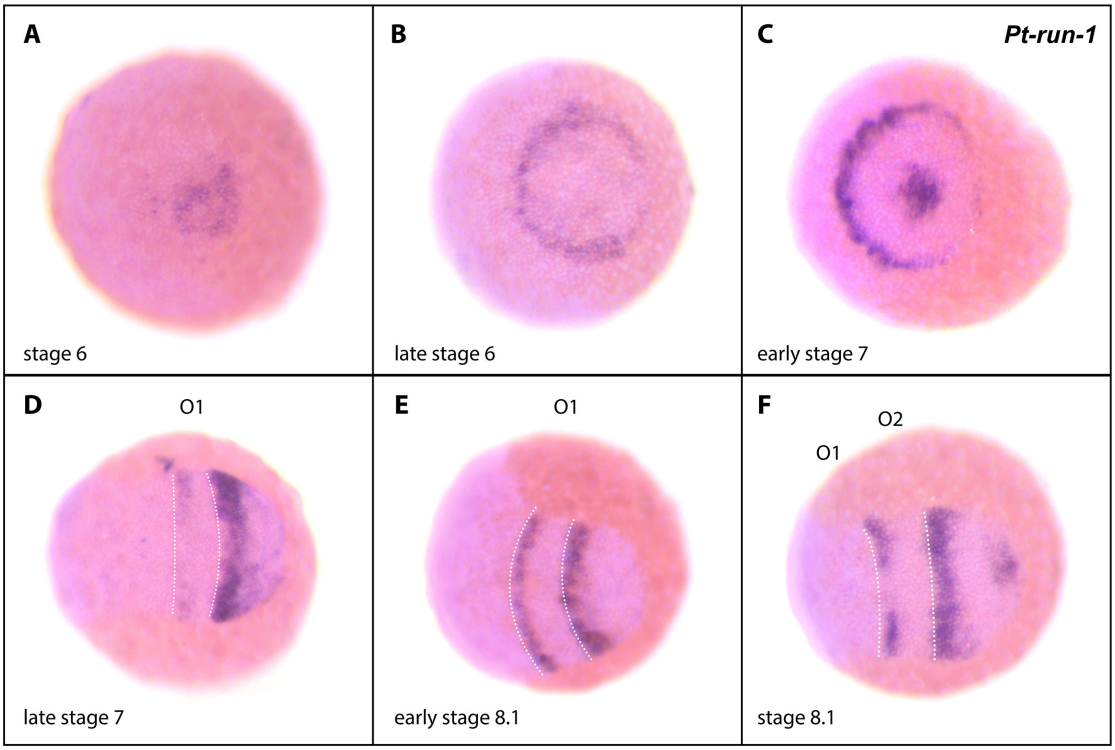

Figure 24 | *Pt-run-1* wild-type expression. Whole mount embryos in a ventral view of stage 6 embryos **(A-C)** and opisthosomal germ band **(D-F)**, respectively. In all panels anterior is to the left and embryos are counterstained with DAPI. *Pt-run-1* is expressed in a circular domain at stage 6 **(A)**, clears from the posterior entirely and refines to a crescent shaped domain at the anterior of the SAZ **(B)**. The expression in the anterior SAZ becomes stronger and a circular domain in the posterior SAZ arises at early stage 7 **(C)**. At a slightly later stage, faint expression arises in the forming O1 segment and refines to a stripe in the anterior SAZ **(D)**. *Pt-run-1* is expressed strongly in O1 and the anterior of the SAZ, but clears from the posterior at early stage 8.1 **(E)**. Expression fades from O1, is expressed in the anterior portion of O2 and in a stripe domain at the anterior and a small patch at the posterior of the SAZ **(F)**.

Expression of *Pt-eve* and *Pt-run* appear in similar domains over the course of posterior development and in order to study their regulatory interactions, I investigated their expression in relation to each other with double in situ hybridisation. *Pt-run-1* expression commences during stage 6 (see fig. 25 A), at approximately the same time that *Pt-eve* can be first detected (see fig. 25 A). Furthermore, *Pt-run-1* and *Pt-eve* expression partially overlap in anterior and posterior SAZ cells at the stages assayed (see fig. 25 A-C). However, *Pt-eve* is expressed approximately 3 cell rows anterior to *Pt-run-1* in forming segments (see fig. 25 A-C).

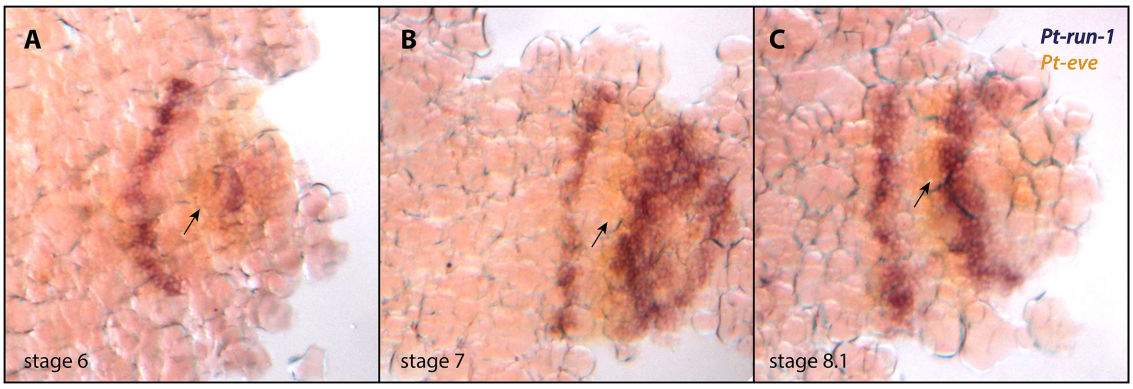

Figure 25 | Double in situ hybridisation of *Pt-run-1* and *Pt-eve* at stages of posterior development. Flat mount embryos in a ventral view of a stage 6 embryo **(A)** and opisthosomal germ band **(B-C)**, respectively. In all panels anterior is to the left. *Pt-run-1* and *Pt-eve* expression largely overlap in the SAZ (arrow in A). Expression of *Pt-eve* is 2-3 cell rows anterior of *Pt-run-1* in forming stripes (arrow in B, C).

4.3.3 Expression of the *Parasteatoda odd-skipped* ortholog

In the *Parasteatoda* genome 2 *odd* paralogs (*Pt-odd-1*> aug3.g10084.t1, Scaffold 1114:68730..184114; *Pt-odd-2*> Locus 17047) could be identified, however only one paralog exhibits opisthosomal expression (Natascha Turetzek, personal communication) that might indicate that this gene is involved

in segmentation (see fig. 26). This gene will be referred to as *Pt-odd-1*. The *Pt-odd-1* transcript is transcribed from the - strand and the coding region is 1.3 kb in length. The Augustus annotation for the *Parasteatoda run-1* ortholog predicts 4 exons.

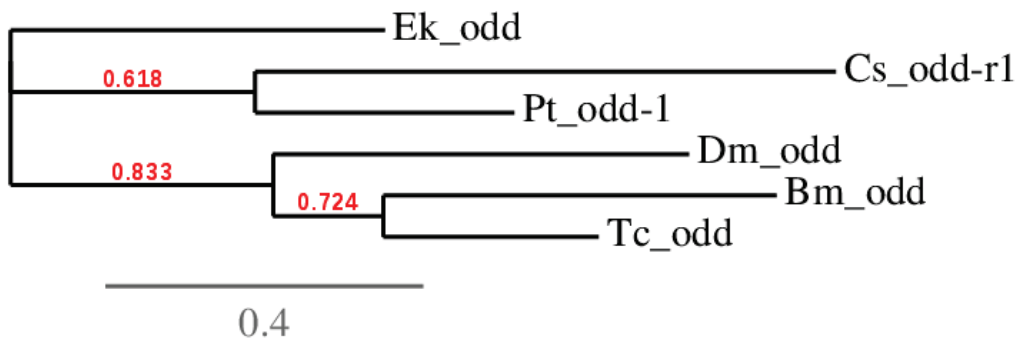

Figure 26 | Phylogenetic analysis of the *Drosophila odd-skipped* orthologs. The gene trees were built by maximum likelihood analysis in PhyML (Guindon and Gascuel, 2003); branch support values (approximate Likelihood-Ratio Test) are indicated in red. The scale bar at the bottom left indicates the branch length, which is proportional to the number of substitutions per site. *Drosophila melanogaster (Dm), Tribolium castanaeum (Tc), Bombyx mori (Bm), Parasteatoda tepidariorum (Pt), Cupiennius salei (Cs), Euperipatoides kanangrensis (Ek).*

Pt-odd-1 expression comes on in the anterior at stage 8.2 in the developing stomodaeum region (data not shown), which persists throughout the stages 8.1-12 (see fig. 27 A-C). At stage 9.2, in the mesoderm of all developing prosomal appendages, a ring-shaped domain of expression can be observed at the base, very faintly within the forming appendages (probably corresponding with segmental borders) and a circular domain at the tip of each appendage (see fig. 27 A). In the opisthosoma, *Pt-odd-1* is expressed at the anterior of O2 and O3 (see fig. 27 A). At stage 10, in the anterior two domains appear in the labrum and expression in the stomodaeum is still visible (see fig. 27 B). The *Pt-odd-1* expression domains at the tip of the developing limbs become stronger

(chevron in fig. 27 B) and in the opisthosoma, expression appears in O3-O5 (see fig. 27 B) at stage 10. At stage 11, *Pt-odd-1* expression in the anterior is restricted to the stomodaeum (see fig. 27 C). Further, the number of circular *Pt-odd-1* expression domains increases (probably corresponding with the increasing development of segmental borders) (see fig. 27 C). *Pt-odd-1* is also expressed in a stripe in the posterior at stage 11 (asterisk in fig. 27 C). Expression of *Pt-odd-1* first emerges in the developing head and prosoma and appears in the opisthosoma only during later stages of development. Thus, the *Pt-odd-1* expression pattern suggests that this gene does not have a crucial function in opisthosomal segment formation of *Parasteatoda*, but might be involved in the development of the walking legs, parts of the head and aspects of opisthosomal appendages.

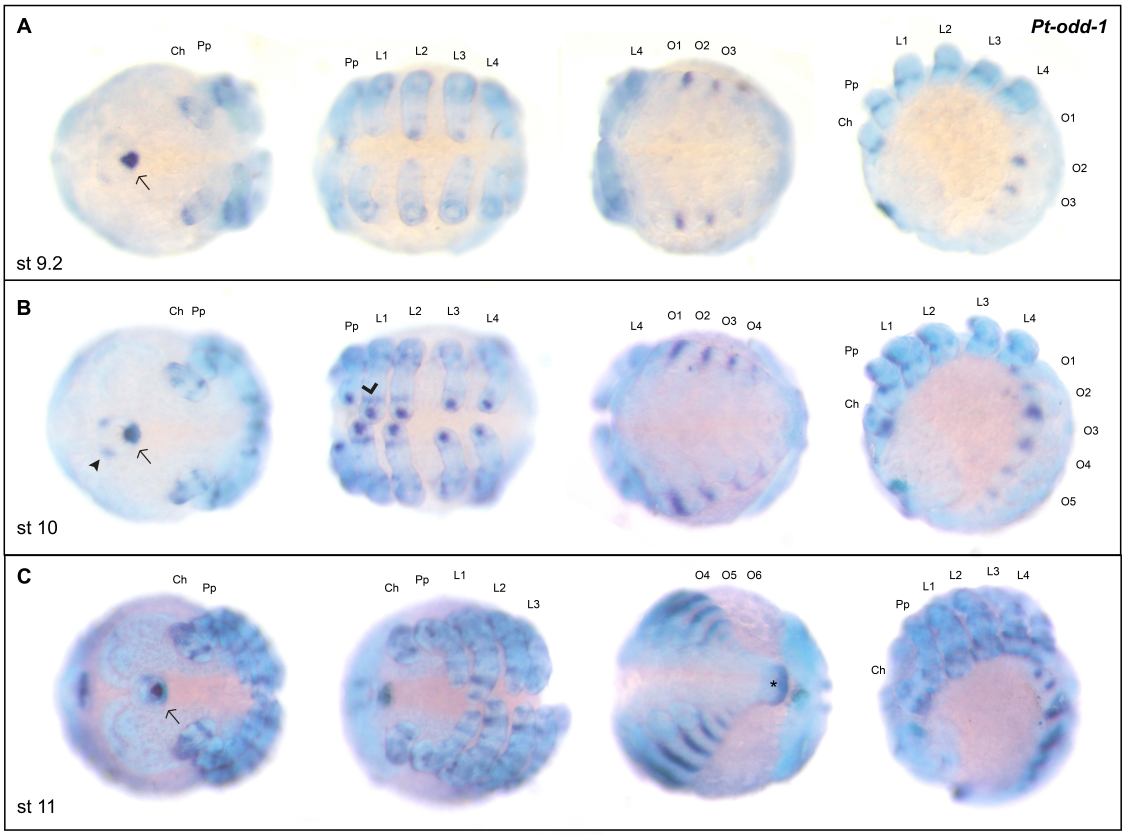

Figure 27 | *Pt-odd-1* wildtype expression. Whole mount embryos in a ventral view of the opisthosomal germ band **(A-C)**, All panels show the same embryo respectively in an anterior (left), a prosomal (2nd view), an opisthosomal (3rd) and a side view (4th view). In all panels anterior is to the left and embryos are counterstained with DAPI. Expression in the stomodaeum of all observed stages is marked with an arrow **(A-C)**. At stage 9.2, a ring-shaped expression domain can be found at the base of the forming appendages **(A)**. There is also expression at the anterior of the O2 and O3 segments **(A)**. At stage 10, probably in accordance with the addition of segments, more rings of expression appear in the appendage mesoderm and the expression at the tip of the appendages becomes stronger **(B)**. With further development, the ring-shaped expression domains in the mesoderm of the appendages increase in number, as well as within the opisthosomal segments **(C)**.

4.3.4 Expression of the *Parasteatoda opa-paired* ortholog

In the *Parasteatoda* genome one *opa* ortholog (*Pt-opa*>aug3.g12202, Scaffold 1447:114106..154022) was identified (see fig. 28). *Pt-opa* is transcribed from the + strand and the coding region is 1.3 kb in length.

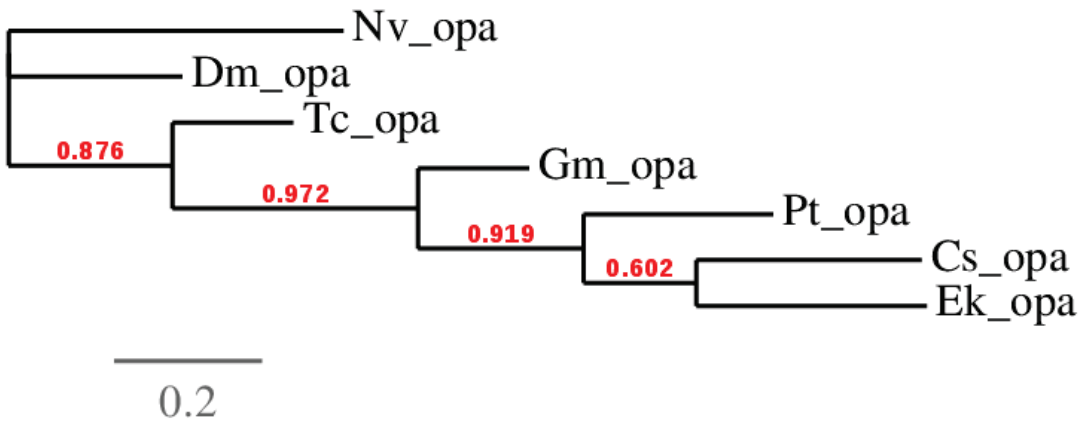

Figure 28 | Phylogenetic analysis of the *Drosophila odd-paired* orthologs. The gene trees were built by maximum likelihood analysis in PhyML (Guindon and Gascuel, 2003); branch support values (approximate Likelihood-Ratio Test) are indicated in red. The scale bar at the bottom left indicates the branch length, which is proportional to the number of substitutions per site. *Nasonia vitripennis (Nv), Drosophila melanogaster (Dm), Tribolium castanaeum (Tc), Glomeris marginata (Gm), Parasteatoda tepidariorum (Pt), Cupiennius salei (Cs), Euperipatoides kanangrensis (Ek).*

Pt-opa expression appears at stage 8 in the developing head and the prosoma. At stage 9.1, *Pt-opa* is expressed in a distinct domain in the PcL (see fig. 29 A), which then splits into an anterior (arrow) and a lateral (arrow head) domain. The superficial ectodermal layer of L1-L4 does not show any signal, but faint expression can be observed in the mesoderm (see fig. 29 B). Interestingly, expression in L2 is stronger compared to expression in the other leg bearing segments (see fig. 29 B). Also at stage 10, a specific domain in the mesoderm of the O2 segment can be observed (see fig. 29 B). In the developing head, expression in the PcL persists (black arrow, arrowhead) and an additional domain appears at the labrum. The mesodermal expression in the limbs

persists and the expression in the appendage of the opisthosomal appendage O2 becomes stronger (see fig. 29 C). Inferred from the expression analysis, *Pt-opa* might be involved in brain development, limb formation and aspects of book lung growth.

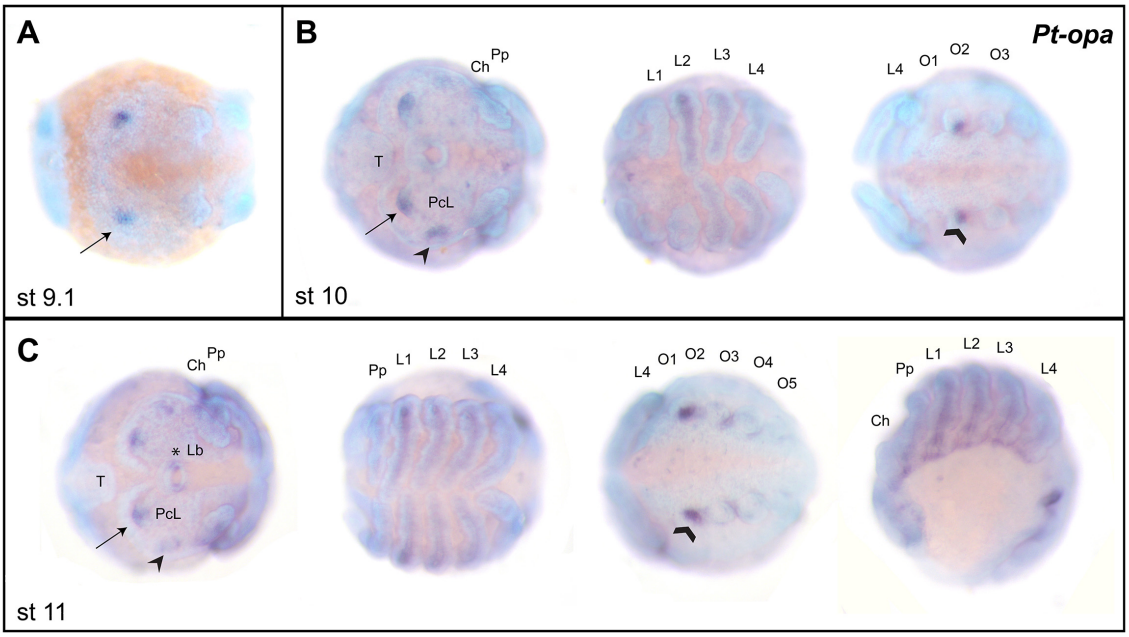

Figure 29 | *Pt-opa* wildtype expression. Whole mount embryos in a ventral view of the opisthosomal germ band **(A-C)**, Panels **B,C** show the same embryo respectively in an anterior (left), a prosomal (2nd view), opisthosomal (3rd) and a side view (4th view in C). In all panels anterior is to the left and embryos are counterstained with DAPI. *Pt-opa* expression commences at stage 9.1 in a distinct domain in the PcL (black arrow, **A**). Further, expression in the PcL splits into two different domains at the anterior (arrow) and a lateral (arrow head) domain **(B)**. At stage 10, faint expression in the developing limb mesoderm can be observed, whereby expression in L2 is stronger compared to the leg bearing segments and there is also a specific domain in the O2 segment **(B)**. At stage 11, the expression in the PcL still persists (black arrow, arrow head) and in addition, an expression domain at the labrum (asterisk) appears **(C)**. The mesoderm expression in the walking legs is unchanged and the expression in the opisthosoma (book lung opening at the posterior of O2) becomes stronger (chevron) **(C)**. The lateral view shows that in addition to the limb mesoderm, there is also expression at the base of each prosomal segment **(C)**.

4.3.5 Expression of the *Parasteatoda sloppy-paired* ortholog

In the *Parasteatoda* genome a single sloppy-paired ortholog (*Pt-slp*>aug3.g19520, Scaffold 3303:1..36954) could be identified (see fig. 30). The *Pt-slp* transcript is transcribed from the - strand and the coding region is 1.3 kb in length. The Augustus annotation for the *Parasteatoda opa* ortholog predicts 4 exons and 4 annotated introns, which exhibit a significant difference in size (intron1= 4276 bp, intron2=15962 bp, intron3=12316 bp, intron4=3105 bp).

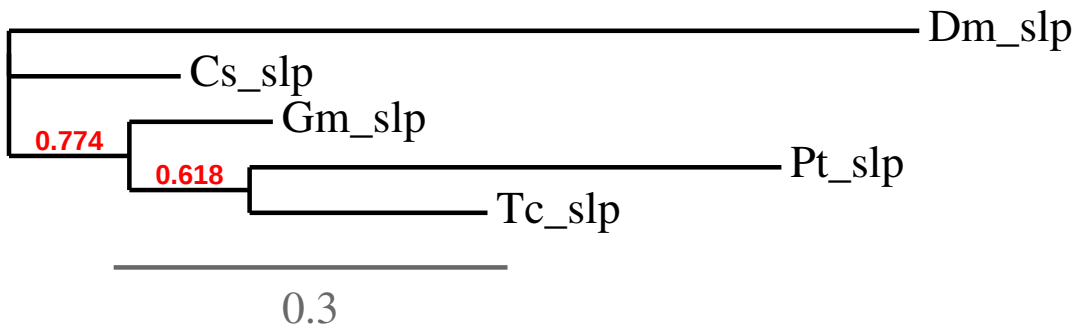

Figure 30 | Phylogenetic analysis of the *Drosophila sloppy-paired* orthologs. The gene trees were built by maximum likelihood analysis in PhyML (Guindon and Gascuel, 2003); branch support values (approximate Likelihood-Ratio Test) are indicated in red. The scale bar at the bottom left indicates the branch length, which is proportional to the number of substitutions per site. *Drosophila melanogaster (Dm), Tribolium castanaeum (Tc), Glomeris marginata (Gm), Parasteatoda tepidariorum (Pt), Cupiennius salei (Cs).*

Expression of *Pt-slp* commences at stage 8.1 in the head lobes in a triangular domain and in the central portion of the prosomal segments L1-L4 (see fig. 31 A). The triangular domains of the developing head become broader at stage 9.1 and two circular domains appear at the labrum and undefined expression around the stomodaeum (see fig. 31 B). The expression in the prosomal and opisthosomal segments becomes stronger and is restricted to the anterior

portion of each segment, excluding the midline (see fig. 31 B). *Pt-slp* expression in the head lobes expands antero-laterally and faint expression arises in the nervous system (see fig. 31 C). The segmental expression becomes more U-shaped in the Pp, Ch, L1-4 and opisthosomal segments (see fig. 31 C). *Pt-slp* expression is not expressed in the SAZ at any of the observed stages, only in the newly formed opisthosomal segments. Due to the expression of *Pt-slp* in the head and the ventral ectoderm, I suggest that *Pt-slp* might be involved in the development of the brain and the central nervous system.

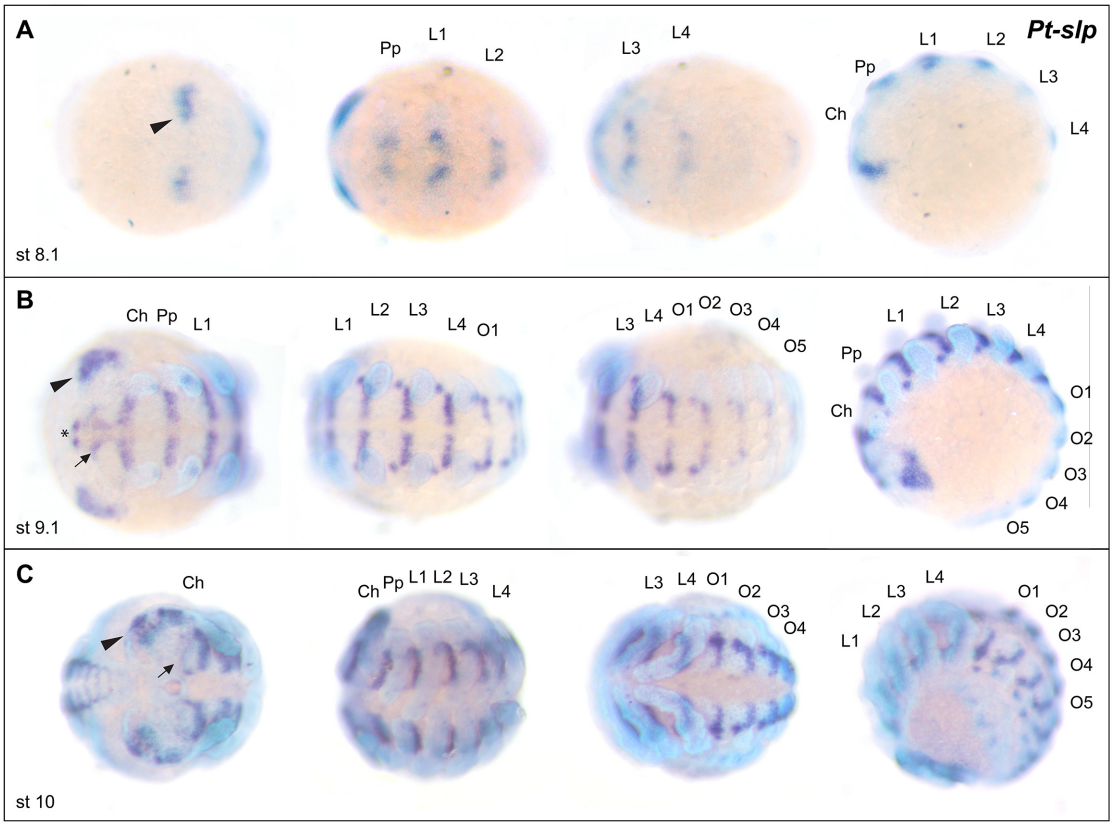

Figure 31 | *Pt-slp* wildtype expression. Whole mount embryos in a ventral view of the opisthosomal germ band **(A-C)**, All panels show the same embryo respectively in an anterior (left), a prosomal (2nd view), opisthosomal (3rd) and a side view (4th view in C). In all panels anterior is to the left and embryos are counterstained with DAPI. *Pt-slp* expression arises in the head lobes (arrow head) and the central part of the prosomal segments **(A)**. Expression in the head lobe exhibits a triangular shape and becomes stronger (arrow head) **(B)**. There is also *Pt-slp* expression around the stomodaeum (arrow) and at the labrum (asterisk) at stage 9.1 **(B)**. Within the prosomal segments and the opisthosomal segments O1-O5, expression can be observed at the anterior of each segment and in a circular lateral domain (B). At stage 10, the anterior expression domain becomes larger at the anterior/lateral part of the head lobes (arrow head) and expression in the developing nervous system appears (arrow; **C**). Strong expression can still be observed in the anterior of the prosomal segments, whereby the lateral domain is fused with the stripe domain at this stage **(C)**.

4.4 Discussion

4.4.1 Expression and role of the *caudal* ortholog in *Parasteatoda*

I have characterised the expression of *Pt-cad* in greater detail compared to previous work (McGregor et al., 2008b; Oda et al., 2007). This shows that it comes on at a similar stage to *Pt-Dl* in the germ disc and subsequently exhibits dynamic expression in the SAZ and is expressed in new segments (see fig.15 and fig. 18). I also tested if *Pt-cad* has an effect on the dynamics of *Pt-Dl* expression and found that *Pt-cad* is not involved in regulating *Pt-Dl* (Schonauer et al., 2016). However, since *Pt-Dl* is required for *Pt-cad* expression (Oda et al., 2007), my results confirm again that *Pt-cad* must be downstream of Delta-Notch signaling in the spider, whilst it is still unclear if *Pt-cad* is a direct target of *Pt-Dl* signaling or if there are intermediate factors (Oda et al., 2007; Schonauer et al., 2016).

In *Strigamia, caudal* (*Sm-cad*) expression precedes morphological segmentation with uniform expression in undifferentiated cells of the blastodisc (Chipman et al., 2004). Throughout posterior development, *Sm-cad* expression is also continuously maintained in the posterior disc and only contracts around the proctodeum upon segment formation (Chipman et al., 2004), in contrast to *Parasteatoda,* where *Pt-cad* expression in the posterior SAZ is more dynamic, alternating between broad expression and clearing from this area (Schonauer et al., 2016). In association with the subsequent elongation of the germ band, *Sm-cad* expression resolves into stripes, reminiscent of *Pt-cad* expression in the spider (Chipman et al., 2004; Schonauer et al., 2016). However, *Sm-cad* expression appears in a double-segmental pattern, in contrast to the single

segmental expression in *Parasteatoda* (Chipman et al., 2004; Schonauer et al., 2016).

The expression profile of *cad* in *Periplaneta* also differs from the spider. *Pa-cad* is expressed broadly in the GZ and establishes a boundary between the undifferentiated GZ and differentiated cells of the forming segments. However, *Pa-cad* is also regulated by Delta-Notch and Wnt signaling in this cockroach (Chesebro et al., 2013) although in contrast to the spider, *Pa-cad* appears to repress *Pa-Dl* (Chesebro et al., 2013). This suggests that while arthropods like *Parasteatoda* and *Periplaneta,* that use similar components including Delta-Notch signaling in GRNs for posterior development, there are differences in their interactions that have evolved since the common ancestor. Indeed, in *Tribolium*, it appears that Delta-Notch signaling may not be employed in posterior segmentation (Aranda et al., 2008), and *Tc-cad* is a maternally deposited morphogen in this beetle which regulates posterior development through control of the spatio-temporal expression of pair-rule genes (Copf et al., 2004; El-Sherif et al., 2014).

4.4.2 Expression analysis of pair-rule gene orthologs in *Parasteatoda*

In this chapter I also report that I found that *Pt-eve* and *Pt-run-1* are expressed in the SAZ and in nascent segments (see fig. 25). The expression domains of both genes predominantly overlap, with *Pt-eve* 2-3 cell rows anterior of *Pt-run-1* at the stages investigated (see fig. 25). As expected, the expression of these genes is similar between *Parasteatoda* and *Cupiennius* (Damen et al., 2000; Schonauer et al., 2016).

Interestingly, the relative expression of pair-rule ortholog genes during segmentation has diverged among arthropods, as the expression of *eve* and *run* do not overlap in *Strigamia* and *Drosophila*, but they do overlap in *Parasteatoda* and *Glomeris* (Frasch et al., 1987; Green and Akam, 2013; Janssen et al., 2011; Schonauer et al., 2016).

In *Strigamia*, three *even-skipped* paralogs have been identified and they differ in expression: *Sm-eve1* is expressed in a double segmental pattern in the posterior disc and resolves into a single segmental expression in the germ band. *Sm-eve2* is only expressed in the posterior disc and does not resolve into a stripe pattern in the germ band and *Sm-eve3* is only expressed in the transition zone, where the germ band arises. However, all three *Sm-eve* paralogs are in phase with each other and hence all three of them are out of phase with *Sm-run* expression (Green and Akam, 2013).

In the spider, the function of *Pt-eve* and *Pt-run-1* appears to be restricted to the posterior and no expression was detected in anterior structures like the prosoma or head, unlike in other arthropods (Brena and Akam, 2013; Brown et al., 1997; Frasch et al., 1987; Janssen et al., 2011; Schonauer et al., 2016). This is further evidence that patterning of the prosoma and the opisthosoma is regulated differently in the spider (Damen et al., 2005; Damen et al., 2000; Pechmann et al., 2011; Pechmann et al., 2009; Schwager et al., 2009).

It has been first established in *Drosophila* that the pair-rule genes can be distinguished by their regulation and function in primary and secondary pair rule genes. In the fruit fly *eve* acts as a primary and *run* as a secondary pair-rule gene (Ingham, 1988), while it has been found in *Tribolium* that *eve* and *run* both

act as primary pair rule genes (Choe et al., 2006). Also in the centipede, *Sm-eve1* and *Sm-run* were classified as primary pair-rule genes, due to their early onset and the double-segmental expression (Green and Akam, 2013). While not all potential regulatory input factors are known, I propose that *Pt-eve* and *Pt-run* act on the same hierarchical level and although they are expressed with single segmental periodicity they potentially act upstream of other pair-rule gene orthologues and thus represent primary-pair rule genes in the spider (Damen, 2007).

Therefore, for further analysis, I suggest testing the interactions between *Pt-eve* and *Pt-run* and other pair-rule genes like *Pt-slp* and *Pt-odd-1*, which show later segmental expression that probably overlaps with either *Pt-cad* or *Pt-eve* and *Pt-run-1*. If *Pt-slp* and *Pt-odd* act as secondary pair-rule genes, I would expect to see an effect in *Pt-eve* and *Pt-run-1* knockdown clones and no effect in *Pt-cad* clones.

In *Parasteatoda, Pt-odd* skipped is expressed in the developing walking legs, the developing head and opisthosomal segments at later stages (see fig. 27). One *odd-skipped* gene has been described in *Drosophila*, which is responsible for the specification of the anterior regions of the segments through interactions with the primary pair-rule genes *even-skipped* and *fushi-tarazu* (Coulter and Wieschaus, 1988). In *Tribolium odd-skipped* is expressed in a double-segmental pattern and has been found to repress *Tc-eve* expression in the pair-rule gene circuit (Choe et al., 2006). In *Cupiennius* expression of the *odd-skipped-related* gene was only detected in the anterior portion of the SAZ and

exhibits a transient pattern which disappears as soon as the segment forms (Damen et al., 2005).

In *Parasteatoda*, *Pt-opa* exhibits faint expression in the developing walking legs, the head and in opisthosomal appendages (see fig. 29). Whilst *odd-paired* expression is initially ubiquitous in *Drosophila*, it does resolve into segmental expression at later stages (Benedyk et al., 1994). In *Cupiennius Cs-opa* is expressed in two stripes in the SAZ and in broad single-segmental stripes in the segments (Damen et al., 2005). This is in contrast to *Parasteatoda,* where *Pt-opa* expression is absent from the opisthosoma at stages of SAZ formation and segmentation. Only at stage 12 a circular domain appears in the O2 segment, which might be associated with the development of appendages arising from this area (see fig. 29 C, chevron). This suggests that *Pt-opa* is not involved in the SAZ and segment formation and the difference between *Pt-opa* and *Cs-opa* expression suggests that they might not be homologs.

Pt-slp expression in *Parasteatoda* displays segmental expression in prosomal and opisthosomal segments and is expressed in the developing head (see fig. 31). In *Drosophila*, two *sloppy paired* paralogs have been identified (*slp1, slp2*), with almost identical expression patterns (Grossniklaus et al., 1992). *Slp1* and *slp2* are secondary pair-rule genes, maintaining segment boundaries downstream of *eve* and also exhibit redundant function in neurodevelopment (Cadigan et al., 1994; Grossniklaus et al., 1992). *Tribolium sloppy-paired* expression commences in anterior segments and resolves into a double-

segmental pattern segmentation (Choe and Brown, 2007). The functional analysis for *Tc-slp* revealed a role in gnathal segment formation, development of even-numbered segments and maintenance of odd-numbered segments of the trunk (Choe and Brown, 2007).

In *Cupiennius*, *Cs-slp* expression is segmental and restricted to the ventral portion of the segments, similar to what I found in early stages of *Parasteatoda* development (see fig.10 A, stage 8.1) (Damen et al., 2005). *Pt-slp* expression also suggests that this gene is involved in nervous system development (fig.31 B,C), like in *Drosophila*. However, my results suggest that *Pt-slp* is not involved in the formation for the SAZ, but potentially in maintaining the segmental borders because it is expressed in fully formed segments.

5 Results Chapter 3: Characterising the GRN underlying posterior segmentation, focusing on the regulatory interactions involving the pair-rule ortholog *even-skipped* in *Parasteatoda*

5.1 The pair-rule genes *Pt-eve* and *Pt-run-1* are regulated by Wnt and Delta-Notch signaling in the posterior

The dynamic expression of *Pt-eve* and *Pt-run-1* in the SAZ and in the forming opisthosomal segments suggests an involvement of these genes in SAZ formation and segmentation in *Parasteatoda*. Furthermore, the expression of *Pt-Wnt8* and *Pt-Delta* (McGregor et al., 2008b; Oda et al., 2007) precede the onset of *Pt-eve* and *Pt-run-1*, suggesting that the pair-rule gene orthologs act downstream, similar to the effect on *Pt-cad*. Hence, the effect of *Pt-Wnt8* and *Pt-Delta,* on *Pt-eve* and *Pt-run-1* were tested.

Knockdown of *Pt-Delta* with pRNAi caused the complete loss of the expression of both *Pt-eve and Pt-run-1* in the SAZ (see figs. 32 B and 31 B). *Pt-eve* and *Pt-run-1* expression was also greatly reduced after pRNAi knockdown of *Pt-Wnt8* RNAi with only a few remaining cells expressing each gene (see fig. 32 C and fig. 33 C). Previous studies of *Pt-Wnt8* RNAi phenotype embryos (McGregor et al., 2008b) suggest that the *Pt-Wnt8* knockdown effect is not complete in all embryos which may explain why a few cells still express *Pt-eve* and *Pt-run-1* expression.

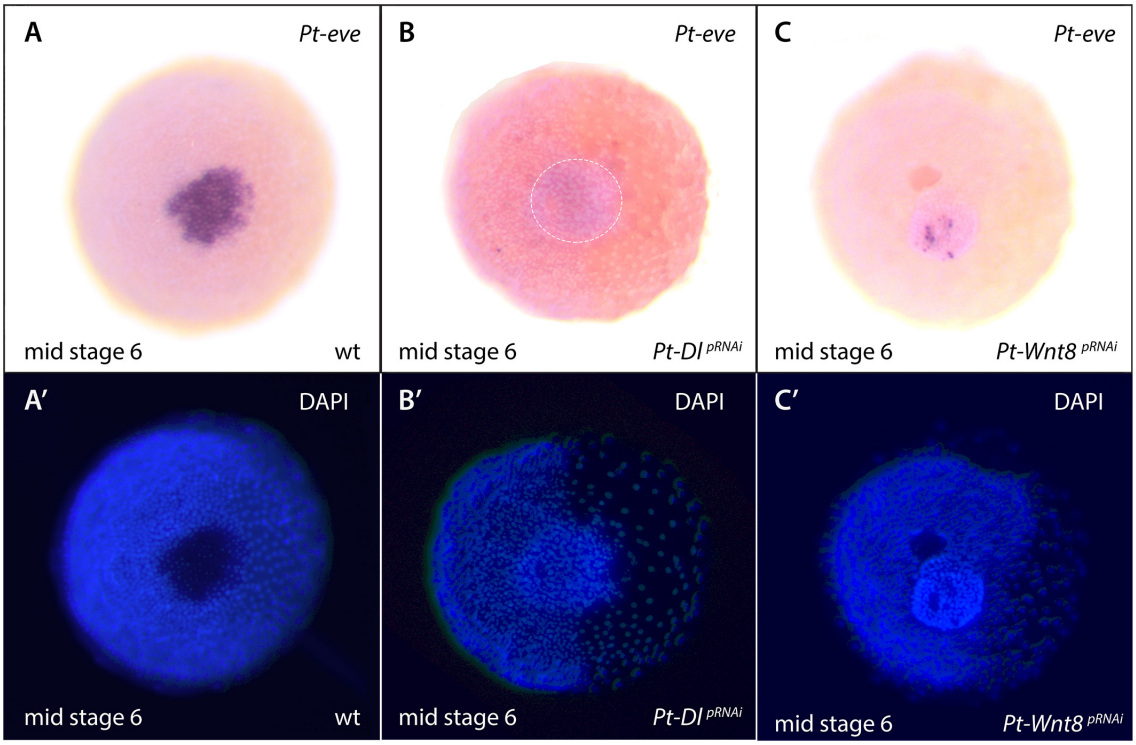

Figure 32 | *Pt-eve* expression in *Pt-Dl* and *Pt-Wnt8* RNAi embryos. Whole mount embryos in a ventral view of stage 6 embryos **(A-C)**. In all panels anterior is to the left and embryos are counterstained with DAPI. Panels **A'-C'** show the DAPI staining of the respective bright field/DAPI overlay images **A-C**. *Pt-eve* wild-type expression in the centre of the germ disc at the stage analysed in the RNAi embryos **(A)**. In *Pt-Dl* pRNAi embryos, *Pt-eve* expression is no longer detectable in the SAZ **(B).** In *Pt-Wnt8* pRNAi embryos expression of *Pt-eve* is reduced to only a few cells **(C)**. The dashed circle in **B** indicates the SAZ **A**.

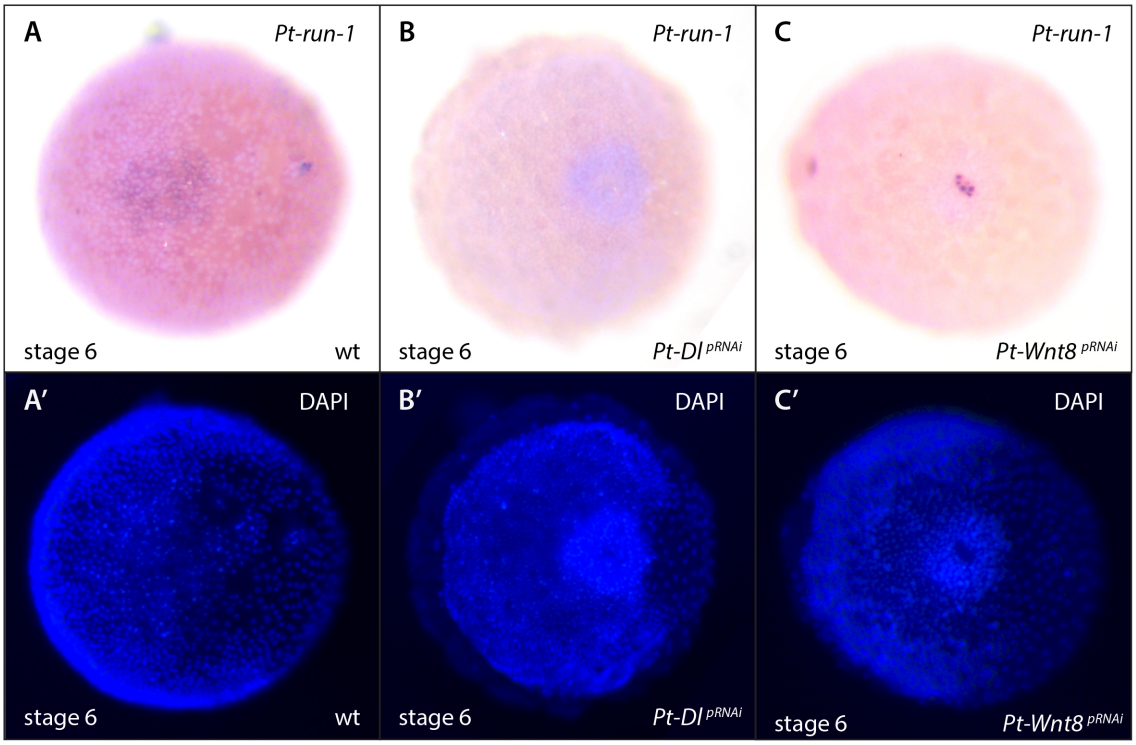

Figure 33 | Effects of *Pt-Dl* and *Pt-Wnt8* on *Pt-run-1* expression. Expression of *Pt-run-1* in wild-type (**A**), *Pt-Dl* pRNAi (**B**) and *Pt-Wnt8* pRNAi (**C**) embryos. In *Pt-Dl* pRNAi embryos, *Pt-run-1* expression is no longer detectable (**B**), compared to a wild-type *Pt-run-1* expression **(A).** Note that the dense accumulations of cells in the posterior of the *Pt-Dl* pRNAi phenotype embryo (B), causes strong background signal in the DAPI staining. In *Pt-Wnt8* pRNAi embryos, expression of *Pt-run-1* is reduced to only a few cells **(C)**. Embryonic *Pt-cad* RNAi results in a loss of expression of *Pt-run-1* in the SAZ (**D**). (**A-C)** whole mount embryos and **D** is a flat mount embryo, showing the posterior end of the opisthosoma with anterior to the left. Panels **A'-D'** show the DAPI staining of the respective bright field/DAPI overlay images **A-D**.

Intriguingly, the effects of *Pt-Wnt8* and *Pt-Delta* RNAi on the expression of *Pt-eve* and *Pt-run-1* are strongly reminiscent of the effect of knockdown of these genes on *Pt-cad* expression (McGregor et al., 2008b; Oda et al., 2007). Therefore, I next investigated if *Pt-cad* is also involved in the regulation of *Pt-eve* and *Pt-run-1*.

5.2 The effect of *Pt-cad* on *Pt-eve*

In order to investigate the possibility that *Pt-cad* could regulate *Pt-eve,* I first, analysed the expression of these two genes in relation to each other during posterior development.

Pt-cad and *Pt-eve* expression are initially detected at mid stage 6 in a small domain in the centre of the germ disc (see fig. 34 A). *Pt-eve* clears from the central part, whereby *Pt-cad* expression persists in this domain (see fig. 34 A'). Subsequently, *Pt-eve* and *Pt-cad* expression expands into an overlapping crescent shaped domain at the anterior of the SAZ, but *Pt-cad* expression then persists in the more anterior cells from which expression of *Pt-eve* has cleared (see fig. 34 B). At stage 7, both *Pt-eve* and *Pt-cad* are expressed in a partially overlapping stripe in the nascent O1 segment: *Pt-eve* is expressed in the anterior-most row of cells, followed by two rows of cells with overlapping expression and *Pt-cad* is expressed alone in approximately two rows of the most posterior cells of the stripe (see fig. 34 C). At this stage a new domain of overlapping expression of *Pt-eve* and *Pt-cad* can also be observed in posterior SAZ cells (see fig. 34 C). The two genes continue to be expressed in a similar fashion during the subsequent addition of segments (see fig. 34 D, E). Thus the relative expression patterns of *Pt-cad* and *Pt-eve* suggest that there might be a regulatory interaction between these two genes, due to a significant degree of overlap.

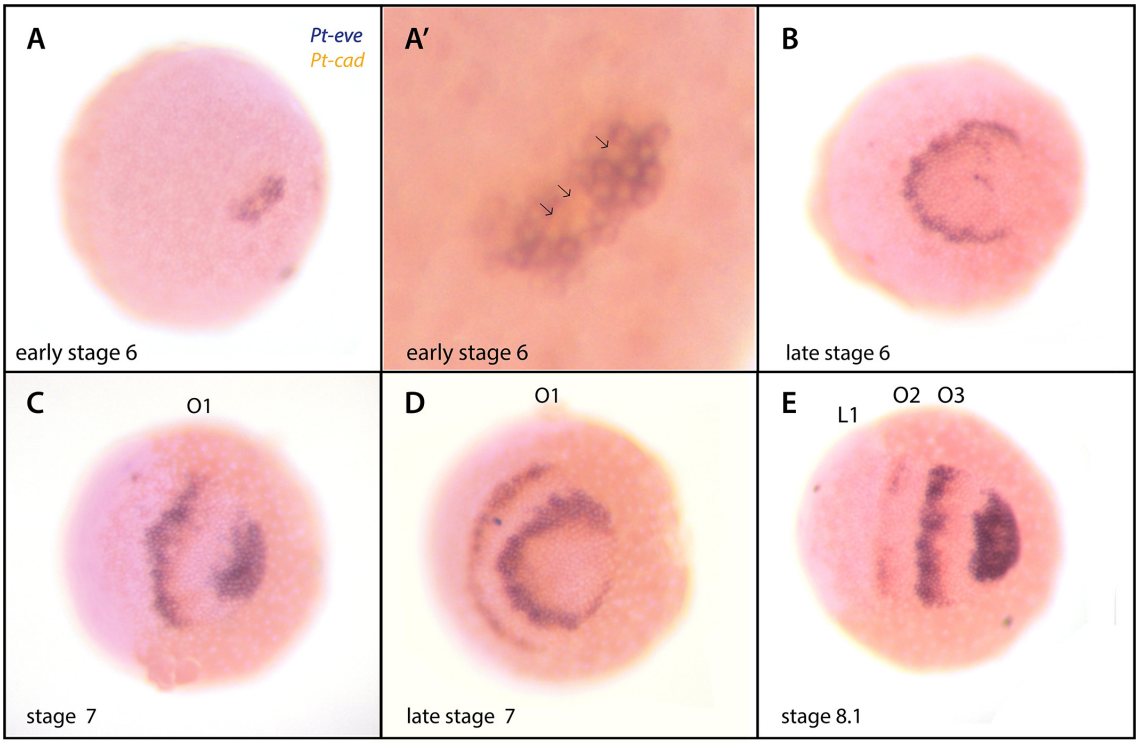

Figure 34 | *Pt-eve and Pt-cad* wild-type expression. Whole mount embryos in a ventral view of stage 6 embryos **(A-C)** and opisthosomal germ band **(C-E)**, respectively. In all panels anterior is to the left and embryos are counterstained with DAPI. *Pt-cad* (orange) and *Pt-eve* (blue) are initially co-expressed in about 15 cells in the SAZ (**A**). However, *Pt-cad* expression remains in cells, where Pt-eve has cleared again (black arrows) **(A')**. Expression of both genes then clears from the posterior and *Pt-cad* and *Pt-eve* are expressed in an overlapping crescent shaped domain, where *Pt-eve* is expressed more anteriorly (**B**). Subsequently, *Pt-eve* and *P-cad* are both again expressed in the posterior SAZ cells (**C**) with successive clearing, and in one (**D**) or two (**E**) of the youngest segments. The *Pt-cad* expression is broader than that of *Pt-eve* and persists for longer in the SAZ (**D-F**).

Despite several attempts previously, the knockdown of *Pt-cad* with parental RNAi did not result in any obvious phenotype (McGregor, personal communication). However, I showed that I could knockdown *Pt-cad* expression in clones by applying eRNAi (Kanayama et al., 2011; Kanayama et al., 2010) (also see chapter 2.4.3.) using two dsRNAs, corresponding to two non-overlapping fragments of the *Pt-cad* coding region (*Pt-cad* fragment 1 16, *Pt-cad* fragment 2 n=11) (data not shown).

The effect of *Pt-cad* eRNAi on *Pt-eve* expression during different stages of posterior development was then investigated (n=16) (see fig. 35 B, D). At stage 6, *Pt-eve* expression was lost or strongly reduced from cells subject to *Pt-cad* knockdown (see fig. 35 B). Similarly, *Pt-cad* eRNAi also results in reduced *Pt-eve* expression within the nascent segment and the SAZ at stage 7 (see fig. 35 D). These results suggest that *Pt-cad* is required for *Pt-eve* expression in *Parasteatoda* and confirms the hypothesis drawn from the previous results that Wnt and Delta-Notch signaling act at least in part via *Pt-cad* to regulate segmentation genes like *Pt-eve*.

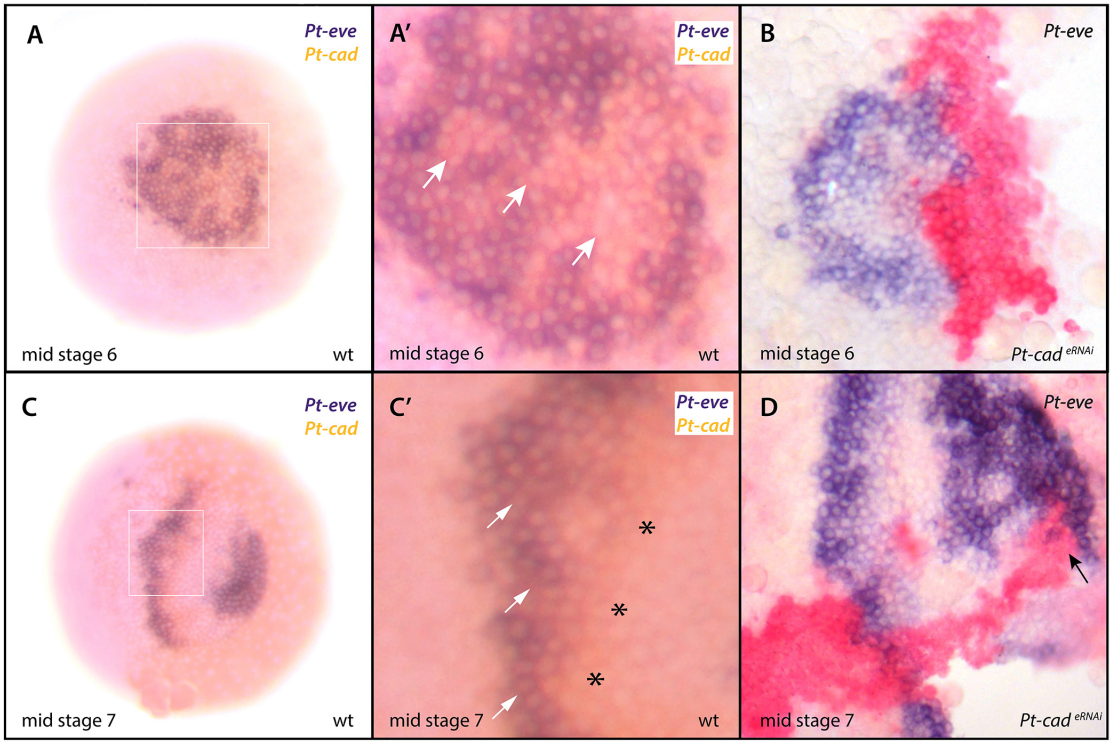

Figure 35 | The effect of *Pt-cad* on *Pt-eve* expression. Whole mount embryos in a ventral view of stage 6 embryos **(A-B)** and opisthosomal germ band **(C-D)**, respectively. In all panels anterior is to the left and embryos are counterstained with DAPI. The effect of *Pt-cad* RNAi on *Pt-eve* in the SAZ and the nascent segments was observed in 16 injected embryos in total.

5.3 The effect of *Pt-cad* on *Pt-run-1*

Pt-cad and *Pt-run-1* are both expressed in the SAZ, with alternating phases of clearing and strong expression, and in stripes in the forming segments (see fig. 18 A-F and fig. 24 A-F). The expression of *Pt-run-1* in relation to *Pt-cad* is reminiscent of to the relative expression of *Pt-eve* to *Pt-cad* (see fig. 34 A-E), whereby *Pt-eve* is 2-3 cell rows anterior of *Pt-run-1*.

Since the effect of pRNAi against Delta/Notch and Wnt8 on *Pt-run-1* expression (see fig. 36 B, C) is reminiscent of the result on *Pt-eve* expression, it has been suggested that this may also be indirect through the loss of *Pt-cad*. Therefore, I then tested whether *Pt-cad* is also required for *Pt-run-1* expression. I found that eRNAi against *Pt-cad* results in the loss of *Pt-run* expression in SAZ cells suggesting that *Pt-cad* is required for *Pt-run-1* expression (1), as well as *Pt-eve* expression (see fig. 36 B).

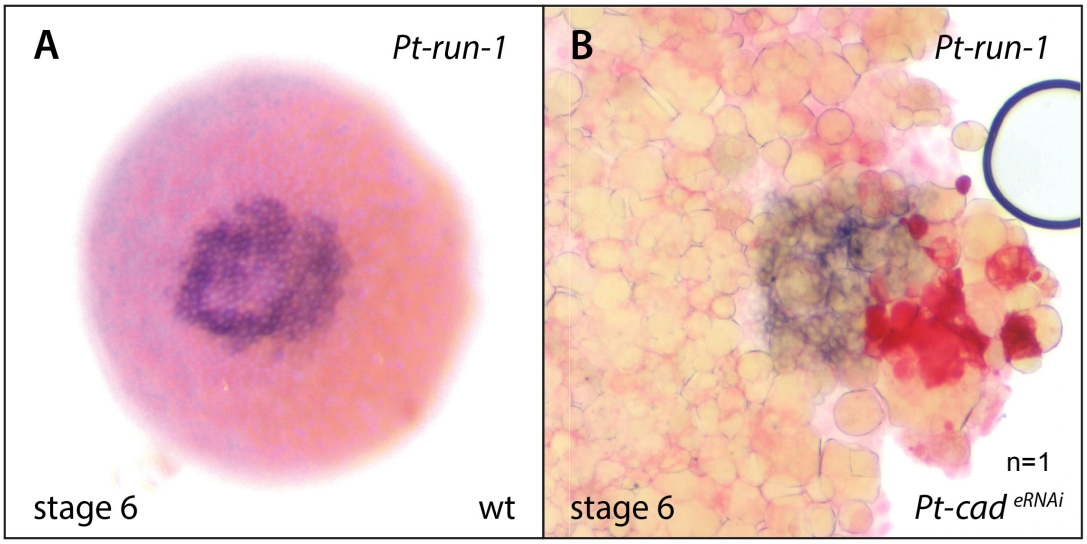

Figure 36 | *Pt-cad* activates *Pt-run-1* expression. Whole mount (**A**) and a flat mount (**B**) embryos of the opisthosoma **(B)**. At stage 6, *Pt-run-1* is expressed in a circular domain in the SAZ (**C**), in a similar expression domain to *Pt-cad* at this stage (see fig 17 A). *Pt-run-1* expression is down regulated in the *Pt-cad* knockdown clone in the SAZ **(B)**.

5.4 Pt-cad is not sufficient for the activation of *Pt-eve*

Since the above experiments show that *Pt-cad* expression necessary to activate *Pt-eve* expression, I then tested if it is sufficient. To do this I injected capped *Pt-cad-eGFP* mRNA into blastomeres at the 16-cell stage and allowed them to develop until stage 5 (i.e. before *Pt-cad* and *Pt-eve* are normally expressed). Clones of cells with nuclear GFP expression were observed (see fig. 37 B), demonstrating that *Pt-cad* was expressed and able to localise to the nuclei (n = 5). These embryos were fixed at stage 5 and an in situ hybridisation for *Pt-eve* was carried out. However, I did not observe expression of *Pt-eve* in any of these cells even after staining until background started to appear. This indicates, that while *Pt-cad* expression is required for *Pt-eve* expression, it is not sufficient in these conditions (see fig. 37 C). Indeed, since some of these cells expressing *Pt-cad*-GFP near the pole of the germ at this stage are likely to also express *Pt-Wnt8* and *Pt*-Dl (McGregor et al., 2008b; Oda et al., 2007), this implies that an additional factor or factors are required to activate *Pt-eve* (see fig. 37 A).

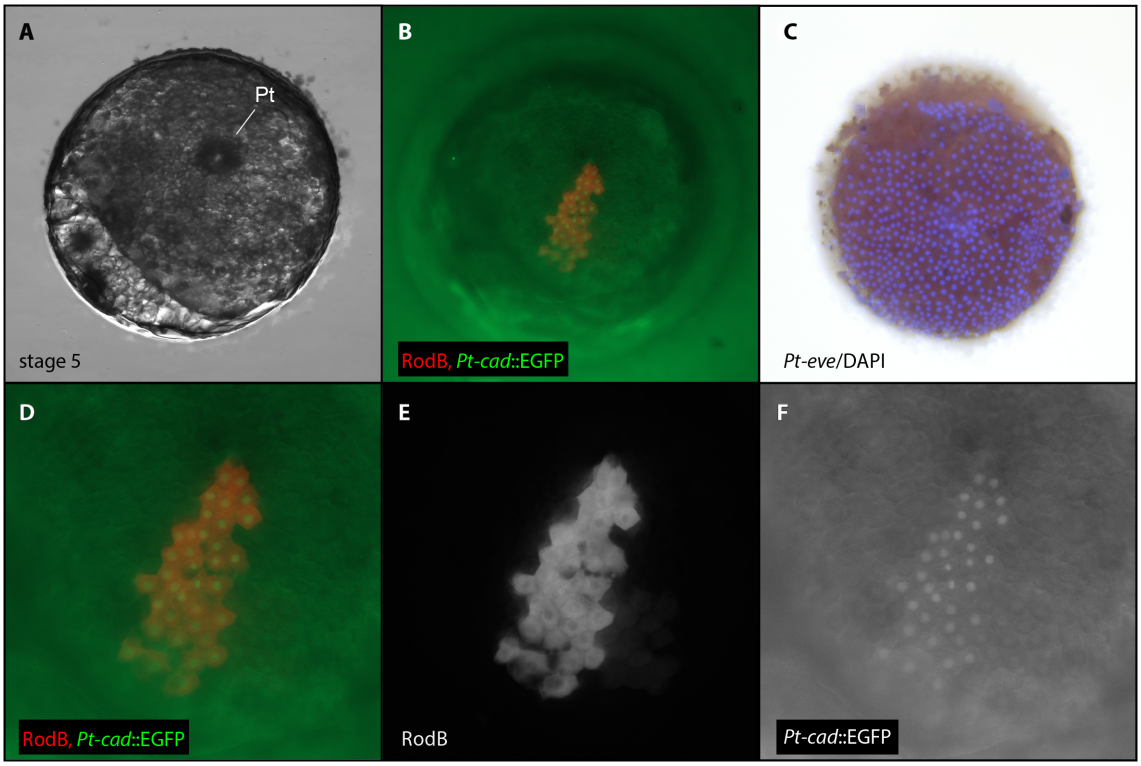

Figure 37 | *Pt-cad* expression is not sufficient to induce *Pt-eve* expression. The injected embryo shown was imaged at stage 5, when the primary thickening (Pt) can be found in the center of the germ disc (**A**). Injection with *Pt-cad*::eGFP/RITC-dextran (at the 16 cell stage) generated a clone of cells which exhibit specific nuclear eGFP expression and exclusively cytoplasmic signal of the fluorescent marker Rhodamine B (RodB) (**B**). After in situ hybridisation, *Pt-eve* expression could not be detected in any cells of the respective *Pt-cad*::eGFP/RITC-dextran injected embryo (**C**). Panels **D-F** show a higher magnification of the same *Pt-cad*::eGFP/RITC-dextran clone, whereby RITC-dextran is only detected in the cytoplasm (**E**) and eGFP is expressed in the nuclei of the clone cells (**F**). Panel **A** shows a bright field image of the injected embryo. Panels **B, D-F** show images of the same live embryo. Panel **C** shows the same embryo after fixation and *Pt-eve* in situ hybridisation, overlaid with a DAPI counterstain image. Abbreviation: Pt, primary thickening.

5.5 Pt-eve does not effect *Pt-cad*

I then tested if *Pt-eve* feeds back to regulate *Pt-cad* expression. As for *Pt-cad*, pRNAi knockdown for *Pt-eve* did not appear to work (McGregor personal communication). Therefore, eRNAi was successfully established for *Pt-eve:* the microinjection of dsRNA covering the entire *Pt-eve* coding region resulted in a loss of *Pt-eve* expression (n = 4). However, the knockdown of *Pt-eve* using eRNAi did not appear to affect *Pt-cad* expression in the SAZ and in the forming

segments unaffected (n = 16) (see fig. 38 B, D). This indicates that *Pt-eve* does not regulate *Pt-cad* expression and is thus downstream of *Pt-cad* in the GRN of segmentation in *Parasteatoda*.

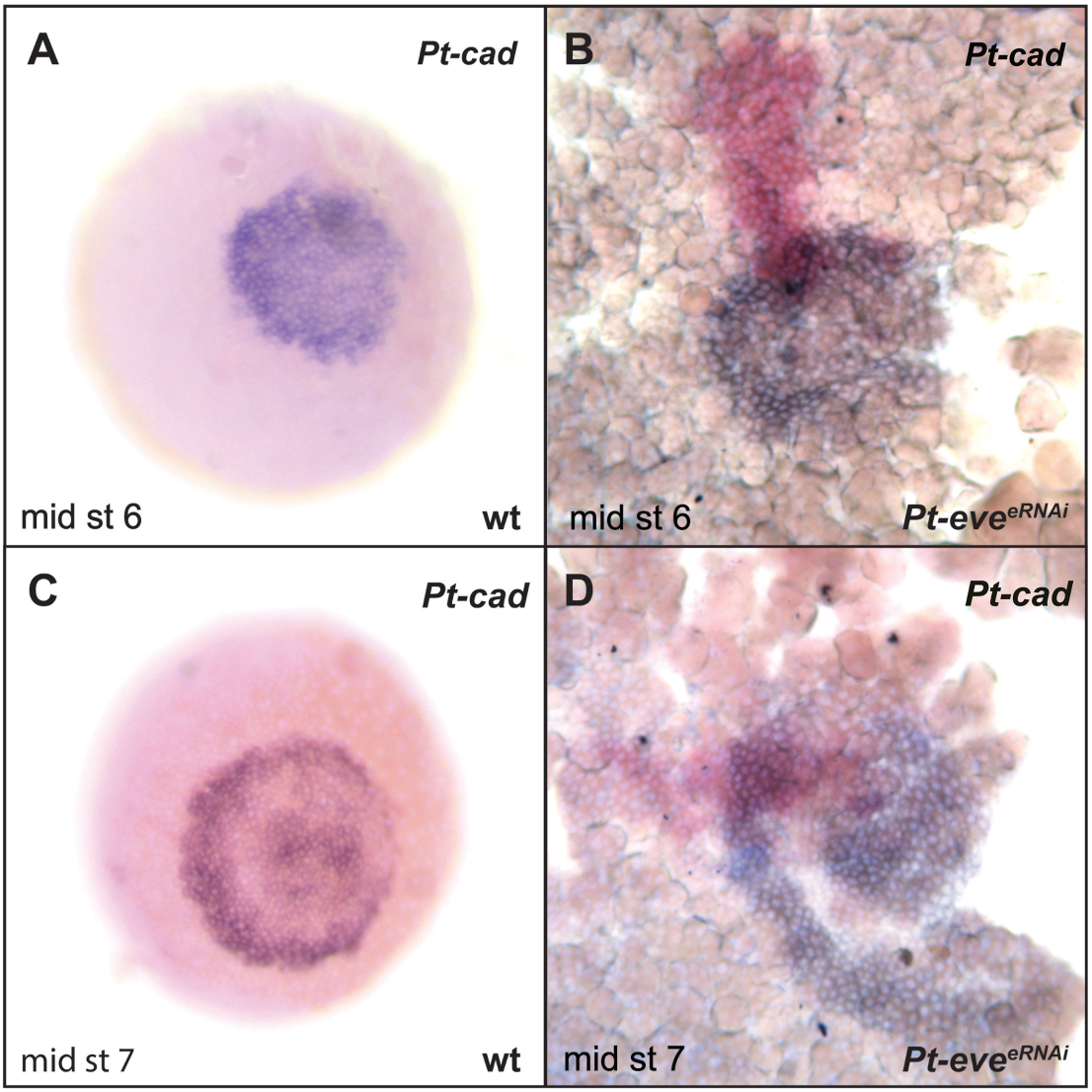

Figure 38 | *Pt-eve* does not have an effect on *Pt-cad* expression. Whole mount embryos in a ventral view of stage 6 embryos **(A-B)** and opisthosomal germ band **(C-D)**, respectively. In all panels anterior is to the left and embryos are counterstained with DAPI. *Pt-cad* is expressed in a circular domain at stage 6 **(A)** and continues to be expressed in the posterior and an anterior SAZ domain at mid stage 7 in wild-type embryos **(C)**. In the areas where the *Pt-eve* knockdown clone overlaps with the *Pt-cad* domain, expression is unaffected in the SAZ at mid stage **(B)** and also in the forming segment at mid stage 7 **(D)**.

5.6 *Pt-eve* and *Pt-run-1* do not regulate each other

In *Tribolium*, it has been reported that a regulatory circuit directs the expression of pair-rule genes in a clock-like mechanism in order to form segments from the SAZ (Choe et al., 2006). In this model *Tc-eve* activates *Tc-run,* which further activates *Tc-odd* and which in turn represses *Tc-eve* (Choe et al., 2006). To test if a similar circuit operates in *Parasteatoda*, I investigated the regulatory interactions between *Pt-eve* and *Pt-run-1*.

To test if *Pt-eve* regulates *Pt-run* in *Parasteatoda* eRNAi knockdown of *Pt-eve* was carried out and the effect on *Pt-run-1* expression at different stages of posterior development was assayed. At all observed stages, no detectable effect of the *Pt-eve* knockdown on *Pt-run* expression could be found (n=12) (see fig. 39 B). This suggests that, in contrast to the pair-rule circuit in *Tribolium*, *Pt-eve* is not required to activate *Pt-run-1* during segment addition in *Parasteatoda*.

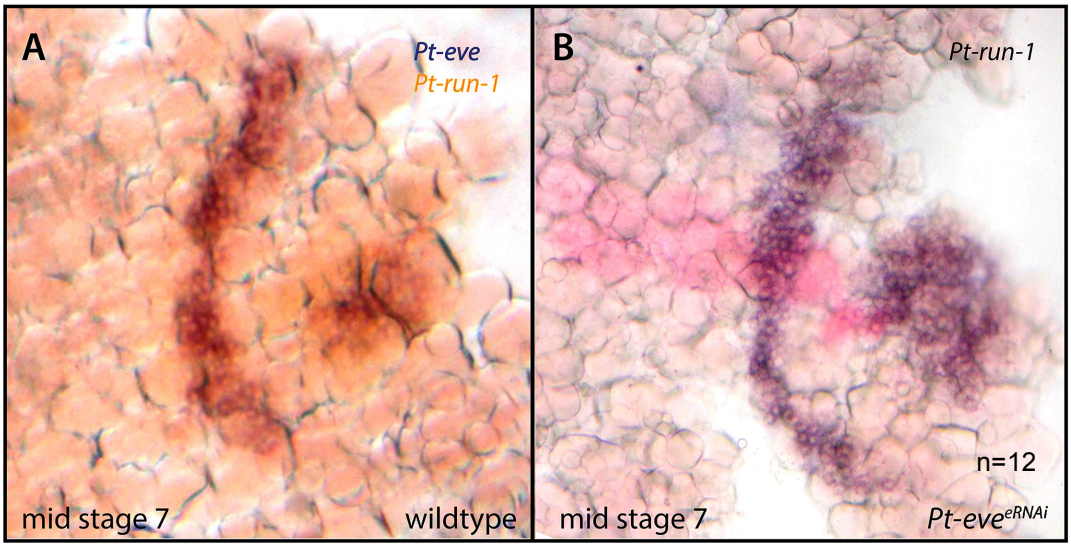

Figure 39 | *Pt-eve* does not have an effect on *Pt-run-1* expression. Flat mount embryos of the opisthosoma **(A,B)**. In all panels anterior is to the left. At mid stage 7 *Pt-eve* and *Pt-run-1* expression overlap in the SAZ and in the forming segment **(A)**. *Pt-run-1* expression appears normal in the *Pt-eve* knockdown area in the SAZ and in the nascent segment **(B)**.

I then tested whether knockdown of *Pt-run-1* affected *Pt-eve* expression. I first showed that two non-overlapping fragments of the *Pt-run-1* CDS were able to knockdown *Pt-run-1* expression in the SAZ and segments (n = 13) (see fig. 40 A, B). However, injection of *Pt-run-1* dsRNA had no discernable effect on *Pt-eve* expression in the SAZ (see fig. 40 D) or in the forming segments (n = 7) (see fig. 40 C). This suggests that *Pt-run-1* does not inhibit *Pt-eve* in *Parasteatoda* and thus does not support the hypothesis of a pair-rule gene circuit regulating segmentation in the spider, at least not exactly like the model described in *Tribolium* (Choe et al., 2006).

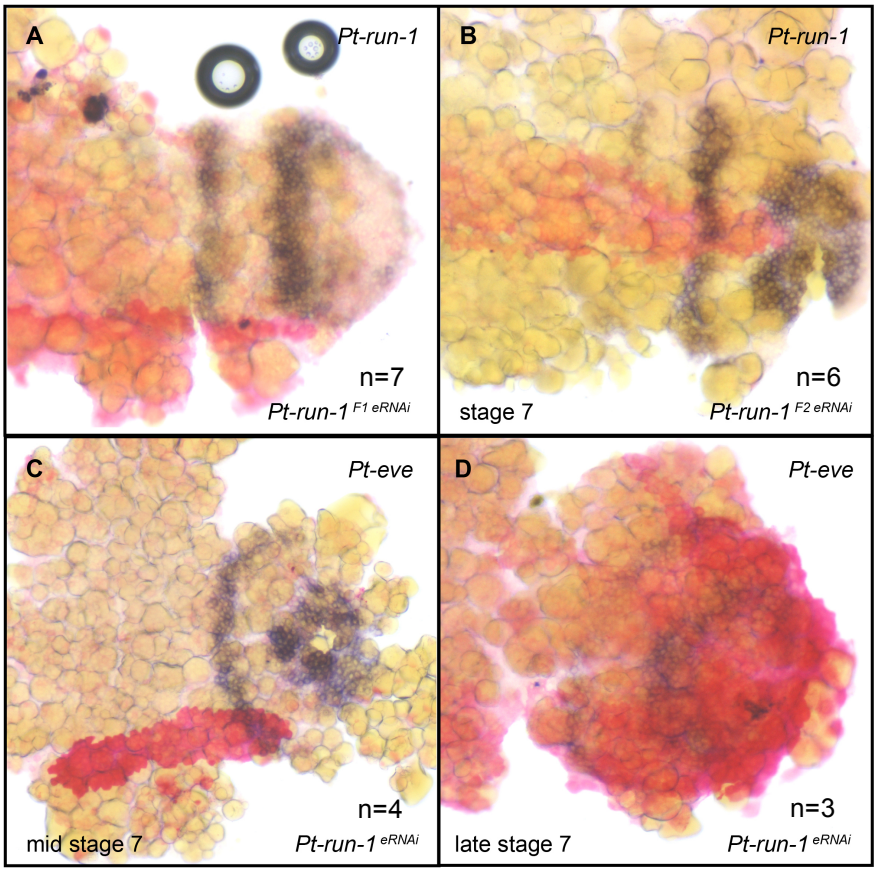

Figure 40 | *Pt-run-1* does not affect *Pt-eve* expression. Flat mount embryos of the opisthosoma **(A-D)**. In all panels anterior is to the left. Two non-overlapping fragments of the *Pt-run-1* CDS, *Pt-run-1* F1 (**A**) and *Pt-run-1* F2 (**B**), were tested for the knockdown of *Pt-run-1* expression. At mid stage 7 *Pt-eve* is expressed in the posterior SAZ and in anterior stripe (**C**), largely overlapping with *Pt-run-1* expression (see fig **A**). *Pt-eve* expression appears normal in the *Pt-run-1* knockdown clone in the nascent segment (**C**) and in the SAZ **(D)**.

5.7 Discussion

I have found that while the knock down of either *Pt-Wnt8* or *Pt-Dl* affects *Pt-eve* and *Pt-run-1* expression, this is probably not a direct effect, but is mediated through *Pt-cad,* which I have shown is required for the expression of both these pair-rule gene orthologues (Schonauer et al., 2016). It appears that *Pt-cad* may not be sufficient to activate *Pt-eve*, however, which would suggest that other factors are required to activate *Pt-eve* and *Pt-run-1* expression that may or may not depend on Wnt8 and Delta-Notch signaling.

Furthermore, I tested if *Pt-eve* expression has an effect on *Pt-cad*. However, no discernable effect on *Pt-cad* expression was observed, which suggests that *Pt-eve* is downstream of Delta-Notch/Wnt8/Cad in *Parasteatoda*.

However the results of the *Pt-cad* overexpression experiment may have to be questioned in terms of the functionality of the tagged *Pt*-Cad protein: it is not clear if the *Pt*-Cad protein is folded correctly and hence functional, since the protein structure might be affected by the GFP tag. To follow this up, GFP could be replaced by a smaller tag (e.g. HA tag ~100bp) in order to label *Pt*-Cad. Furthermore, the position of the GFP tag at the C-terminus might interfere with the function of homeodomain, which is only ~ 30 aa upstream of the C-terminus. Therefore, tagging the *Pt*-Cad protein at the N-terminus could help prevent potential interference with folding and function of the protein in this case. Moreover, it would be desirable in terms of a control, to be able to detect the *Pt*-Cad protein itself, rather than just the marker, i.e. with an antibody staining, however, as far as I am aware there is no cross-reacting antibody available.

In *Tribolium, Tc-eve* is also regulated by *Tc-cad* (El-Sherif et al., 2014) and therefore, also considering findings in *Periplaneta* (Chesebro et al., 2013), it appears that the regulation of *eve* by *cad* may have been ancestral feature of arthropods. Furthermore in the proposed pair-rule circuit in *Tribolium*, *Tc-eve* activates *Tc-run,* which in turn activates *Tc-odd* (Choe et al., 2006). *Tc-odd* then represses *Tc-eve* in even-numbered parasegments and thus primary *Tc-eve* stripes are generated (Choe et al., 2006). Given the largely overlapping expression patterns in the SAZ and the developing segments of *Parasteatoda*, I tested if a similar circuit operated in this spider. However, the knockdown of *Pt-eve* left *Pt-run-1* unaffected and there was also no effect on *Pt-eve* in *Pt-run-1* knockdown clones. This suggests that the pair-rule gene orthologs examined are not connected in a *Tribolium*-like pair-rule gene circuit (Choe et al., 2006; Schonauer et al., 2016). On the contrary the effect of *Pt-Dl, Pt-Wnt8* and *Pt-cad* RNAi knockdown on *Pt-eve* and *Pt-run-1* suggests that pair-rule gene orthologs are instead only regulated by such upstream factors. Summarizing these results, I suggest that pair-rule gene orthologues in the spider are not regulated by a pair-rule gene circuit, but a Delta-Notch/Wnt/Cad organizer, which might be ancestral to all arthropods (Chesebro et al., 2013; Schonauer et al., 2016). Furthermore, my results suggest that the pair-rule gene circuit as established in *Tribolium* is a derived mechanism for generating a segmental pattern that may not be dependent on Delta-Notch signaling.

6 Results Chapter 4: Investigating the expression of frizzled receptor genes during spider embryogenesis

During embryonic development Wnt signaling is fundamental for cell-cell communication in multiple developmental processes like cell division, cell fate decision, cell morphology and cell movement (Logan and Nusse, 2004). In the case of the canonical pathway, secreted Wnt glycoprotein ligands bind the 7-transmembrane receptors of the Frizzled family and a lipoprotein receptor-related protein (LRP) co-receptor (*arrow* in *Drosophila*) and thereby trigger the phosphorylation of the downstream factor Dishevelled. This results in the inhibition of a multi-protein complex (including GSK3 (glycogen synthase kinase 3), APC (adenomatosis polyposis coli protein) and Axin) that normally leads to the degradation of β-catenin (Komiya and Habas, 2008), which instead now increases in concentration and enters the nucleus where it binds to LEF/TCF regulates transcription (Behrens et al., 1996) (see fig. 41).

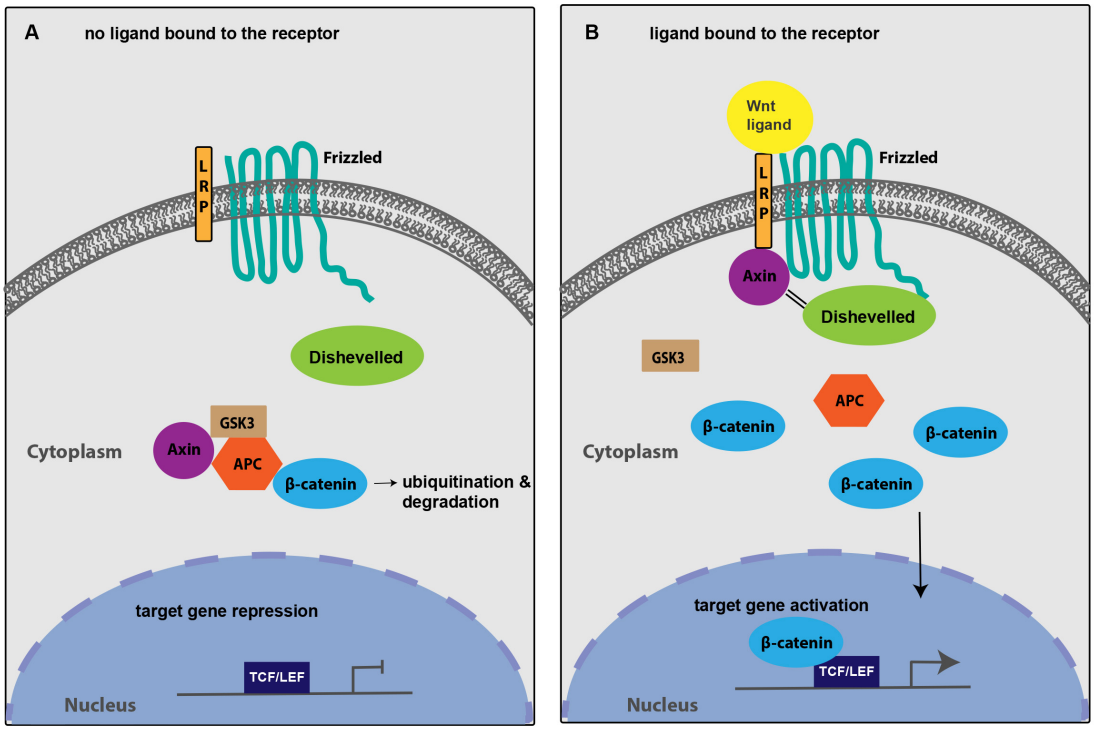

Figure 41 | Canonical Wnt signaling pathway. (A) If no ligand is bound to the receptor an enzyme complex consisting of axin, GSK3 B, APC prevents β-catenin from entering the nucleus. The downstream factor Dishevelled is expressed ubiquitously in the cytoplasm. Target gene expression is inhibited by Lef/TCF. **(B)** The binding of a Wnt ligand to the frizzled and the co-receptor LRP causes the phosphorylation of Dishevelled and binding to the Frizzled receptor. Also, axin binds the LRP co-receptor, which subsequently falls apart and allows β-catenin to enter the nucleus and activate target gene expression. Illustration redrawn from (Staal and Clevers, 2005).

Wnt ligands

Metazoans have 13 Wnt ligands, although deuterostomes have lost *Wnt A* (Kusserow et al., 2005) and protostomes have lost Wnt3 (Cho et al., 2010; Garriock et al., 2007; Janssen et al., 2010). *Parasteatoda* has 12 Wnt ligand genes, having lost *Wnt9* and *Wnt10* but containing duplicates of *Wnt7* and *Wnt11 (Janssen et al., 2010)*. Insects on the other hand have lost several Wnts and only *Wnt9* and *Wnt7* are found in *Tribolium* and *Drosophila* respectively (Janssen et al., 2010). However, the loss of Wnts in some insects does not seem to represent a general arthropod feature, as the crustacean *Daphnia* has

retained 12 and the myriapod *Strigamia* 11 Wnt ligands (Hayden and Arthur, 2014; Janssen et al., 2010). Comparative analysis of Wnt expression and function across protostomes illustrated that many Wnt ligands are likely involved in segment formation (Hogvall et al., 2014; Janssen et al., 2010; Murat et al., 2010).

Frizzled receptors

Other functionally important components of the Wnt signaling pathway are the frizzled receptors, which consist of a conserved cysteine-rich domain (CRD), followed by a variable region (see fig. 42). The adjacent 7 trans-membrane domain transverses the plasma membrane and is followed by the N-terminal KTXXXW motif, which is part of the intracellular domain (MacDonald and He, 2012; Park et al., 1994b) (see fig. 42). The CRD has been found to be responsible for ligand recognition and the trans-membrane domain works as an anchor for the corresponding Wnt protein. The KTXXXW motif transduces the signal through phosphorylating the intracellular downstream target Dishevelled (Huang and Klein, 2004; Umbhauer et al., 2000) (see fig. 42).

Figure 42 | General structure of the frizzled receptors. The cysteine-rich domain (CRD) is located at the C-terminal end, adjacent to a variable part of the receptor. The 7 trans-membrane domain, which transverses the cell membrane, binds the Wnt ligand, whereas the KTXXXW motif at the N-terminus, activates the intracellular downstream cascade.

Four frizzled genes have been described in *Drosophila* and these receptors are involved in cell polarity and amongst other functions, regulate bristle orientation in epidermal cells (Adler, 2002; Wang et al., 1996). In *Drosophila,* Frizzled and DFrizzled-2 both act as *wingless* (*wg*) receptors, which amongst other functions, maintain *en* expression in an adjacent stripe of all developing segments (Bhanot et al., 1996; Bhanot et al., 1999; Martinez-Arias and Lawrence, 1985).

In *Tribolium* there are three frizzled genes (*Tc-Fz1, Tc-Fz-2, Tc-Fz-4*) and the co-receptor *arrow,* regulating GZ maintenance, axis elongation and leg development (Beermann et al., 2011; Bolognesi et al., 2009). The knockdown of both *Tc-Fz1* and *Tc-Fz2* and *Tc-arrow*, respectively caused a reduction of the GZ and malformation of the pre-segmental region, located just anterior to the GZ. This functional analysis evidenced a crucial role for Wnt signaling in the posterior of the beetle during axis elongation and segmentation (Beermann et al., 2011).

Wnt signaling has been shown to be essential for segmentation in spiders (McGregor et al., 2008b) and four frizzled receptors have been identified in *Parasteatoda* (Janssen et al., 2015), however its unclear which Wnt ligands use which receptor for signal transduction. To gain insights into frizzled receptor evolution and to investigate the potential role of frizzled receptors in spider segmentation, I studied the expression of frizzled receptors in *Parasteatoda.*

6.1 Analysis of the *Parasteatoda* frizzled receptors expression over the course of embryonic development

To investigate the roles of the four frizzled receptors (*Pt-fz1*, *Pt-fz2*, *Pt-fz4a, Pt-fz4b*) during embryogenesis in *Parasteatoda* in situ hybridisation was carried out for each of these genes.

6.1.1 *Pt-fz1* expression in *Parasteatoda*

Pt-fz1 is expressed ubiquitously at low levels during stages 5-12. However, stronger and more specific expression was observed at stage 9.1 at the margin of the segmental grooves in the ventral neuroectoderm of the prosomal and the opisthosomal segments (see fig. 43).

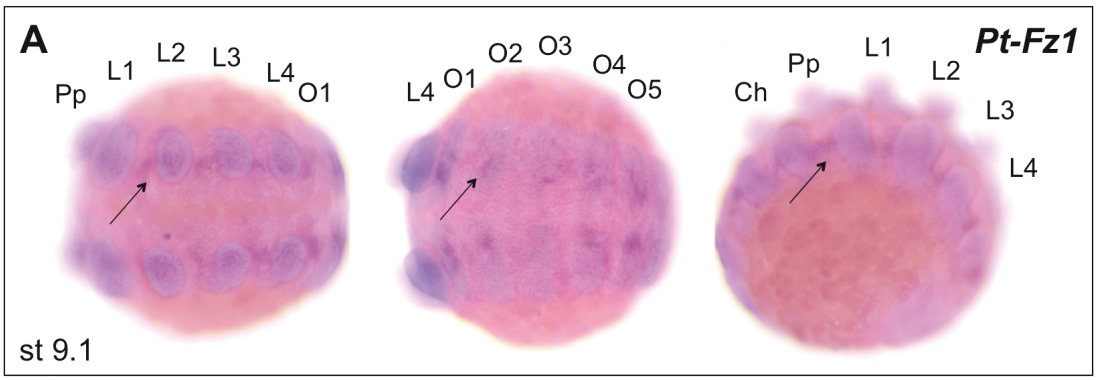

Figure 43 | Expression of *Pt-Fz*1. The same embryo is shown in a prosomal (left), an opisthosomal (middle) and a lateral (right) view. Anterior is to the left and the embryo is counterstained with DAPI. **(A)** Expression in the ventral neuroectoderm of the segmental grooves (arrows) becomes apparent at stage 9.1.

6.1.2 *Pt-fz2* expression in *Parasteatoda*

Pt-fz2 expression commences at stage 5 in a broad ring encompassing the germ disc (see fig. 44). During stage 6, expression is restricted to an anterior stripe encompassing the germ disc (see fig. 44 A). This anterior domain broadens during stage 7 and will become the future prosoma (fig. 44 B). *Pt-fz2* is subsequently expressed in a narrow stripe along the anterior margin of the germ band and in the prosomal segments at stage 8.1 (see fig. 44 C). At this stage expression in L3 and L4 is much broader compared to L1 and L2 (see fig. 44 C). At stage 8.2, when prosomal segments become morphologically visible and the first opisthosomal segment (O1) has formed, *Pt-fz2* is expressed in the anterior portion of each segment and in the segmental groove (see fig. 44 D). At this stage the expression at the anterior margin of the germ broadens (see fig. 44 D). At stage 9.2, strong *Pt-fz2* expression in the developing head refines to the anterior portion of each precheliceral lobe (PcL) and surrounds the stomodeum (see fig. 44 E, white arrow). Strong *Pt-fz2* expression can also be observed in the ventral neuroectoderm and the dorsal periphery of each segment and in nascent opisthosomal segments (see fig. 44 E). However, no expression of *Pt-fz2* was observed in the SAZ at any stage.

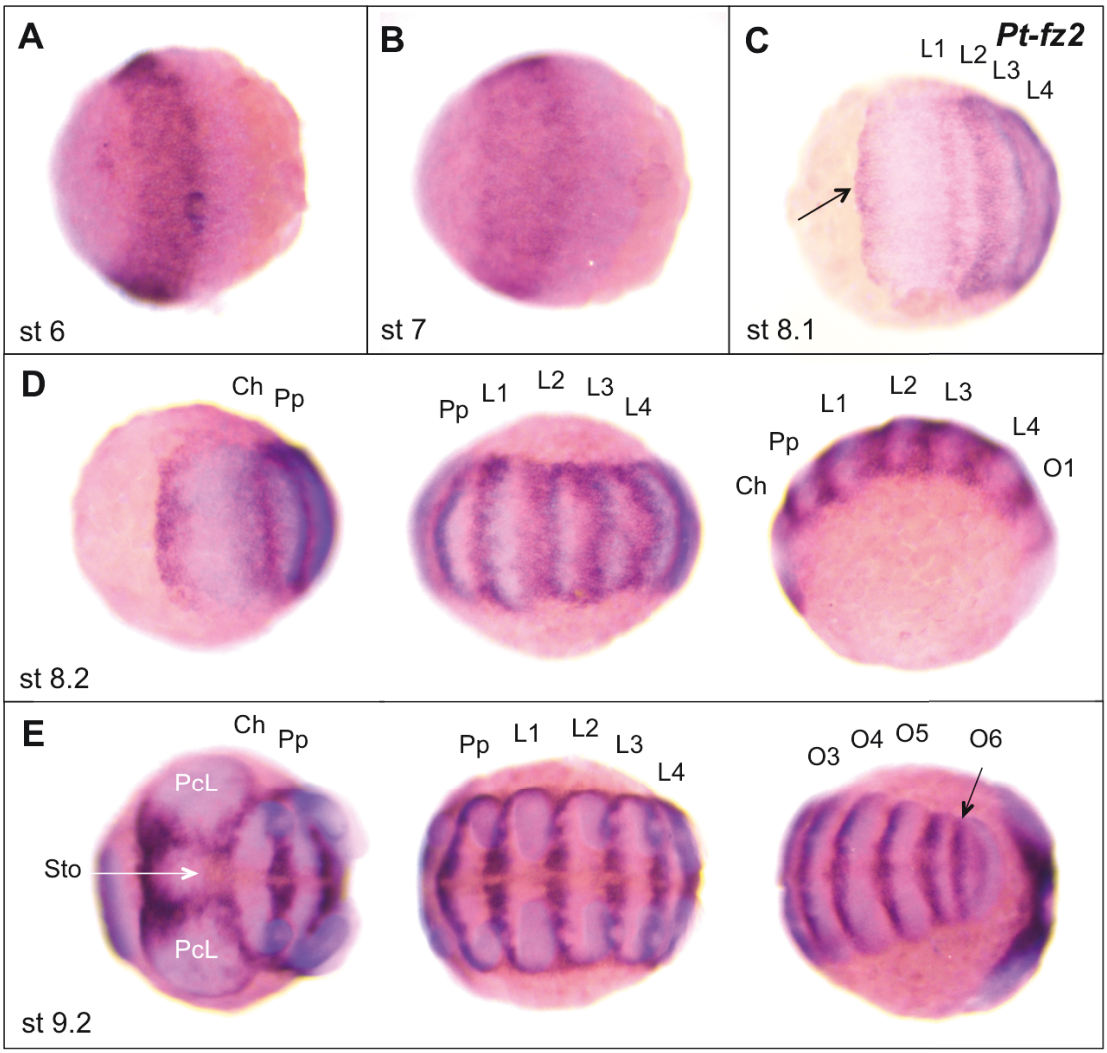

Figure 44 | *Pt-fz2* wildtype expression during stages 6-9.2. Panel **D** and **E** show the same embryo, respectively in an anterior (left), prosomal (middle), and a lateral (right) **(D)** or an opisthosomal (right) **(E)** view. In all panels anterior is to the left and embryos are counterstained with DAPI. At stage 6 *Pt-fz2* is expressed in a stripe in the anterior **(A)**, which becomes wider at a slightly later stage **(B)**. In the developing embryo, *Pt-fz2* expression expands in the forming prosomal segments, whereby expression in L3 and L4 is much broader than in L1 and L2 **(C)**. *Pt-fz2* is also expressed in a thin stripe at the anterior of the germ band at stage 8.1 (**C,** black arrow). At stage 8.2 *Pt-fz2* is expressed in the anterior portion for each segment and in the segmental groove **(D)**. The *Pt-fz2* expression domain at the anterior margin of the developing head lobe has become broader at stage 8.2 **(D)**. At stage 9.2, *Pt-fz2* expression head lobe expression refines to the anterior of each precheliceral lobe (PcL) and the future stomodaeum area (Sto, white arrow, **E**). Strong expression can also be found in the ventral neuroectoderm and the dorsal periphery of each segment, however the SAZ does not show *Pt-fz2* expression (black arrow indicates expression in the youngest opisthosomal segment O6, **E)**.

6.1.3 Pt-fz4-1 expression in *Parasteatoda*

Pt-fz4-1 expression was first detected at stage 8.2 in the segmental groove posterior of the O2 segment and in the forming O3 segment (see fig. 45 A). *Pt-fz4-1* expression was also detected later in the mesoderm of the developing limbs and in a definite domain of future neural tissue at the precheliceral lobes at stage 9.2 (see fig. 45 B). At a later stage, *Pt-fz4-1* becomes stronger and more broadly expressed in the limb mesoderm and expands also in the ventral neuroectoderm (see fig. 45 C). The expression in the head lobes continues throughout stage 9.2 (see fig. 45 C). At stage 12 *Pt-fz4-1* is strongly expressed in the limb mesoderm and in the mesoderm of the opisthosomal segments (see fig. 45 D). The faint expression in the head is restricted to the anterior border of the lobes and the labrum (L) region (see fig. 45 D; Lb, white arrow).

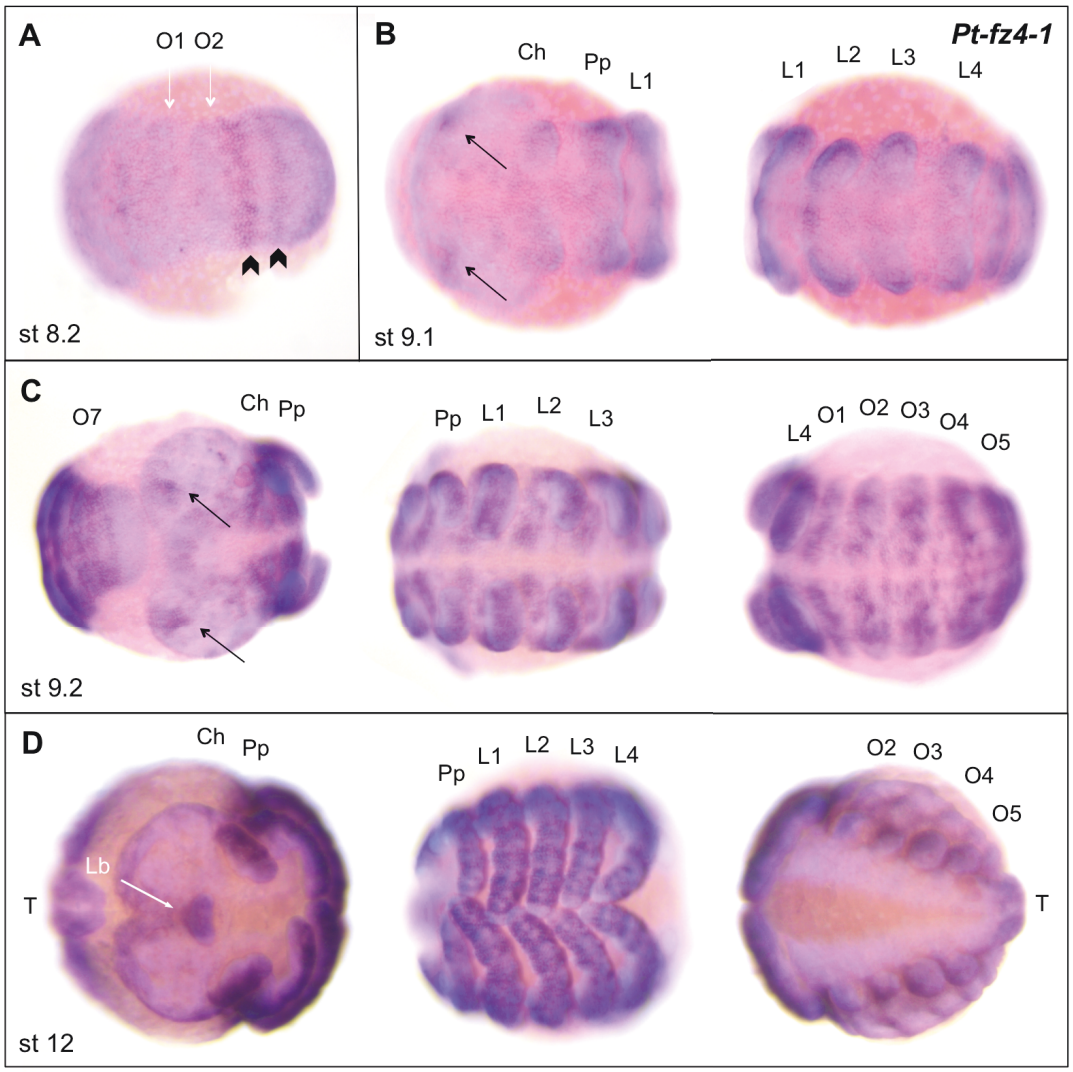

Figure 45 | *Pt-fz4-1* wildtype expression during stages 8.2-12. Panels **C** and **D** shows the same embryo in an anterior (left), prosomal (middle) and opisthosomal (right) view. In all panels anterior is to the left and embryos are counterstained with DAPI. *Pt-fz4-1* was first detected at stage 8.2 in a stripe domain (arrowhead) at the posterior of the O2 segment (arrow) and in a stripe (chevron) at the anterior portion of the SAZ **(A)**. At stage 9.1, faint *Pt-fz4-1* expression can be detected in the mesoderm of the forming limbs and in circular domains in the precheliceral lobes (arrows) **(B)**. *Pt-fz4-1* is strongly expressed in the limb mesoderm, the ventral neuroectoderm and the head lobes (arrows) at stage 9.2 **(C)**. *Pt-fz4-1* expression continues in the limbs and the opisthosomal mesoderm **(D)**. The expression in the head lobe is restricted to the anterior border and the labrum area (arrow. **D**).

6.1.4 *Pt-fz4-2* expression in *Parasteatoda*

Pt-fz4-2 expression arises as an anterior stripe at stage 6 in a similar domain and at a similar time point to *Pt-fz4-1* (see fig. 45 A, 45 A). However, compared to *Pt-fz4-1* (see fig.45 A), the expression domain is initially narrower and does not become as broad at stage 8.1 (see fig. 46 B). Later, at stage 8.2, *Pt-fz4-2* is strongly expressed in the segmental grooves in the pro- and opisthosomal segments and in a ring around the future labrum (see fig. 46 C). The expression of *Pt-fz4-2* retracts to the dorsal periphery of each segment at stage 9.2 and the domain at the labrum becomes more defined (see fig. 46 C). *Pt-fz4-2* is strongly expressed in the limb and opisthosomal mesoderm at stage 12 (see fig. 46 D), and at this stage is still expressed in the labrum and also becomes apparent in a specific area anterior to this structure (see fig. 46 D). However, *Pt-fz4-2* expression was not detected in the SAZ at any of the observed stages (see fig. 46 C-E).

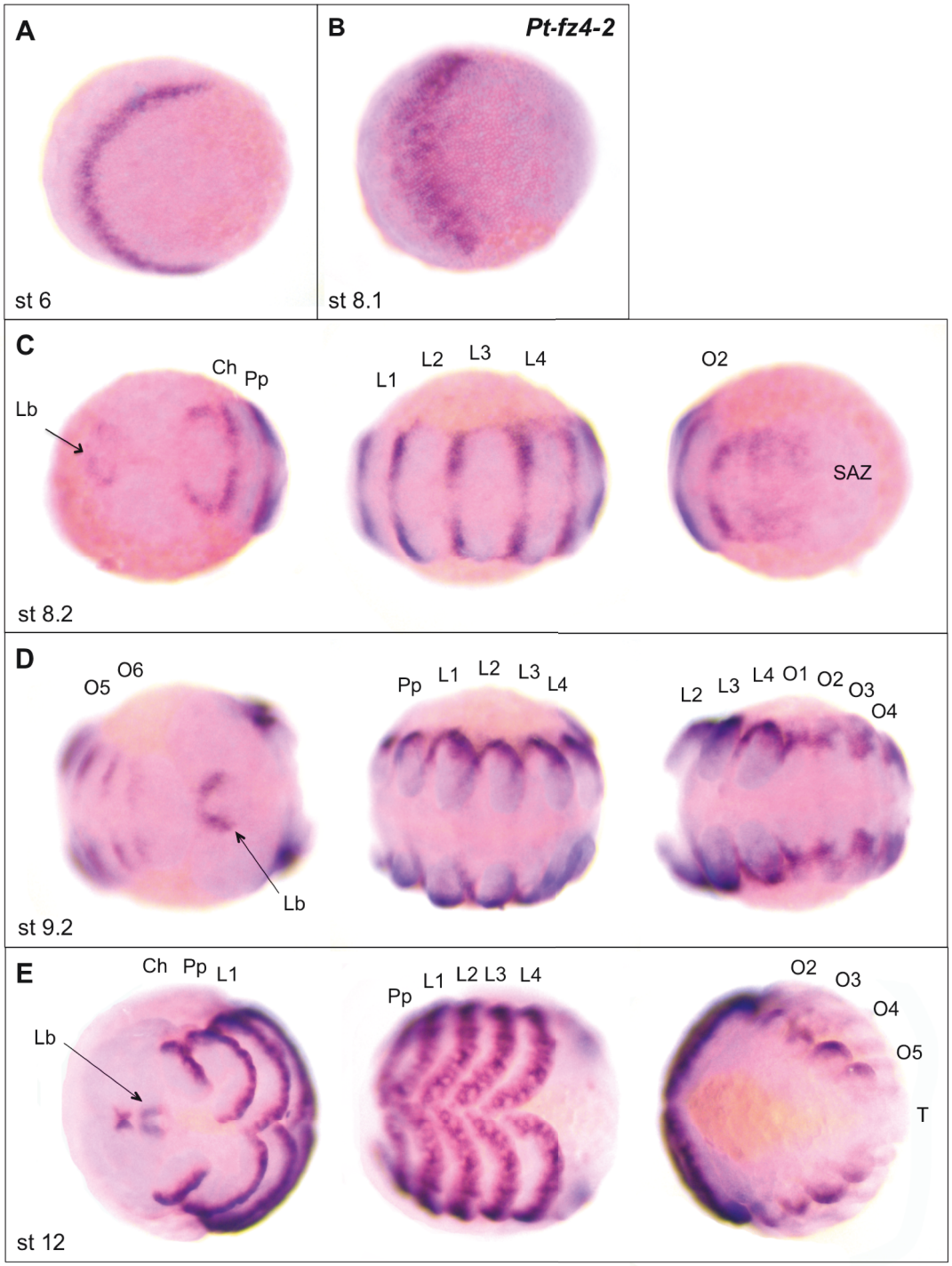

Figure 46 | *Pt-fz4-2* wildtype expression during stages 6-12. Panels **C,D,E** show the same embryo respectively in an anterior (left), a prosomal (middle) and an opisthosomal (right) view. In all panels anterior is to the left and embryos are counterstained with DAPI. *Pt-fz4a* is first expressed in an anterior stripe domain at stage 6 (A). At stage 7 the expression domain becomes slightly broader (B). At stage 8.2, *Pt-fz4b* is expressed in pro- and opisthosomal segmental grooves and in a ring domain around the forming labrum (Lb, arrow) area (C). The expression of *Pt-fz4b* is retracted to the dorsal periphery of each segment at stage 9.2 and the domain at the labrum area (Lb, arrow) becomes more defined (C). Further, *Pt-fz4a* is strongly expressed in the limb and opisthosomal mesoderm at stage 13 (D). At the anterior, *Pt-fz4a* is continuously expressed in the labrum (Lb, arrow) and additionally appears in the stomodaeum (Sto, arrow)(D).

Summarising the results of the frizzled receptor expression analysis in *Parasteatoda,* while *Pt-fz2* and *Pt-fz4-2* are expressed in pattern possibly consistent with a role in segmentation, only *Pt-Fz1* out of the four frizzled genes was expressed in the SAZ during any of the stages analysed.

6.2 Secreted frizzled-related proteins in *Parasteatoda*

Secreted frizzled-related proteins (Sfrp) have been identified as Wnt signaling antagonists in vertebrates where they play a major role in embryonic development (Chapman et al., 2004; Esteve and Bovolenta, 2006; Leimeister et al., 1998; Rattner et al., 1997). Sfrps contain a frizzled-like CRD domain at their amino-terminal end, but lack the characteristic Frizzled trans-membrane domain, which suggests that they are secreted (Rattner et al., 1997).

In the *Parasteatoda* genome, a single secreted frizzled-related protein (*Pt-Sfrp*) was identified (Hilbrant and McGregor unpublished data) (see fig. 47).

```
Pt-Sfrp          PSCVDIPENLTLCHGIGYTQMRLPNLLDHDTMAEVSQQAGSWVPLLNIECHPDTQLFLCSL
Sm-Sfrp5         .T.....R.M....D....K..................S......F.LK..S.........
Smim-Sfrp5       .T.M.....................................................

Pt-Sfrp          FSPVCLDRPIYPCRSLCDKVRAGCESRMQAYGFPWPDMVKCDKFPVDNDMCISVQANANTE
Sm-Sfrp5         ................EA..QG..G..RV..Y....FLR.E...L......TA.SGKS.A
Smim-Sfrp5       ................EA.QK...G..R.........R.....I...........S..G
```

Figure 47 | Alignment of the *Sfrp* frizzled-like CRD domain. Identical aa are represented with dots and sequences are in order of similarity identified in protein BLAST. *Parasteatoda tepidariorum (Pt), Strigamia maritima* (*Sm), Stegodyphus mimosarum (Smim).*

Previous characterisation of the structure and function of Sfrps was predominantly carried out in vertebrates, with representatives identified in a few

invertebrates and evidence for Sfrps missing in arthropods (Bovolenta et al., 2008).

However recently, five trans-membrane frizzled-receptors, as well as other frizzled-related genes, like a secreted Frizzled-related protein were also identified in the *Strigamia maritima* genome (Chipman et al., 2014).

6.2.1 Expression of *Pt-Sfrp* in *Parasteatoda*

Pt-Sfrp expression was first detected in a broad stripe at the anterior of the germ band at around stage 7 (see fig. 48 A), similarly to that described above for *Pt-fz2* and *Pt-fz4-2* (see fig. 44 A and 46 A). Later, *Pt-Srfp* is expressed in a broad stripe in the anterior SAZ, which resolves in ectodermal strips of the segmental grooves of prosomal and opisthosomal segments, but expression is absent from the midline (see fig. 48 B-D). The strong segmental expression continued until stage 10.2, the latest stage observed (see fig. 48 F-I).

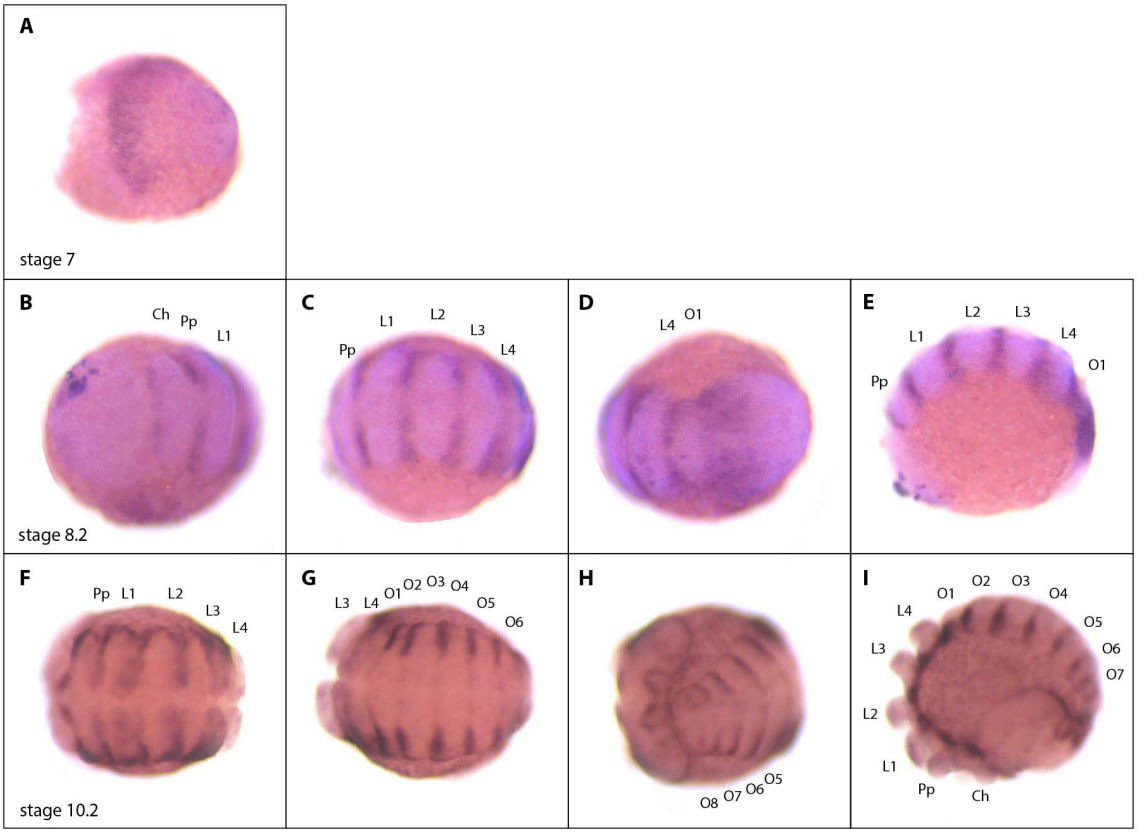

Figure 48 | *Pt-Sfrp* wildtype expression at stage 8.2. Panels **B-E** and **F-I** show the same embryo respectively in an anterior (**B**), a prosomal (**C,F**), an opisthosomal (**D,G,H**) and a side view (**E,I**). In all panels anterior is to the left and embryos **A-E** are counterstained with DAPI. *Pt-Sfrp* expression commences in a broad anterior stripe (A). Later *Pt-Sfrp* expression is restricted to the lateral parts of the segmental groove (dashed lines in **C**) and in a broad band in anterior SAZ (dashed lines in **D**). At stage 10.2 *Pt-Sfrp* continues to be restricted to the lateral ectoderm of the segmental grooves (**F-I**).

6.3 Discussion

A previous study confirmed that there are four subfamilies of frizzled genes in metazoans (Schenkelaars et al., 2015). Four frizzled genes (*Pt-fz1*, *Pt-fz2*, *Pt-fz4a* and *Pt-fz4b*) were identified previously in *Parasteatoda* (Janssen et al., 2015) (see fig. 48), but it appears that *fz3* has been lost in this spider and there has been a duplication of *fz4* (Janssen et al., 2015).

The phylogenetic analysis including several panarthropod species (*Tribolium castaneum* (*Tc*), Zootermopsis nevadensis (*Zn), Glomeris marginata* (*Gm*), *Strigamia maritima (Sm), Parasteatoda tepidariorum* (*Pt*), *Pholcus phalangoides* (*Pp*), *Stegodyphus mimosarum* (Stm), *Ixodes scapularis (Is)*, *Mesobuthus martensii (Mm)* and *Euperipatoides kanangrensis* (Ek)) confirmed four Frizzled receptor subfamilies, reported in metazoans previously (Janssen et al., 2015; Schenkelaars et al., 2015). Moreover it could be shown that *Gm, Sm, Mm, Zn, Pp* assemble in a Frizzled 3 cluster, whereas Fz3 appears lost in *Pt, Is* and *Tc* (Janssen et al., 2015). Interestingly, duplications of the Frizzled 4 subfamily could be found for two other spiders (*Pt, Stm,*) and a scorpion (*Mm*), but not for the third spider (*Pp*) included in the analysis. Tree from (Janssen et al., 2015).

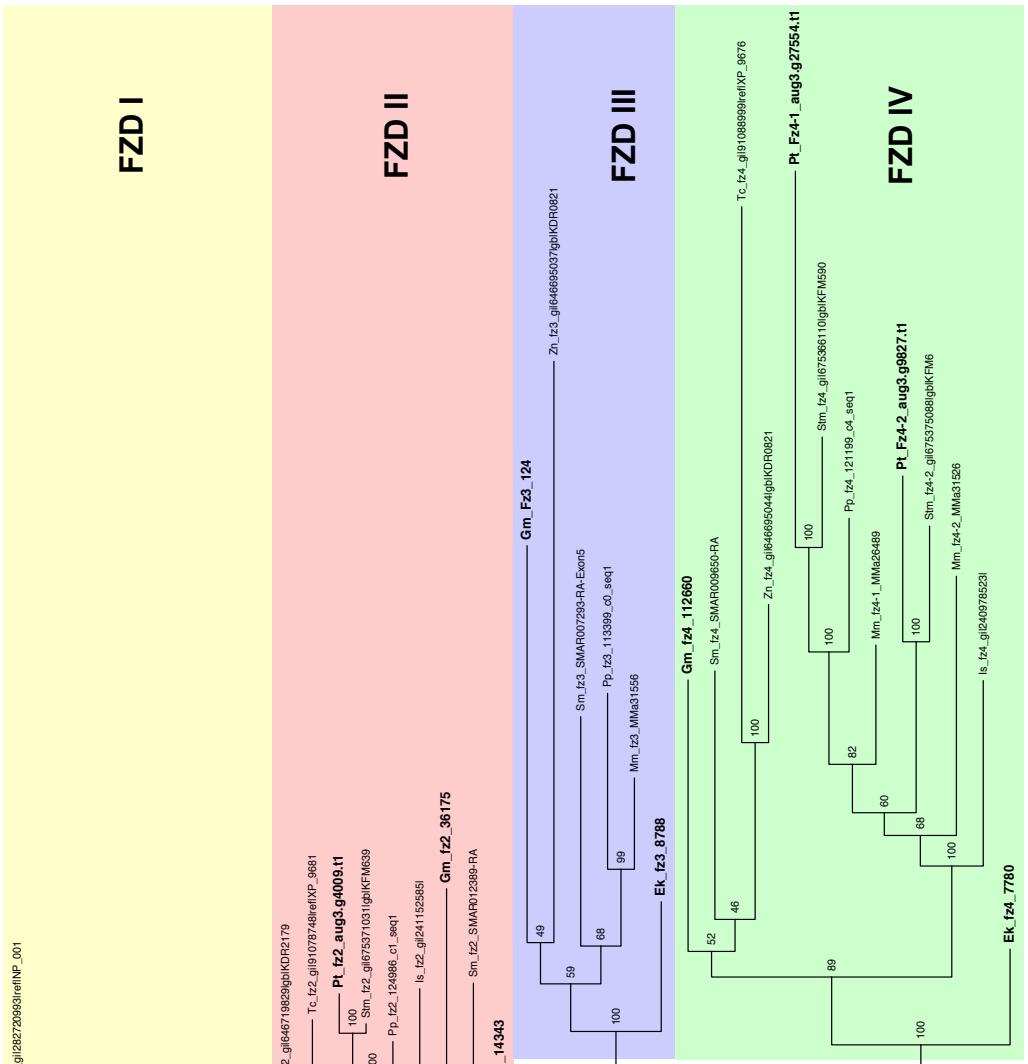

Figure 49 | Phylogenetic analysis of the frizzled receptors. Maximum likelihood tree of frizzled receptor amino acid sequences among metazoans. The bootstrap values from the maximum likelihood analysis are given at the nodes. Included species: *Tribolium castaneum* (*Tc*), Zootermopsis nevadensis (*Zn*), *Glomeris marginata* (*Gm*), *Strigamia maritima* (*Sm*), *Parasteatoda tepidariorum* (*Pt*), *Pholcus phalangoides* (*Pp*), *Stegodyphus mimosarum* (Stm), *Ixodes scapularis* (*Is*), *Mesobuthus martensii* (*Mm*) and *Euperipatoides kanangrensis* (Ek). Provided by Maarten Hilbrant for (Janssen et al., 2015).

6.3.1 Expression analysis of the *Parasteatoda* frizzled genes

Taken together, the analysis of the expression patterns of the Frizzled genes in *Parasteatoda* suggest they are involved in neuroectoderm development, segment border formation and maintenance and development of anterior structures (see figs. 43 - 46). Comparing these expression patterns among arthropods provides some useful insights into the roles of these genes and their evolution.

Fz1 is expressed ubiquitously in embryos of *Parasteatoda,* the millipede *Glomeris,* and the onychophoran *Euperipatoides* as well as *Drosophila* and *Tribolium*. However, *fz1* expression can be observed in a segmental pattern in *Parasteatoda* and *Euperipatoides* at later stages. This suggests that *Fz1* could be involved in segmentation across panarthropods (Beermann et al., 2011; Janssen et al., 2015; Muller et al., 1999; Park et al., 1994a). Although this is a bit speculative when inferred from ubiquitous expression in the absence of functional data.

Fz2 expression in *Parasteatoda* and *Glomeris* resembles expression in *Drosophila* and *Tribolium*, which starts out as a broad anterior domain and progresses into expression in segmental stripes (Beermann et al., 2011; Muller et al., 1999). Therefore, it has been suggested that *Fz2* might also be involved in segmentation in *Parasteatoda* and *Glomeris*, but not across panarthropods, since no segmental expression was detected in *Euperipatoides* (Janssen et al., 2015).

In the case of *Fz4*, a single copy was identified in both *Glomeris* and *Euperipatoides* (Janssen et al., 2015) (see fig. 45 & 46). Comparison of *Fz4* expression domains between these two species and the *Parasteatoda*

paralogs suggest that they perform various functions including nervous system development, segmentation and limb development (Janssen et al., 2015). The two *fz4* paralogs in *Parasteatoda* show similar expression in the labrum and the walking legs (Janssen et al., 2015). While *Parasteatoda fz4-1* is expressed early in the developing nervous system and the head lobes, *Pt-fz4-2* exhibits specific segmental expression in prosomal and opisthosomal segments (Janssen et al., 2015). Generally, *Pt-fz4-1* appears to be expressed more broadly, compared to the restricted expression of *Pt-fz4-2*, which might indicate subfunctionalization of those duplicated genes (Force et al., 1999; Lynch and Force, 2000).

6.3.2 Investigating Frizzled function in the spider

It has been hypothesized that frizzled receptors act redundantly or require combinatorial action. In *Tribolium* for example, only the combined knockdown of *fz1* and *fz2* causes germ band phenotypes, whereas *fz2* RNAi does not have an effect and *fz1* knockdown leads to limb malformations (Beermann et al., 2011).

Individual pRNAi knockdown of the four *Parasteatoda* frizzled genes showed no detectable effect (data not shown). Hence, to obtain a better understanding of the function of frizzled receptors in *Parasteatoda*, double or even triple RNAi against different combinations of frizzled receptors should be undertaken.

Another interesting aspect of frizzled receptor function concerns which Wnt ligands bind to each of them. To date, there is no experimental evidence about which Wnt ligand binds to which Frizzled receptor in *Parasteatoda* and this would be particularly interesting to know with respect to segmentation. *Wnt5, Wnt7-1, Wnt8* and *Wnt11-2* are all expressed in the SAZ in *Parasteatoda* (Janssen et al., 2010), while *Pt-fz1* is expressed ubiquitously and *Pt-fz4a* and *Pt-fz4b* expression is only observed at the anterior border of the SAZ at stage 9 (see figs. 45 and 46 D). This suggests that *Pt-fz1* is the receptor used in the SAZ with perhaps *Pt-fz4-1* and *Pt-fz4-2* also acting during formation of some segments. To help understand these potential roles and interaction better, it would be useful to characterise in detail where each Wnt ligand protein is expressed perhaps by tagging them using CRISPR/Cas9.

6.3.3 Sfrp in *Parasteatoda*

In humans five Sfrps have been identified (SFRP 1-5), which are also present in all vertebrates (Bovolenta et al., 2008). Additionally, non-mammalian vertebrates like *Xenopus*, zebrafisha and chicks exhibit another subgroup (Sizzled, Crescent, Tlc), which is similar in sequence to the human SFRP1/2/5 cluster (Bovolenta et al., 2008). In invertebrates, Sfrp homologs have been discovered in the purple sea urchin (Lapraz et al., 2006), the nematode *Caenorhabditis elegans* (Bovolenta et al., 2008), the sea squirt *Ciona intestinalis* (Hino et al., 2003) and in the sponge *Lubomirskia baicalensis (Adell et al., 2007)*, which indicates the ancient origin of this signaling molecule family. Although, initially believed to be lost in arthropods, based on

the lack of Sfrps in the *Drosophila* genome, Sfrp homologs have also been discovered in the milipede *Strigamia maritima* (Chipman et al., 2014) and the spider *Parasteatoda* (M. Hilbrant and A. McGregor).

It was thought that SFRPs act as Wnt signaling antagonists in vertebrates but they have in fact been shown to play different roles in vertebrate development, where they activate as well as inhibit Wnt-signaling in different processes (Bovolenta et al., 2008; Esteve et al., 2011; Leyns et al., 1997; Wang et al., 1997). Furthermore it was shown that Sfrps interact with frizzled receptors (Bafico et al., 1999) and each other to inhibit function (Yoshino et al., 2001).

To obtain a better understanding of the function and mechanism of Sfrps in arthropods, Sfrps in other arthropod species need to be identified and functionally tested. In the case of the *Parasteatoda* homolog, a more detailed time series could be carried out and RNAi against the *Pt-Sfrp* could be undertaken. As Sfrps have been shown to interact with frizzled receptors (Bafico et al., 1999), *Pt-Sfrp* RNAi knockdown should also be carried out in *Parasteatoda* and the effect on embryogenesis and the expression of other Wnt signaling components assayed.

7. General discussion

7.1. Functional division of the SAZ and interaction between Delta-Notch and Wnt8 signaling pathways

This PhD provides further evidence that the *Parasteatoda* SAZ is subdivided into a posterior domain with high *Pt-Wnt8* expression, and an anterior *Pt-Wnt8* domain with relatively lower *Pt-Wnt8* expression both of which are regulated by Delta-Notch signaling (Schonauer et al., 2016) (see fig. 49). I propose, that *Pt-Dl* expression, cyclically progressing from the posterior to the anterior SAZ and on to the nascent segments, is primarily responsible for *Pt-Wnt8* repression in the anterior. These alternating states of *Pt-Dl* expression and consequently *Pt-Wnt8* repression in the anterior and vice versa, might enable the differentiation of cells and thus facilitate subsequent formation of segments from the SAZ at regular intervals. Whereas *Pt-N,* with its continuous expression in the SAZ, might be responsible for the maintenance of *Pt-Wnt8* expression in the posterior SAZ.

A similar functional compartmentalisation of the GZ, the SAZ equivalent in the cockroach, could be shown in *Periplaneta*: *Pa-Dl* expression oscillates through the GZ via activation by *Pa-Wnt1* in the posterior and repression by *Pa-cad* in a broad domain in the anterior part (Chesebro et al., 2013). Only when *Pa-Dl* expression exceeds a certain threshold, anterior of the *Pa-cad* domain, is segmentation gene expression activated, ensuring the sequential formation of segments in the cockroach (Chesebro et al., 2013).

Whilst no other comprehensive description of Delta-Notch and Wnt signaling interplay regulating sequential segment formation has been reported in other arthropods, expression and/or function of components of the Delta-Notch and Wnt signaling pathway suggest that they are likely to be crucial for short germ segmentation more widely.

In the centipede *Strigamia,* oscillating *Sm-Dl* expression has been observed throughout posterior development including the transition from double-segmental to single segmental expression during trunk segment formation (Chipman and Akam, 2008). In the cricket *Gryllus*, as well as in the milkweed bug *Oncopeltus* and the flour beetle *Tribolium*, functional analysis of components of the Wnt signaling pathway confirmed a role in posterior segment formation, however, no involvement of Delta-Notch signaling in segmentation has yet been found in those insects (Angelini and Kaufman, 2005; Aranda et al., 2008; Bolognesi et al., 2008; Kainz et al., 2011; Miyawaki et al., 2004).

However, it is still unclear how the dynamic *Pt-Dl* and *Pt-N* expression is generated and how *Pt-Dl* activates *Pt-Wnt8* in the posterior and represses in the anterior SAZ. Indeed, the loss of *Pt-N* expression in *Pt-Dl* RNAi embryos potentially suggests auto-inhibitory mechanism of this signaling pathway. Investigating the regulatory interactions between *Pt-Dl* and *Pt-N* further, could also give insight into the dynamics of their expression (see Discussion in Chapter 3 for further detail).

Furthermore, the effect of *Pt-Dl* and *Pt-N* on downstream factors should be studied in more detail: whilst the effect of *Pt-Dl* and *Pt-N* on *Pt-Wnt8* appears

similar, differences in their wild-type expression patterns suggest that they might be responsible for different aspects of gene expression of the SAZ. To address this question, a more detailed time series of *Pt-Dl* and *Pt-N* double in situ analysis is needed, to get more information about their relative expression patterns at different stages of posterior development and in different compartments of the germ band. In addition, the generation of *Pt-Dl* RNAi clones and subsequent in situ hybridisation to assay *Pt-N* expression at different developmental stages would also be insightful. Hereby, the effect on *Pt-N* with the *Pt-Dl* clone can be compared to interactions with the surrounding wild-type tissue. These observations might elucidate the regulation between *Pt-Dl* and *Pt-N* in different compartments of the *Parasteatoda* SAZ and thereby explain the differential effect on *Pt-Wnt8* expression in the posterior and anterior SAZ.

7.2. The regulation of pair-rule gene orthologues

I also demonstrated that Delta-Notch and Wnt signaling together with *caudal* are required for pair-rule gene expression in the spider. In addition, I also showed that *Pt-cad* is downstream of *Pt-Dl.* However, *Pt-cad* does not appear to be sufficient for *Pt-eve* activation. I could also show that *Pt-eve* does not activate *Pt-cad*, which suggests that *Pt-eve* acts downstream of *Pt-cad* (see fig. 50). These findings confirm that the regulation and expression of the pair-rule genes investigated, is not achieved by a pair-rule gene circuit, exactly as described in *Tribolium* (Choe et al., 2006), but appear to be regulated by Delta-Notch/Wnt/Cad in parallel.

Whilst it is challenging to infer the molecular composition and structure of segmentation in the common ancestor of arthropods from studying individual components of a presumably complex GRN, a common principle can be identified in several arthropod representatives: observations in *Parasteatoda*, together with evidence from *Periplaneta, Tribolium* and *Gryllus*, allow the conclusion, that *even-skipped* regulation by *caudal,* directed by upstream signaling pathways is ancestral to all arthropods (Chesebro et al., 2013; El-Sherif et al., 2014; Pueyo et al., 2008; Schonauer et al., 2016; Shinmyo et al., 2005) (and see Discussion in Chapter 5).

Furthermore, expression of pair-rule genes in *Strigamia, Cupiennius* and *Parasteatoda* suggest that segments were added one by one ancestrally and the double segmental pattern, observed in *Drosophila* and during the addition of many of the trunk segments in *Strigamia* possibly represents convergent evolution in geophilomorph centipedes and insects (Brena and Akam, 2013; Chipman and Akam, 2008; Chipman et al., 2004; Choe et al., 2006; Damen, 2004; Damen, 2007; Damen et al., 2000; Davis et al., 2001; Frasch and Levine, 1987; Green and Akam, 2013; Janssen et al., 2011; Leite and McGregor, 2016; Patel et al., 1994; Sarrazin et al., 2012; Schonauer et al., 2016; Schoppmeier and Damen, 2005a).

The expression profile of *Pt-eve* and *Pt-run-1* exhibits an early expression onset and a single segmental pattern in the SAZ and forming segments. Also, both genes are regulated by *Pt-cad* amongst other factors. Taken together, these findings suggest that both genes act on the same hierarchical level and function as primary pair-rule genes in *Parasteatoda*. I would be interested to investigate the regulation of the other pair-rule genes. For example, I suggest

analysing *Pt-odd-1* or *Pt-slp* in *Pt-eve* and *Pt-run* eRNAi embryos to determine if expression is lost in the clone area.

In case of a negative result showing no change to *Pt-odd-1* and *Pt-slp* expression, one might have to consider knocking down *Pt-eve* and *Pt-run-1* at the same time, as one of the primary pair rule genes might be sufficient for *Pt-odd-1* and *Pt-slp* expression.

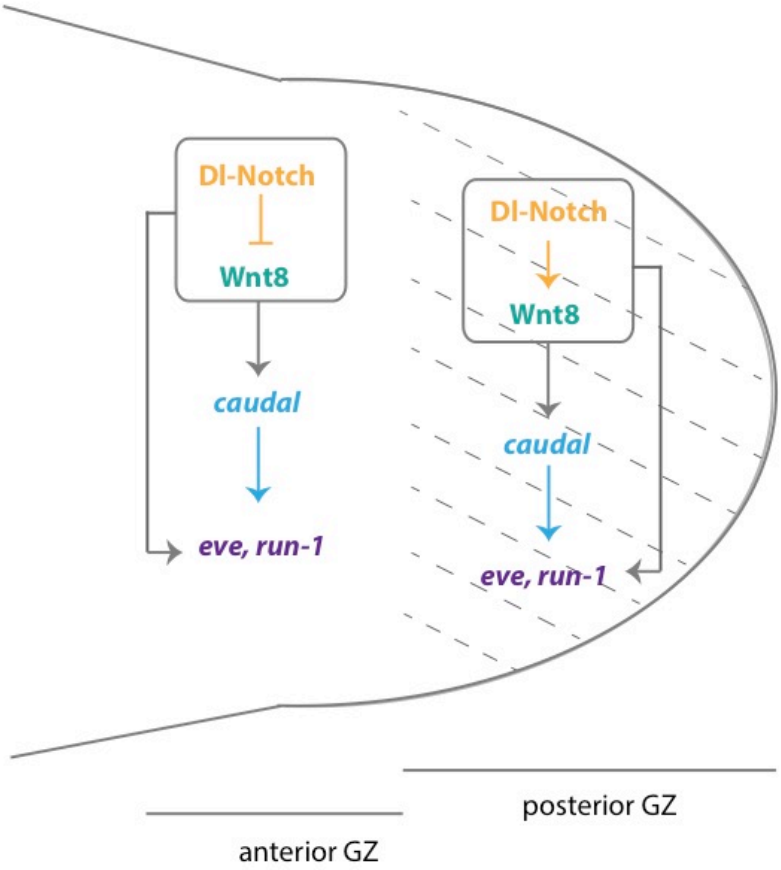

Figure 50 | Summary of the GRN of posterior development in *Parasteatoda*. In the posterior of the SAZ (hatched area), Dl-N (orange) activates Wnt8 (green) expression to maintain cells in an undifferentiated state. Wnt8 is then required for dynamic expression of Dl, which results in the formation of a stripe of Dl expression in anterior SAZ cells (white background). Wnt8 and Dl-N are also required to activate caudal (blue) expression. These factors activate eve and run-1 (both violet) expression. In anterior SAZ cells, Dl then subsequently suppresses Wnt8 expression and in combination with caudal, eve and runt expression leads to segment formation. Arrowheads and flat arrows indicate activation and repression, respectively, although it is not known if these interactions are direct or whether additional factors are required. Also for simplicity, the regulation of Wnt8 by Dl and N is depicted, rather than the regulation of Dl and N expression on each other. This schematic representation of the SAZ of *Parasteatoda* does not depict a particular stage of development, but aims to highlight the differences in regulation between the anterior and posterior SAZ.

7.3. The Evolution of Segmentation

Our knowledge about arthropod segmentation to this date allows two different scenarios explaining the evolution of segmentation: namely that the common bilaterian ancestor was segmented and utilized a Delta-Notch/Wnt signaling based mechanism to generate segments sequentially. In this case, it could be argued that the lack of involvement of Delta-Notch signaling in segmentation in insects like *Tribolium* and *Drosophila* is a derived state of segmentation (Aranda et al., 2008).

Alternatively, Delta-Notch/Wnt-based segmentation as observed in vertebrates and arthropods like *Parasteatoda* and *Periplaneta* (and potentially other arthropods) could have evolved independently by co-option of signaling pathways or other factors. Evidence for such an evolutionary history might be that some factors are 'plugged-in' to the network differently: *caudal*, for example represses Delta in the GZ of the cockroach, whereas it has no effect on *Pt-Dl* expression in the spider (Chesebro et al., 2013; Schonauer et al., 2016).

Nevertheless, we have to bear in mind that we may so far have only examined in detail a small part of a presumably complex GRN consisting of numerous factors, intertwined by regulatory mechanisms, which ensure the correct expression at the right time, in the correct place. And whilst expression patterns give us a good indication about a potential role, only the functional analysis of the GRN components in other arthropods, and outgroups like Onycophorans (Janssen and Budd, 2013; Strausfeld et al., 2006) and Priapulids (Webster et al., 2006) as well as annelids is likely to provide

sufficient information to address the question of evolution of segmentation in bilateria further.

7.4. Future directions to understand segment addition in *Parasteatoda*

Parasteatoda has proven to be an excellent model organism for studying arthropod segmentation, due to the easy access to embryos, their well described embryonic development, the gene knockdown techniques including the generation of somatic clones and the reliable mRNA staining protocol (Hilbrant et al., 2012). However, during the course of my work some additional questions arose that could be addressed in future experiments to provide a better understanding of the mechanisms of sequential segment addition in the spider.

The results showing that *Pt-cad* is not sufficient to activate *Pt-eve* in the posterior and most likely requires other unknown factors. This highlights the fact that there are certainly more components involved in regulating the formation of the SAZ, its maintenance and the subsequent formation of segments from this tissue. Therefore, an unbiased, non-candidate gene approach towards identifying other parts of the GRN of posterior segmentation is required. This could be carried out by preparing RNA-seq libraries of SAZ tissue from wild-type embryos and for example *Pt-Wnt8* RNAi knockdown embryos at different stages (before SAZ formation / when the SAZ has formed / after formation of the first segment). This would generate the expression profile of all the genes expressed at different stages of posterior development and those that are regulated by Wnt8 signaling; thus providing

new candidates for further expression and functional studies and broadening our understating of the GRN for posterior segment addition in *Parasteatoda*.

Another aspect of segmentation opened up during my PhD work, concerns the mesoderm. Previous work in the spider showed that the knockdown of *Pt-Dl* disrupts the equal formation of caudal meso- and ectoderm, through overexpression of the mesodermal determination gene *twist* (*Pt-twist*) and the lack of *Pt-cad* in the posterior (Oda et al., 2007). Note that previous analysis also showed that *Pt-twi* is involved in mesoderm development in the spider (Yamazaki et al., 2005). Intriguingly, I observed *Pt-twi* expression in the prosoma which suggests that cells delineate from one stripe domain and migrate to an anterior stripe (Schoenauer, unpublished). To better understand the development and segmentation of the mesoderm, I would attempt to fluorescently label and observe *Pt-twi* using CRISPR/Cas9 and Pt-Twi protein expression over the course of posterior development. In parallel, I would functionally analyse this gene and further using embryonic RNAi to investigate the regulatory interactions with the already known factors such as *Pt-Dl*.

As outlined earlier, the labelling of components of the SAZ could not only provide information on the gene expression dynamics, but would also allow the tracking of cell movements over the course of posterior development. It could be shown previously that there is not a significant rate of cell proliferation happening in the SAZ during elongation of the germ band (McGregor et al., 2008b). In *Tribolium*, fluorescently labelled clones of cells revealed differences in cell behaviour dependent on their location and

differences in the segment addition rate over the course of posterior development (Nakamoto et al., 2015). By labelling components of the GRN of segmentation, the protein localization in correlation with development time, the timing of segment addition and cell movements in the SAZ could be elucidated. This would provide a better understanding of cell behaviour underlying SAZ function to compliment our genetic insights.

8. References

Adell, T., Thakur, A. N. and Muller, W. E. (2007). Isolation and characterization of Wnt pathway-related genes from Porifera. *Cell Biol Int* **31**, 939-949.

Adler, P. N. (2002). Planar signaling and morphogenesis in Drosophila. *Dev Cell* **2**, 525-535.

Affolter, M., Schier, A. and Gehring, W. J. (1990). Homeodomain proteins and the regulation of gene expression. *Curr Opin Cell Biol* **2**, 485-495.

Aguinaldo, A. M., Turbeville, J. M., Linford, L. S., Rivera, M. C., Garey, J. R., Raff, R. A. and Lake, J. A. (1997). Evidence for a clade of nematodes, arthropods and other moulting animals. *Nature* **387**, 489-493.

Akam, M. (1987). The molecular basis for metameric pattern in the Drosophila embryo. *Development* **101**, 1-22.

Akiyama-Oda, Y. and Oda, H. (2003). Early patterning of the spider embryo: a cluster of mesenchymal cells at the cumulus produces Dpp signals received by germ disc epithelial cells. *Development* **130**, 1735-1747.

---- (2006). Axis specification in the spider embryo: dpp is required for radial-to-axial symmetry transformation and sog for ventral patterning. *Development* **133**, 2347-2357.

Anderson, D. T. (1973). Embryology and Phylogeny in Annelids and Arthropods. *Pergamon Press, Oxford*.

Angelini, D. R. and Kaufman, T. C. (2005). Functional analyses in the milkweed bug Oncopeltus fasciatus (Hemiptera) support a role for Wnt signaling in body segmentation but not appendage development. *Dev Biol* **283**, 409-423.

Aranda, M., Marques-Souza, H., Bayer, T. and Tautz, D. (2008). The role of the segmentation gene hairy in Tribolium. *Dev Genes Evol* **218**, 465-477.

Auer, T. O., Duroure, K., De Cian, A., Concordet, J. P. and Del Bene, F. (2014). Highly efficient CRISPR/Cas9-mediated knock-in in zebrafish by homology-independent DNA repair. *Genome Res* **24**, 142-153.

Aulehla, A. and Herrmann, B. G. (2004). Segmentation in vertebrates: clock and gradient finally joined. *Genes Dev* **18**, 2060-2067.

Baena-Lopez, L. A., Alexandre, C., Mitchell, A., Pasakarnis, L. and Vincent, J. P. (2013). Accelerated homologous recombination and subsequent genome modification in Drosophila. *Development* **140**, 4818-4825.

Bafico, A., Gazit, A., Pramila, T., Finch, P. W., Yaniv, A. and Aaronson, S. A. (1999). Interaction of frizzled related protein (FRP) with Wnt ligands and the frizzled receptor suggests alternative mechanisms for FRP inhibition of Wnt signaling. *J Biol Chem* **274**, 16180-16187.

Balavoine, G. (2014). Segment formation in Annelids: patterns, processes and evolution. *Int J Dev Biol* **58**, 469-483.

Balavoine, G. and Adoutte, A. (2003). The segmented urbilateria: a testable scenario. *Integr Comp Biol* **43**, 137-147.

Bassett, A. R. and Liu, J. L. (2014). CRISPR/Cas9 and genome editing in Drosophila. *J Genet Genomics* **41**, 7-19.

Bassett, A. R., Tibbit, C., Ponting, C. P. and Liu, J. L. (2013). Highly efficient targeted mutagenesis of Drosophila with the CRISPR/Cas9 system. *Cell Rep* **4**, 220-228.

Beermann, A., Pruhs, R., Lutz, R. and Schroder, R. (2011). A context-dependent combination of Wnt receptors controls axis elongation and leg development in a short germ insect. *Development* **138**, 2793-2805.

Behrens, J., von Kries, J. P., Kuhl, M., Bruhn, L., Wedlich, D., Grosschedl, R. and Birchmeier, W. (1996). Functional interaction of beta-catenin with the transcription factor LEF-1. *Nature* **382**, 638-642.

Benedyk, M. J., Mullen, J. R. and DiNardo, S. (1994). odd-paired: a zinc finger pair-rule protein required for the timely activation of engrailed and wingless in Drosophila embryos. *Genes Dev* **8**, 105-117.

Berleth, T., Burri, M., Thoma, G., Bopp, D., Richstein, S., Frigerio, G., Noll, M. and Nusslein-Volhard, C. (1988). The role of localization of bicoid RNA in organizing the anterior pattern of the Drosophila embryo. *EMBO J* **7**, 1749-1756.

Bhanot, P., Brink, M., Samos, C. H., Hsieh, J. C., Wang, Y., Macke, J. P., Andrew, D., Nathans, J. and Nusse, R. (1996). A new member of the frizzled family from Drosophila functions as a Wingless receptor. *Nature* **382**, 225-230.

Bhanot, P., Fish, M., Jemison, J. A., Nusse, R., Nathans, J. and Cadigan, K. M. (1999). Frizzled and Dfrizzled-2 function as redundant receptors for Wingless during Drosophila embryonic development. *Development* **126**, 4175-4186.

Bhaya, D., Davison, M. and Barrangou, R. (2011). CRISPR-Cas systems in bacteria and archaea: versatile small RNAs for adaptive defense and regulation. *Annu Rev Genet* **45**, 273-297.

Bissen, S. T. and Weisblat, D. A. (1989). The durations and compositions of cell cycles in embryos of the leech, Helobdella triserialis. *Development* **106**, 105-118.

Bolognesi, R., Farzana, L., Fischer, T. D. and Brown, S. J. (2008). Multiple Wnt genes are required for segmentation in the short-germ embryo of Tribolium castaneum. *Curr Biol* **18**, 1624-1629.

Bolognesi, R., Fischer, T. D. and Brown, S. J. (2009). Loss of Tc-arrow and canonical Wnt signaling alters posterior morphology and pair-rule gene expression in the short-germ insect, Tribolium castaneum. *Dev Genes Evol* **219**, 369-375.

Bothma, J. P., Garcia, H. G., Esposito, E., Schlissel, G., Gregor, T. and Levine, M. (2014). Dynamic regulation of eve stripe 2 expression reveals transcriptional bursts in living Drosophila embryos. *Proc Natl Acad Sci U S A* **111**, 10598-10603.

Bovolenta, P., Esteve, P., Ruiz, J. M., Cisneros, E. and Lopez-Rios, J. (2008). Beyond Wnt inhibition: new functions of secreted Frizzled-related proteins in development and disease. *J Cell Sci* **121**, 737-746.

Brena, C. and Akam, M. (2013). An analysis of segmentation dynamics throughout embryogenesis in the centipede Strigamia maritima. *BMC Biol* **11**, 112.

Brown, S. J., Parrish, J. K., Beeman, R. W. and Denell, R. E. (1997). Molecular characterization and embryonic expression of the even-skipped ortholog of Tribolium castaneum. *Mech Dev* **61**, 165-173.

Bucher, G. and Klingler, M. (2004). Divergent segmentation mechanism in the short germ insect Tribolium revealed by giant expression and function. *Development* **131**, 1729-1740.

Cadigan, K. M., Grossniklaus, U. and Gehring, W. J. (1994). Localized expression of sloppy paired protein maintains the polarity of Drosophila parasegments. *Genes Dev* **8**, 899-913.

Cao, Z., Yu, Y., Wu, Y., Hao, P., Di, Z., He, Y., Chen, Z., Yang, W., Shen, Z., He, X., et al. (2013). The genome of Mesobuthus martensii reveals a unique adaptation model of arthropods. *Nat Commun* **4**, 2602.

Carroll, S. B. (1990). Zebra patterns in fly embryos: activation of stripes or repression of interstripes? *Cell* **60**, 9-16.

---- (2008). Evo-devo and an expanding evolutionary synthesis: a genetic theory of morphological evolution. *Cell* **134**, 25-36.

Castresana, J. (2000). Selection of conserved blocks from multiple alignments for their use in phylogenetic analysis. *Mol Biol Evol* **17**, 540-552.

Chapman, S. C., Brown, R., Lees, L., Schoenwolf, G. C. and Lumsden, A. (2004). Expression analysis of chick Wnt and frizzled genes and selected inhibitors in early chick patterning. *Dev Dyn* **229**, 668-676.

Chesebro, J. E., Pueyo, J. I. and Couso, J. P. (2012). Interplay between a Wnt-dependent organiser and the Notch segmentation clock regulates posterior development in Periplaneta americana. *Biology Open*.

Chesebro, J. E., Pueyo, J. I. and Couso, J. P. (2013). Interplay between a Wnt-dependent organiser and the Notch segmentation clock regulates posterior development in Periplaneta americana. *Biol Open* **2**, 227-237.

Chevenet, F., Brun, C., Banuls, A. L., Jacq, B. and Christen, R. (2006). TreeDyn: towards dynamic graphics and annotations for analyses of trees. *BMC Bioinformatics* **7**, 439.

Chipman, A. D. (2010). Parallel evolution of segmentation by co-option of ancestral gene regulatory networks. *Bioessays* **32**, 60-70.

Chipman, A. D. and Akam, M. (2008). The segmentation cascade in the centipede Strigamia maritima: involvement of the Notch pathway and pair-rule gene homologues. *Dev Biol* **319**, 160-169.

Chipman, A. D., Arthur, W. and Akam, M. (2004). A double segment periodicity underlies segment generation in centipede development. *Curr Biol* **14**, 1250-1255.

Chipman, A. D., Ferrier, D. E., Brena, C., Qu, J., Hughes, D. S., Schroder, R., Torres-Oliva, M., Znassi, N., Jiang, H., Almeida, F. C., et al. (2014). The first myriapod genome sequence reveals conservative arthropod gene content and genome organisation in the centipede Strigamia maritima. *PLoS Biol* **12**, e1002005.

Cho, S. J., Valles, Y., Giani, V. C., Jr., Seaver, E. C. and Weisblat, D. A. (2010). Evolutionary dynamics of the wnt gene family: a lophotrochozoan perspective. *Molecular biology and evolution* **27**, 1645-1658.

Choe, C. P. and Brown, S. J. (2007). Evolutionary flexibility of pair-rule patterning revealed by functional analysis of secondary pair-rule genes, paired and sloppy-paired in the short-germ insect, Tribolium castaneum. *Dev Biol* **302**, 281-294.

Choe, C. P., Miller, S. C. and Brown, S. J. (2006). A pair-rule gene circuit defines segments sequentially in the short-germ insect Tribolium castaneum. *Proc Natl Acad Sci U S A* **103**, 6560-6564.

Cong, L., Ran, F. A., Cox, D., Lin, S., Barretto, R., Habib, N., Hsu, P. D., Wu, X., Jiang, W., Marraffini, L. A., et al. (2013). Multiplex genome engineering using CRISPR/Cas systems. *Science* **339**, 819-823.

Cooke, J. (1998). A gene that resuscitates a theory--somitogenesis and a molecular oscillator. *Trends Genet* **14**, 85-88.

Cooke, J. and Zeeman, E. C. (1976). A clock and wavefront model for control of the number of repeated structures during animal morphogenesis. *J Theor Biol* **58**, 455-476.

Copf, T., Schroder, R. and Averof, M. (2004). Ancestral role of caudal genes in axis elongation and segmentation. *Proc Natl Acad Sci U S A* **101**, 17711-17715.

Coulter, D. E. and Wieschaus, E. (1988). Gene activities and segmental patterning in Drosophila: analysis of odd-skipped and pair-rule double mutants. *Genes Dev* **2**, 1812-1823.

Couso, J. P. (2009). Segmentation, metamerism and the Cambrian explosion. *Int J Dev Biol* **53**, 1305-1316.

Damen, W. G. (2002). Parasegmental organization of the spider embryo implies that the parasegment is an evolutionary conserved entity in arthropod embryogenesis. *Development* **129**, 1239-1250.

---- (2004). Arthropod segmentation: why centipedes are odd. *Curr Biol* **14**, R557-559.

---- (2007). Evolutionary conservation and divergence of the segmentation process in arthropods. *Dev Dyn* **236**, 1379-1391.

Damen, W. G., Janssen, R. and Prpic, N. M. (2005). Pair rule gene orthologs in spider segmentation. *Evol Dev* **7**, 618-628.

Damen, W. G., Weller, M. and Tautz, D. (2000). Expression patterns of hairy, even-skipped, and runt in the spider Cupiennius salei imply that these genes were segmentation genes in a basal arthropod. *Proc Natl Acad Sci U S A* **97**, 4515-4519.

Davis, G. K., Jaramillo, C. A. and Patel, N. H. (2001). Pax group III genes and the evolution of insect pair-rule patterning. *Development* **128**, 3445-3458.

Davis, G. K. and Patel, N. H. (1999). The origin and evolution of segmentation. *Trends Cell Biol* **9**, M68-72.

---- (2002). Short, long, and beyond: molecular and embryological approaches to insect segmentation. *Annu Rev Entomol* **47**, 669-699.

de Celis, J. F. and Bray, S. (1997). Feed-back mechanisms affecting Notch activation at the dorsoventral boundary in the Drosophila wing. *Development* **124**, 3241-3251.

De Robertis, E. M. (2008). The molecular ancestry of segmentation mechanisms. *Proc Natl Acad Sci U S A* **105**, 16411-16412.

De Robertis, E. M. and Sasai, Y. (1996). A common plan for dorsoventral patterning in Bilateria. *Nature* **380**, 37-40.

de Rosa, R., Grenier, J. K., Andreeva, T., Cook, C. E., Adoutte, A., Akam, M., Carroll, S. B. and Balavoine, G. (1999). Hox genes in brachiopods and priapulids and protostome evolution. *Nature* **399**, 772-776.

de Rosa, R., Prud'homme, B. and Balavoine, G. (2005). Caudal and even-skipped in the annelid Platynereis dumerilii and the ancestry of posterior growth. *Evol Dev* **7**, 574-587.

Dearden, P. K. and Akam, M. (2001). Early embryo patterning in the grasshopper, Schistocerca gregaria: wingless, decapentaplegic and caudal expression. *Development* **128**, 3435-3444.

Dearden, P. K., Donly, C. and Grbić, M. (2002). Expression of pair-rule gene homologues in a chelicerate: early patterning of the two-spotted spider mite Tetranychus urticae. *Development* **129**, 5461-5472.

del Alamo, D., Rouault, H. and Schweisguth, F. (2011). Mechanism and significance of cis-inhibition in Notch signalling. *Curr Biol* **21**, R40-47.

Dereeper, A., Guignon, V., Blanc, G., Audic, S., Buffet, S., Chevenet, F., Dufayard, J. F., Guindon, S., Lefort, V., Lescot, M., et al. (2008). Phylogeny.fr: robust phylogenetic analysis for the non-specialist. *Nucleic Acids Res* **36**, W465-469.

Dray, N., Tessmar-Raible, K., Le Gouar, M., Vibert, L., Christodoulou, F., Schipany, K., Guillou, A., Zantke, J., Snyman, H., Behague, J., et al. (2010). Hedgehog signaling regulates segment formation in the annelid Platynereis. *Science* **329**, 339-342.

Driever, W. and Nusslein-Volhard, C. (1988a). The bicoid protein determines position in the Drosophila embryo in a concentration-dependent manner. *Cell* **54**, 95-104.

---- (1988b). A gradient of bicoid protein in Drosophila embryos. *Cell* **54**, 83-93.

Dubrulle, J., McGrew, M. J. and Pourquie, O. (2001). FGF signaling controls somite boundary position and regulates segmentation clock control of spatiotemporal Hox gene activation. *Cell*, 219-232.

Dunlop, J. A. (2010). Geological history and phylogeny of Chelicerata. *Arthropod Struct Dev* **39**, 124-142.

Dunlop, J. A. and Arango, C. P. (2005). Pycnogonid affinities: a review. *Journal of Zoological Systematics and Evolutionary Research* **43**, 8-21.

Edgar, R. C. (2004). MUSCLE: a multiple sequence alignment method with reduced time and space complexity. *BMC Bioinformatics* **5**, 113.

El-Sherif, E., Zhu, X., Fu, J. and Brown, S. J. (2014). Caudal regulates the spatiotemporal dynamics of pair-rule waves in Tribolium. *PLoS Genet* **10**, e1004677.

Erwin, D. H. and Davidson, E. H. (2002). The last common bilaterian ancestor. *Development* **129**, 3021-3032.

Esteve, P. and Bovolenta, P. (2006). Secreted inducers in vertebrate eye development: more functions for old morphogens. *Curr Opin Neurobiol* **16**, 13-19.

Esteve, P., Sandonis, A., Ibanez, C., Shimono, A., Guerrero, I. and Bovolenta, P. (2011). Secreted frizzled-related proteins are required for Wnt/beta-catenin signalling activation in the vertebrate optic cup. *Development* **138**, 4179-4184.

Farzana, L. and Brown, S. J. (2008). Hedgehog signaling pathway function conserved in Tribolium segmentation. *Dev Genes Evol* **218**, 181-192.

Ferjentsik, Z., Hayashi, S., Dale, J. K., Bessho, Y., Herreman, A., De Strooper, B., del Monte, G., de la Pompa, J. L. and Maroto, M. (2009). Notch is a critical component of the mouse somitogenesis

oscillator and is essential for the formation of the somites. *PLoS Genet* **5**, e1000662.

Fischer, A. H., Henrich, T. and Arendt, D. (2010). The normal development of Platynereis dumerilii (Nereididae, Annelida). *Front Zool* **7**, 31.

Force, A., Lynch, M., Pickett, F. B., Amores, A., Yan, Y. L. and Postlethwait, J. (1999). Preservation of duplicate genes by complementary, degenerative mutations. *Genetics* **151**, 1531-1545.

Frasch, M., Hoey, T., Rushlow, C., Doyle, H. and Levine, M. (1987). Characterization and localization of the even-skipped protein of Drosophila. *EMBO J* **6**, 749-759.

Frasch, M. and Levine, M. (1987). Complementary patterns of even-skipped and fushi tarazu expression involve their differential regulation by a common set of segmentation genes in Drosophila. *Genes Dev* **1**, 981-995.

Friedland, A. E., Tzur, Y. B., Esvelt, K. M., Colaiácovo, M. P., Church, G. M. and Calarco, J. A. (2013). Heritable genome editing in C. elegans via a CRISPR-Cas9 system. *Nat Methods* **10**, 741-743.

Garriock, R. J., Warkman, A. S., Meadows, S. M., D'Agostino, S. and Krieg, P. A. (2007). Census of vertebrate Wnt genes: isolation and developmental expression of Xenopus Wnt2, Wnt3, Wnt9a, Wnt9b, Wnt10a, and Wnt16. *Developmental dynamics : an official publication of the American Association of Anatomists* **236**, 1249-1258.

Gaul, U. and Jackle, H. (1990). Role of gap genes in early Drosophila development. *Adv Genet* **27**, 239-275.

Gazave, E., Guillou, A. and Balavoine, G. (2014). History of a prolific family: the Hes/Hey-related genes of the annelid Platynereis. *Evodevo* **5**, 29.

Gilbert, S. F., Opitz, J. M. and Raff, R. A. (1996). Resynthesizing evolutionary and developmental biology. *Dev Biol* **173**, 357-372.

Gilles, A. F. and Averof, M. (2014). Functional genetics for all: engineered nucleases, CRISPR and the gene editing revolution. *Evodevo* **5**, 43.

Gilles, A. F., Schinko, J. B. and Averof, M. (2015). Efficient CRISPR-mediated gene targeting and transgene replacement in the beetle Tribolium castaneum. *Development* **142**, 2832-2839.

Giribet, G. and Edgecombe, G. D. (2012). Reevaluating the arthropod tree of life. *Annu Rev Entomol* **57**, 167-186.

Giribet, G., Richter, S., Edgecombe, G.D., Wheeler, W.C. (2005). The position of crustaceans within Arthropoda – evidence from nine molecular loci and morphology. . Crustacea and Arthropod Relationships. Crustacean Issues, 16. CRC Press, Taylor & Francis, pp. 307–352. .

Goto, T., Macdonald, P. and Maniatis, T. (1989). Early and late periodic patterns of even skipped expression are controlled by distinct regulatory elements that respond to different spatial cues. *Cell* **57**, 413-422.

Graham, A., Butts, T., Lumsden, A. and Kiecker, C. (2014). What can vertebrates tell us about segmentation? *Evodevo* **5**, 24.

Gratz, S. J., Ukken, F. P., Rubinstein, C. D., Thiede, G., Donohue, L. K., Cummings, A. M. and O'Connor-Giles, K. M. (2014). Highly specific and efficient CRISPR/Cas9-catalyzed homology-directed repair in Drosophila. *Genetics* **196**, 961-971.

Grbic, M., Van Leeuwen, T., Clark, R. M., Rombauts, S., Rouze, P., Grbic, V., Osborne, E. J., Dermauw, W., Ngoc, P. C., Ortego, F., et al. (2011). The genome of Tetranychus urticae reveals herbivorous pest adaptations. *Nature* **479**, 487-492.

Green, J. and Akam, M. (2013). Evolution of the pair rule gene network: Insights from a centipede. *Dev Biol* **382**, 235-245.

Grossniklaus, U., Pearson, R. K. and Gehring, W. J. (1992). The Drosophila sloppy paired locus encodes two proteins involved in segmentation that show homology to mammalian transcription factors. *Genes Dev* **6**, 1030-1051.

Guindon, S., Dufayard, J. F., Lefort, V., Anisimova, M., Hordijk, W. and Gascuel, O. (2010). New algorithms and methods to estimate maximum-likelihood phylogenies: assessing the performance of PhyML 3.0. *Syst Biol* **59**, 307-321.

Hagedorn, E. J., Bayraktar, J. L., Kandachar, V. R., Bai, T., Englert, D. M. and Chang, H. C. (2006). Drosophila melanogaster auxilin regulates the internalization of Delta to control activity of the Notch signaling pathway. *Journal of Cell Biology* **173**, 443-452.

Hall, B. K. (2003). Evo-Devo: evolutionary developmental mechanisms. *Int J Dev Biol* **47**, 491-495.

Harding, K., Wedeen, C., McGinnis, W. and Levine, M. (1985). Spatially regulated expression of homeotic genes in Drosophila. *Science* **229**, 1236-1242.

Hayden, L. and Arthur, W. (2014). The centipede Strigamia maritima possesses a large complement of Wnt genes with diverse expression patterns. *Evol Dev* **16**, 127-138.

Heemskerk, J., DiNardo, S., Kostriken, R. and O'Farrell, P. H. (1991). Multiple modes of engrailed regulation in the progression towards cell fate determination. *Nature* **352**, 404-410.

Hilbrant, M., Damen, W. G. and McGregor, A. P. (2012). Evolutionary crossroads in developmental biology: the spider Parasteatoda tepidariorum. *Development* **139**, 2655-2662.

Hino, K., Satou, Y., Yagi, K. and Satoh, N. (2003). A genomewide survey of developmentally relevant genes in Ciona intestinalis. VI. Genes for Wnt, TGFbeta, Hedgehog and JAK/STAT signaling pathways. *Dev Genes Evol* **213**, 264-272.

Hogvall, M., Schonauer, A., Budd, G. E., McGregor, A. P., Posnien, N. and Janssen, R. (2014). Analysis of the Wnt gene repertoire in an onychophoran provides new insights into the evolution of segmentation. *Evodevo* **5**, 14.

Huang, H. C. and Klein, P. S. (2004). The Frizzled family: receptors for multiple signal transduction pathways. *Genome Biol* **5**, 234.

Ingham, P. (1988). Interactions between the pair-rule genes runt, hairy, even-skipped and fushi tarazu and the establishment of periodic pattern in the Drosophila embryo. *Development* **104**, 51-60.

Ingham, P. W. and McMahon, A. P. (2001). Hedgehog signaling in animal development: paradigms and principles. *Genes Dev* **15**, 3059-3087.

Ingham, P. W., Taylor, A. M. and Nakano, Y. (1991). Role of the Drosophila patched gene in positional signalling. *Nature* **353**, 184-187.

Irish, V. F., Martinez-Arias, A. and Akam, M. (1989). Spatial regulation of the Antennapedia and Ultrabithorax homeotic genes during Drosophila early development. *EMBO J* **8**, 1527-1537.

Irvine, K. D. (1999). Fringe, Notch, and making developmental boundaries. *Curr Opin Genet Dev* **9**, 434-441.

Janssen, R. and Budd, G. E. (2013). Deciphering the onychophoran 'segmentation gene cascade': Gene expression reveals limited involvement of pair rule gene orthologs in segmentation, but a highly conserved segment polarity gene network. *Dev Biol* **382**, 224-234.

Janssen, R., Budd, G. E., Prpic, N. M. and Damen, W. G. (2011). Expression of myriapod pair rule gene orthologs. *Evodevo* **2**, 5.

Janssen, R., Le Gouar, M., Pechmann, M., Poulin, F., Bolognesi, R., Schwager, E. E., Hopfen, C., Colbourne, J. K., Budd, G. E., Brown, S. J., et al. (2010). Conservation, loss, and redeployment of Wnt ligands in protostomes: implications for understanding the evolution of segment formation. *BMC Evol Biol* **10**, 374.

Janssen, R., Schönauer, A., Weber, M., Turetzek, N., Hogvall, M., Goss, G., Patel, N. and McGregor, A. a. H., M (2015). The evolution and expression of panarthropod frizzled genes. *Frontiers in Ecology and Evolution*.

Janssens, H., Siggens, K., Cicin-Sain, D., Jimenez-Guri, E., Musy, M., Akam, M. and Jaeger, J. (2014). A quantitative atlas of Even-skipped and Hunchback expression in Clogmia albipunctata (Diptera: Psychodidae) blastoderm embryos. *Evodevo* **5**, 1.

Jaynes, J. B. and Fujioka, M. (2004). Drawing lines in the sand: even skipped et al. and parasegment boundaries. *Dev Biol* **269**, 609-622.

Jiang, Y. J., Aerne, B. L., Smithers, L., Haddon, C., Ish-Horowicz, D. and Lewis, J. (2000). Notch signalling and the synchronization of the somite segmentation clock. *Nature* **408**, 475-479.

Kageyama, R., Niwa, Y., Isomura, A., Gonzalez, A. and Harima, Y. (2012). Oscillatory gene expression and somitogenesis. *Wiley Interdiscip Rev Dev Biol* **1**, 629-641.

Kainz, F., Ewen-Campen, B., Akam, M. and Extavour, C. G. (2011). Notch/Delta signalling is not required for segment generation in the basally branching insect Gryllus bimaculatus. *Development* **138**, 5015-5026.

Kanayama, M., Akiyama-Oda, Y., Nishimura, O., Tarui, H., Agata, K. and Oda, H. (2011). Travelling and splitting of a wave of hedgehog expression involved in spider-head segmentation. *Nat Commun* **2**, 500.

Kanayama, M., Akiyama-Oda, Y. and Oda, H. (2010). Early embryonic development in the spider Achaearanea tepidariorum: Microinjection verifies that cellularization is complete before the blastoderm stage. *Arthropod Struct Dev* **39**, 436-445.

Kimmel, C. B. (1996). Was Urbilateria segmented? *Trends Genet* **12**, 329-331.

Kistler, K. E., Vosshall, L. B. and Matthews, B. J. (2015). Genome engineering with CRISPR-Cas9 in the mosquito Aedes aegypti. *Cell Rep* **11**, 51-60.

Komiya, Y. and Habas, R. (2008). Wnt signal transduction pathways. *Organogenesis* **4**, 68-75.

Kornberg, T., Siden, I., O'Farrell, P. and Simon, M. (1985). The engrailed locus of Drosophila: in situ localization of transcripts reveals compartment-specific expression. *Cell* **40**, 45-53.

Kusserow, A., Pang, K., Sturm, C., Hrouda, M., Lentfer, J., Schmidt, H. A., Technau, U., von Haeseler, A., Hobmayer, B., Martindale, M. Q., et al. (2005). Unexpected complexity of the Wnt gene family in a sea anemone. *Nature* **433**, 156-160.

Lall, S. and Patel, N. H. (2001). Conservation and divergence in molecular mechanisms of axis formation. *Annu Rev Genet* **35**, 407-437.

Lapraz, F., Rottinger, E., Duboc, V., Range, R., Duloquin, L., Walton, K., Wu, S. Y., Bradham, C., Loza, M. A., Hibino, T., et al. (2006). RTK and TGF-beta signaling pathways genes in the sea urchin genome. *Dev Biol* **300**, 132-152.

Lawrence, P. A. (1992). *The making of a fly: the genetics of animal design*. Oxford, UK: Blackwell Scientific.

Lehmann, R. and Nusslein-Volhard, C. (1991). The maternal gene nanos has a central role in posterior pattern formation of the Drosophila embryo. *Development* **112**, 679-691.

Leimeister, C., Bach, A. and Gessler, M. (1998). Developmental expression patterns of mouse sFRP genes encoding members of the secreted frizzled related protein family. *Mech Dev* **75**, 29-42.

Leite, D. J. and McGregor, A. P. (2016). Arthropod evolution and development: recent insights from chelicerates and myriapods. *Curr Opin Genet Dev* **39**, 93-100.

Leite, D. J., Ninova, M., Hilbrant, M., Arif, S., Griffiths-Jones, S., Ronshaugen, M. and McGregor, A. P. (2016). Pervasive microRNA duplication in chelicerates: insights from the embryonic microRNA repertoire of the spider Parasteatoda tepidariorum. *Genome Biol Evol*.

Lewis, E. B. (1978). A gene complex controlling segmentation in Drosophila. *Nature* **276**, 565-570.

Leyns, L., Bouwmeester, T., Kim, S. H., Piccolo, S. and De Robertis, E. M. (1997). Frzb-1 is a secreted antagonist of Wnt signaling expressed in the Spemann organizer. *Cell* **88**, 747-756.

Liu, P. Z. and Kaufman, T. C. (2004a). hunchback is required for suppression of abdominal identity, and for proper germband growth and segmentation in the intermediate germband insect Oncopeltus fasciatus. *Development* **131**, 1515-1527.

---- (2004b). Kruppel is a gap gene in the intermediate germband insect Oncopeltus fasciatus and is required for development of both blastoderm and germband-derived segments. *Development* **131**, 4567-4579.

---- (2005). even-skipped is not a pair-rule gene but has segmental and gap-like functions in Oncopeltus fasciatus, an intermediate germband insect. *Development* **132**, 2081-2092.

Liu, P. Z. and Patel, N. H. (2010). giant is a bona fide gap gene in the intermediate germband insect, Oncopeltus fasciatus. *Development* **137**, 835-844.

Logan, C. Y. and Nusse, R. (2004). The Wnt signaling pathway in development and disease. *Annu Rev Cell Dev Biol* **20**, 781-810.

Lynch, M. and Force, A. (2000). The probability of duplicate gene preservation by subfunctionalization. *Genetics* **154**, 459-473.
MacDonald, B. T. and He, X. (2012). Frizzled and LRP5/6 receptors for Wnt/β-catenin signaling. *Cold Spring Harb Perspect Biol* **4**.
Macdonald, P. M. and Struhl, G. (1986). A molecular gradient in early Drosophila embryos and its role in specifying the body pattern. *Nature* **324**, 537-545.
Maderspacher, F., Bucher, G. and Klingler, M. (1998). Pair-rule and gap gene mutants in the flour beetle Tribolium castaneum. *Dev Genes Evol* **208**, 558-568.
Marie, B. and Bacon, J. P. (2000). Two engrailed-related genes in the cockroach: cloning, phylogenetic analysis, expression and isolation of splice variants. *Dev Genes Evol* **210**, 436-448.
Marques-Souza, H., Aranda, M. and Tautz, D. (2008). Delimiting the conserved features of hunchback function for the trunk organization of insects. *Development* **135**, 881-888.
Martinez-Arias, A. and Lawrence, P. A. (1985). Parasegments and compartments in the Drosophila embryo. *Nature* **313**, 639-642.
McGregor, A. P. (2005). How to get ahead: the origin, evolution and function of bicoid. *Bioessays* **27**, 904-913.
McGregor, A. P., Hilbrant, M., Pechmann, M., Schwager, E. E., Prpic, N. M. and Damen, W. G. (2008a). Cupiennius salei and Achaearanea tepidariorum: Spider models for investigating evolution and development. *Bioessays* **30**, 487-498.
McGregor, A. P., Pechmann, M., Schwager, E. E. and Damen, W. G. (2009). An ancestral regulatory network for posterior development in arthropods. *Commun Integr Biol* **2**, 174-176.
McGregor, A. P., Pechmann, M., Schwager, E. E., Feitosa, N. M., Kruck, S., Aranda, M. and Damen, W. G. (2008b). Wnt8 is required for growth-zone establishment and development of opisthosomal segments in a spider. *Curr Biol* **18**, 1619-1623.
Micchelli, C. A., Rulifson, E. J. and Blair, S. S. (1997). The function and regulation of cut expression on the wing margin of Drosophila: Notch, Wingless and a dominant negative role for Delta and Serrate. *Development* **124**, 1485-1495.
Minelli, A. (2015). *Introduction, Non-Bilateria, Acoelomorpha, Xenoturbellida, Chaetognatha*: Springer.
Mito, T., Sarashina, I., Zhang, H., Iwahashi, A., Okamoto, H., Miyawaki, K., Shinmyo, Y., Ohuchi, H. and Noji, S. (2005). Non-canonical functions of hunchback in segment patterning of the intermediate germ cricket Gryllus bimaculatus. *Development* **132**, 2069-2079.
Mittmann, B. and Wolff, C. (2012). Embryonic development and staging of the cobweb spider Parasteatoda tepidariorum C. L. Koch, 1841 (syn.: Achaearanea tepidariorum; Araneomorphae; Theridiidae). *Dev Genes Evol* **222**, 189-216.
Miyawaki, K., Mito, T., Sarashina, I., Zhang, H., Shinmyo, Y., Ohuchi, H. and Noji, S. (2004). Involvement of Wingless/Armadillo signaling in the posterior sequential segmentation in the cricket, Gryllus bimaculatus (Orthoptera), as revealed by RNAi analysis. *Mech Dev* **121**, 119-130.

Mlodzik, M. and Gehring, W. J. (1987). Expression of the caudal gene in the germ line of Drosophila: formation of an RNA and protein gradient during early embryogenesis. *Cell* **48**, 465-478.

Mohler, J. and Vani, K. (1992). Molecular organization and embryonic expression of the hedgehog gene involved in cell-cell communication in segmental patterning of Drosophila. *Development* **115**, 957-971.

Muller, H. A., Samanta, R. and Wieschaus, E. (1999). Wingless signaling in the Drosophila embryo: zygotic requirements and the role of the frizzled genes. *Development* **126**, 577-586.

Murat, S., Hopfen, C. and McGregor, A. P. (2010). The function and evolution of Wnt genes in arthropods. *Arthropod Struct Dev* **39**, 446-452.

Nakamoto, A., Hester, S. D., Constantinou, S. J., Blaine, W. G., Tewksbury, A. B., Matei, M. T., Nagy, L. M. and Williams, T. A. (2015). Changing cell behaviours during beetle embryogenesis correlates with slowing of segmentation. *Nat Commun* **6**, 6635.

Nakanishi, T., Kato, Y., Matsuura, T. and Watanabe, H. (2014). CRISPR/Cas-mediated targeted mutagenesis in Daphnia magna. *PLoS One* **9**, e98363.

Nakayama, T., Fish, M. B., Fisher, M., Oomen-Hajagos, J., Thomsen, G. H. and Grainger, R. M. (2013). Simple and efficient CRISPR/Cas9-mediated targeted mutagenesis in Xenopus tropicalis. *Genesis* **51**, 835-843.

Nomura-Kitabayashi, A., Takahashi, Y., Kitajima, S., Inoue, T., Takeda, H. and Saga, Y. (2002). Hypomorphic Mesp allele distinguishes establishment of rostrocaudal polarity and segment border formation in somitogenesis. *Development* **129**, 2473-2481.

Nossa, C. W., Havlak, P., Yue, J. X., Lv, J., Vincent, K. Y., Brockmann, H. J. and Putnam, N. H. (2014). Joint assembly and genetic mapping of the Atlantic horseshoe crab genome reveals ancient whole genome duplication. *Gigascience* **3**, 9.

Nusslein-Volhard, C. and Wieschaus, E. (1980). Mutations affecting segment number and polarity in Drosophila. *Nature* **287**, 795-801.

Oda, H., Nishimura, O., Hirao, Y., Tarui, H., Agata, K. and Akiyama-Oda, Y. (2007). Progressive activation of Delta-Notch signaling from around the blastopore is required to set up a functional caudal lobe in the spider Achaearanea tepidariorum. *Development* **134**, 2195-2205.

Olesnicky, E. C., Brent, A. E., Tonnes, L., Walker, M., Pultz, M. A., Leaf, D. and Desplan, C. (2006). A caudal mRNA gradient controls posterior development in the wasp Nasonia. *Development* **133**, 3973-3982.

Pankratz, M. and Jäckle, H. (1993). Blastoderm segmentation. In *The development of Drosophila melanogaster* (ed. M. B. a. A. M. Arias), pp. pp. 467-516: Cold Spring Harbor Press.

Pankratz, M. J., Seifert, E., Gerwin, N., Billi, B., Nauber, U. and Jackle, H. (1990). Gradients of Kruppel and knirps gene products direct pair-rule gene stripe patterning in the posterior region of the Drosophila embryo. *Cell* **61**, 309-317.

Park, W. J., Liu, J. and Adler, P. N. (1994a). Frizzled gene expression and development of tissue polarity in the Drosophila wing. *Dev Genet* **15**, 383-389.

---- (1994b). The frizzled gene of Drosophila encodes a membrane protein with an odd number of transmembrane domains. *Mech Dev* **45**, 127-137.

Patel, N. H. (2003). The ancestry of segmentation. *Dev Cell* **5**, 2-4.

Patel, N. H., Condron, B. G. and Zinn, K. (1994). Pair-rule expression patterns of even-skipped are found in both short- and long-germ beetles. *Nature* **367**, 429-434.

Patel, N. H., Kornberg, T. B. and Goodman, C. S. (1989a). Expression of engrailed during segmentation in grasshopper and crayfish. *Development* **107**, 201-212.

Patel, N. H., Martin-Blanco, E., Coleman, K. G., Poole, S. J., Ellis, M. C., Kornberg, T. B. and Goodman, C. S. (1989b). Expression of engrailed proteins in arthropods, annelids, and chordates. *Cell* **58**, 955-968.

Pearson, J. C., Lemons, D. and McGinnis, W. (2005). Modulating Hox gene functions during animal body patterning. *Nat Rev Genet* **6**, 893-904.

Pechmann, M., Khadjeh, S., Turetzek, N., McGregor, A. P., Damen, W. G. and Prpic, N. M. (2011). Novel function of Distal-less as a gap gene during spider segmentation. *PLoS Genet* **7**, e1002342.

Pechmann, M., McGregor, A. P., Schwager, E. E., Feitosa, N. M. and Damen, W. G. (2009). Dynamic gene expression is required for anterior regionalization in a spider. *Proc Natl Acad Sci U S A* **106**, 1468-1472.

Peel, A. and Akam, M. (2003). Evolution of segmentation: rolling back the clock. *Curr Biol* **13**, R708-710.

Peel, A. D. (2008). The evolution of developmental gene networks: lessons from comparative studies on holometabolous insects. *Philos Trans R Soc Lond B Biol Sci* **363**, 1539-1547.

Peel, A. D., Chipman, A. D. and Akam, M. (2005). Arthropod segmentation: beyond the Drosophila paradigm. *Nat Rev Genet* **6**, 905-916.

Platt, R. J., Chen, S., Zhou, Y., Yim, M. J., Swiech, L., Kempton, H. R., Dahlman, J. E., Parnas, O., Eisenhaure, T. M., Jovanovic, M., et al. (2014). CRISPR-Cas9 knockin mice for genome editing and cancer modeling. *Cell* **159**, 440-455.

Posnien, N., Zeng, V., Schwager, E. E., Pechmann, M., Hilbrant, M., Keefe, J. D., Damen, W. G., Prpic, N. M., McGregor, A. P. and Extavour, C. G. (2014). A comprehensive reference transcriptome resource for the common house spider Parasteatoda tepidariorum. *PLoS One* **9**, e104885.

Pourquie, O. (2001). Vertebrate somitogenesis. *Annual review of cell and developmental biology* **17**, 311-350.

---- (2003). Vertebrate somitogenesis: a novel paradigm for animal segmentation? *Int J Dev Biol* **47**, 597-603.

Prpic, N. M., Schoppmeier, M. and Damen, W. G. (2008a). Collection and fixation of spider embryos. *CSH Protoc* **2008**, pdb prot5067.

---- (2008b). Gene Silencing via Embryonic RNAi in Spider Embryos. *CSH Protoc* **2008**, pdb prot5070.

---- (2008c). Whole-mount in situ hybridization of spider embryos. *CSH Protoc* **2008**, pdb prot5068.

---- (2008d). Whole-mount in situ hybridization of spider embryos. *CSH Protoc* **2008**, pdb.prot5068.

Prud'homme, B., de Rosa, R., Arendt, D., Julien, J. F., Pajaziti, R., Dorresteijn, A. W., Adoutte, A., Wittbrodt, J. and Balavoine, G. (2003). Arthropod-like expression patterns of engrailed and wingless in the annelid Platynereis dumerilii suggest a role in segment formation. *Curr Biol* **13**, 1876-1881.

Pueyo, J. I., Lanfear, R. and Couso, J. P. (2008). Ancestral Notch-mediated segmentation revealed in the cockroach Periplaneta americana. *Proc Natl Acad Sci U S A* **105**, 16614-16619.

Ran, F. A., Hsu, P. D., Lin, C. Y., Gootenberg, J. S., Konermann, S., Trevino, A. E., Scott, D. A., Inoue, A., Matoba, S., Zhang, Y., et al. (2013). Double nicking by RNA-guided CRISPR Cas9 for enhanced genome editing specificity. *Cell* **154**, 1380-1389.

Rattner, A., Hsieh, J. C., Smallwood, P. M., Gilbert, D. J., Copeland, N. G., Jenkins, N. A. and Nathans, J. (1997). A family of secreted proteins contains homology to the cysteine-rich ligand-binding domain of frizzled receptors. *Proc Natl Acad Sci U S A* **94**, 2859-2863.

Regier, J. C., Shultz, J. W., Zwick, A., Hussey, A., Ball, B., Wetzer, R., Martin, J. W. and Cunningham, C. W. (2010). Arthropod relationships revealed by phylogenomic analysis of nuclear protein-coding sequences. *Nature* **463**, 1079-1083.

Ren, X., Yang, Z., Xu, J., Sun, J., Mao, D., Hu, Y., Yang, S. J., Qiao, H. H., Wang, X., Hu, Q., et al. (2014). Enhanced specificity and efficiency of the CRISPR/Cas9 system with optimized sgRNA parameters in Drosophila. *Cell Rep* **9**, 1151-1162.

Rivera-Pomar, R. and Jackle, H. (1996). From gradients to stripes in Drosophila embryogenesis: filling in the gaps. *Trends in genetics : TIG* **12**, 478-483.

Rivera-Pomar, R., Lu, X., Perrimon, N., Taubert, H. and Jackle, H. (1995). Activation of posterior gap gene expression in the Drosophila blastoderm. *Nature* **376**, 253-256.

Rota-Stabelli, O., Campbell, L., Brinkmann, H., Edgecombe, G. D., Longhorn, S. J., Peterson, K. J., Pisani, D., Philippe, H. and Telford, M. J. (2011). A congruent solution to arthropod phylogeny: phylogenomics, microRNAs and morphology support monophyletic Mandibulata. *Proc Biol Sci* **278**, 298-306.

Rota-Stabelli, O., Daley, A. C. and Pisani, D. (2013). Molecular timetrees reveal a Cambrian colonization of land and a new scenario for ecdysozoan evolution. *Curr Biol* **23**, 392-398.

Saga, Y. (2007). Segmental border is defined by the key transcription factor Mesp2, by means of the suppression of Notch activity. *Dev Dyn* **236**, 1450-1455.

Sander, J. D. and Joung, J. K. (2014). CRISPR-Cas systems for editing, regulating and targeting genomes. *Nat Biotechnol* **32**, 347-355.

Sanggaard, K. W., Bechsgaard, J. S., Fang, X., Duan, J., Dyrlund, T. F., Gupta, V., Jiang, X., Cheng, L., Fan, D., Feng, Y., et al. (2014). Spider genomes provide insight into composition and evolution of venom and silk. *Nat Commun* **5**, 3765.

Sarrazin, A. F., Peel, A. D. and Averof, M. (2012). A segmentation clock with two-segment periodicity in insects. *Science* **336**, 338-341.

Schenkelaars, Q., Fierro-Constain, L., Renard, E., Hill, A. L. and Borchiellini, C. (2015). Insights into Frizzled evolution and new perspectives. *Evol Dev* **17**, 160-169.

Scholtz, G. (1998). Cleavage, germ band formation and head segmentation: the ground pattern of the Euarthropoda. In *Arthropod Relationships* (ed. R. A. Fortey & R. H. Thomas). London, UK: Springer Science+Business Media Dordrecht.

---- (2002). The Articulata hypothesis - or what is a segment? *Organisms Diversity and Evolution* **2**, 18.

Schonauer, A., Paese, C. L., Hilbrant, M., Leite, D. J., Schwager, E. E., Feitosa, N. M., Eibner, C., Damen, W. G. and McGregor, A. P. (2016). The Wnt and Delta-Notch signalling pathways interact to direct pair-rule gene expression via caudal during segment addition in the spider Parasteatoda tepidariorum. *Development*.

Schoppmeier, M. and Damen, W. G. (2005a). Expression of Pax group III genes suggests a single-segmental periodicity for opisthosomal segment patterning in the spider Cupiennius salei. *Evol Dev* **7**, 160-169.

---- (2005b). Suppressor of Hairless and Presenilin phenotypes imply involvement of canonical Notch-signalling in segmentation of the spider Cupiennius salei. *Dev Biol* **280**, 211-224.

Schroder, R. (2003). The genes orthodenticle and hunchback substitute for bicoid in the beetle Tribolium. *Nature* **422**, 621-625.

Schwager, E. E., Pechmann, M., Feitosa, N. M., McGregor, A. P. and Damen, W. G. (2009). hunchback functions as a segmentation gene in the spider Achaearanea tepidariorum. *Curr Biol* **19**, 1333-1340.

Schwager, E. E., Schönauer, A., Leite, D., Sharma, P. P. and McGregor, A. P. (2015). Chelicerata. In *Evolutionary Developmental Biology of Invertebrates 3: Ecdysozoa I: Non-Tetraconata* (ed. A. Wanninger). Wien: Springer-Verlag.

Scott, M. P. and Carroll, S. B. (1987). The segmentation and homeotic gene network in early Drosophila development. *Cell* **51**, 689-698.

Shinmyo, Y., Mito, T., Matsushita, T., Sarashina, I., Miyawaki, K., Ohuchi, H. and Noji, S. (2005). caudal is required for gnathal and thoracic patterning and for posterior elongation in the intermediate-germband cricket Gryllus bimaculatus. *Mech Dev* **122**, 231-239.

Song, M. H., Huang, F. Z., Chang, G. Y. and Weisblat, D. A. (2002). Expression and function of an even-skipped homolog in the leech Helobdella robusta. *Development* **129**, 3681-3692.

Song, M. H., Huang, F. Z., Gonsalves, F. C. and Weisblat, D. A. (2004). Cell cycle-dependent expression of a hairy and Enhancer of split (hes) homolog during cleavage and segmentation in leech embryos. *Dev Biol* **269**, 183-195.

Sprinzak, D., Lakhanpal, A., Lebon, L., Santat, L. A., Fontes, M. E., Anderson, G. A., Garcia-Ojalvo, J. and Elowitz, M. B. (2010). Cis-interactions between Notch and Delta generate mutually exclusive signalling states. *Nature* **465**, 86-90.

St Johnston, D. and Nusslein-Volhard, C. (1992). The origin of pattern and polarity in the Drosophila embryo. *Cell* **68**, 201-219.

Staal, F. J. and Clevers, H. C. (2005). WNT signalling and haematopoiesis: a WNT-WNT situation. *Nat Rev Immunol* **5**, 21-30.

Stansbury, M. S. and Moczek, A. P. (2013). The Evolvability of Arthropods. In *Arthropod Biology and Evolution (Molecules, Development, Morphology)* (ed. A. Minelli, G. Boxshall & G. Fusco). Berlin Heidelberg, Germany: Springer.

Stauber, M., Jackle, H. and Schmidt-Ott, U. (1999). The anterior determinant bicoid of Drosophila is a derived Hox class 3 gene. *Proc Natl Acad Sci U S A* **96**, 3786-3789.

Stollewerk, A., Schoppmeier, M. and Damen, W. G. (2003). Involvement of Notch and Delta genes in spider segmentation. *Nature* **423**, 863-865.

Strausfeld, N. J., Strausfeld, C. M., Loesel, R., Rowell, D. and Stowe, S. (2006). Arthropod phylogeny: onychophoran brain organization suggests an archaic relationship with a chelicerate stem lineage. *Proc Biol Sci* **273**, 1857-1866.

Takeuchi, H. and Haltiwanger, R. S. (2010). Role of glycosylation of Notch in development. *Semin Cell Dev Biol* **21**, 638-645.

Takke, C. and Campos-Ortega, J. A. (1999). her1, a zebrafish pair-rule like gene, acts downstream of notch signalling to control somite development. *Development* **126**, 3005-3014.

Tautz, D. (2004). Segmentation. *Dev Cell* **7**, 301-312.

Umbhauer, M., Djiane, A., Goisset, C., Penzo-Mendez, A., Riou, J. F., Boucaut, J. C. and Shi, D. L. (2000). The C-terminal cytoplasmic Lys-thr-X-X-X-Trp motif in frizzled receptors mediates Wnt/beta-catenin signalling. *EMBO J* **19**, 4944-4954.

Wang, H., Yang, H., Shivalila, C. S., Dawlaty, M. M., Cheng, A. W., Zhang, F. and Jaenisch, R. (2013). One-step generation of mice carrying mutations in multiple genes by CRISPR/Cas-mediated genome engineering. *Cell* **153**, 910-918.

Wang, S., Krinks, M., Lin, K., Luyten, F. P. and Moos, M., Jr. (1997). Frzb, a secreted protein expressed in the Spemann organizer, binds and inhibits Wnt-8. *Cell* **88**, 757-766.

Wang, Y., Macke, J. P., Abella, B. S., Andreasson, K., Worley, P., Gilbert, D. J., Copeland, N. G., Jenkins, N. A. and Nathans, J. (1996). A large family of putative transmembrane receptors homologous to the product of the Drosophila tissue polarity gene frizzled. *J Biol Chem* **271**, 4468-4476.

Webster, B. L., Copley, R. R., Jenner, R. A., Mackenzie-Dodds, J. A., Bourlat, S. J., Rota-Stabelli, O., Littlewood, D. T. and Telford, M. J. (2006). Mitogenomics and phylogenomics reveal priapulid worms as extant models of the ancestral Ecdysozoan. *Evol Dev* **8**, 502-510.

Wei, W., Xin, H., Roy, B., Dai, J., Miao, Y. and Gao, G. (2014). Heritable genome editing with CRISPR/Cas9 in the silkworm, Bombyx mori. *PLoS One* **9**, e101210.

Weisblat, D. A., Kim, S. Y. and Stent, G. S. (1984). Embryonic origins of cells in the leech Helobdella triserialis. *Dev Biol* **104**, 65-85.

Weygoldt, P. and Paulus, H. F. (1979). Untersuchungen zur Morphologie, Taxonomie und Phylogenie der Chelicerata. *Journal of Zoological Systematics and Evolutionary Research* **17**.

Wu, C. and Alwine, J. C. (2004). Secondary structure as a functional feature in the downstream region of mammalian polyadenylation signals. *Molecular and cellular biology* **24**, 2789-2796.

Yamazaki, K., Akiyama-Oda, Y. and Oda, H. (2005). Expression patterns of a twist-related gene in embryos of the spider Achaearanea tepidariorum reveal divergent aspects of mesoderm development in the fly and spider. *Zoolog Sci* **22**, 177-185.

Yoshino, K., Rubin, J. S., Higinbotham, K. G., Uren, A., Anest, V., Plisov, S. Y. and Perantoni, A. O. (2001). Secreted Frizzled-related proteins can regulate metanephric development. *Mech Dev* **102**, 45-55.

Zackson, S. L. (1982). Cell clones and segmentation in leech development. *Cell* **31**, 761-770.

Zeng, V. and Extavour, C. G. (2012). ASGARD: an open-access database of annotated transcriptomes for emerging model arthropod species. *Database (Oxford)* **2012**, bas048.